USE OF REFINED ANALYSIS METHODS FOR IMPROVED ESTIMATION OF LIVE LOAD DEMANDS IN LOAD RATING OF GIRDER AND SLAB BRIDGES

Dissertation

by

ABDOU K. NDONG

Submitted to the School of Engineering and Applied Science at

University of Virginia

In partial fulfillment of the requirements for the degree of

DOCTOR OF PHILOSOPHY

in

Engineering Systems and Environment

December 2022

APPROVAL SHEET

The dissertation

is submitted in partial fulfillment of the requirements

for the degree of

Doctor of Philosophy

Abdou K. Ndong

The thesis has been read and approved by the examining committee:

Osman E. Ozbulut (Advisor)
_____

Jose Gomez (Chair)
_____

Devin K. Harris
_____

Natasha Smith
_____

Bernard Kassner
_____

Accepted for the School of Engineering and Applied Science:

Jennifer West, Dean, School of Engineering and Applied Science

December 2022

USE OF REFINED ANALYSIS METHODS FOR IMPROVED ESTIMATION OF LIVE LOAD DEMANDS IN LOAD RATING OF GIRDER AND SLAB BRIDGES

ABSTRACT

Bridge load rating assesses the safe live load carrying capacity of an existing or newly designed bridge structure. In addition to load rating with previously defined standard legal-load rating vehicles, the Federal Highway Administration has required states to rate all the bridges with specialized hauling vehicles (SHVs) and emergency vehicles (EVs) by the end of 2022. SHVs refers to single unit trucks with closely spaced multiple axles, typically ranging from four to seven. They meet the axle and gross weight limits defined by Federal Formula B, but they have axle configurations that are different than those of standard legal vehicles. Emergency vehicles are designed for use under emergency conditions such as fires or other hazardous conditions. They can have considerably higher axle weight and gross weight than standard legal vehicles. It is recognized that the load effects (bending moment and shear) produced by SHVs and EVs on certain bridge types and spans might be greater than those caused by the previous legal loads. Therefore, a number of bridges within VDOT's inventory may require posting when they are rated with these specialized vehicles.

The goal of this study is to assess the likelihood of an increase in load rating factor through refined analysis methods for the bridge classes potentially vulnerable to load ratings under consideration of the new federal regulations. Typically, live load effects on bridges are estimated using live load distribution factor equations in load rating of bridges. Refined methods of analysis can more accurately describe the distribution of load sharing with a bridge and possibly improve the overall load ratings. This study focused on the evaluation of live load distribution factors for girder bridges and live load resisting effective bridge widths for slab bridges through refined analysis. Considering the population of bridges affected by the SHV ratings and route importance, three bridge classes (simple span steel girder bridges, reinforce concrete T-beam bridges, and concrete slab bridges) were selected for the refined analysis. Girder bridges were modeled using the plate with an eccentric beam analysis approach, while plate elements were used to model slab bridges using a structural analysis software package. The selected modeling approaches were

validated through the simulation of the bridge structures with available field-testing results from the literature. A total of 71 in-service bridges belonging to the three selected bridge classes were then modeled and analyzed to compute the load distribution factors for girder bridges or effective widths for slab bridges, and the results were compared with those obtained from the code-specified equations. Using the data obtained from these numerical simulations, a series of multi-parameter linear regression models were developed to predict the percent change in distribution factor and effective width, respectively for girder and slab bridges with different geometrical characteristics. For girder bridges, the results indicate that moment distribution factors obtained from refined analysis will likely improve rating factors for SHVs, while the shear distribution factors will likely be larger. For the slab bridges, refined analysis tends to result in a higher effective slab width when compared to the AASHTO LRFD approach. The developed regression equations can be used as screening tools to provide guidance on the use of refined methods of analysis to improve the load ratings of bridges vulnerable to posting from previously existing load rating classifications as well as the recently introduced vehicles.

DEDICATION

Dedicated to my inspiring parents, Amy Sene and El Hadj Ibrahim Ndong and siblings, for being the pillows, role models, catapults, cheerleading squad and sounding boards I have needed

ACKNOWLEDGEMENTS

NOMENCLATURE

ABBREVIATION	DESCRIPTION
AASHTO	American Association of State Highway and Transportation Officials
DF or g	Distribution Factor
DOT	Department of Transportation
EV	Emergency Vehicle
FAST Act	Fixing America's Surface Transportation Act
FHWA	Federal Highway Administration
LRFD	Load and Resistance Factor Design
MBE	Manual for Bridge Evaluation
NCHRP	National Cooperative Highway Research Program
PEB	Plate with Eccentric Beam
RC	Reinforced Concrete
RF	Rating Factor
R_{max}	Maximum moment or shear
SHV	Specialized Hauling Vehicle
SU	Single Unit
U.S.C.	United States Code
VDOT	Virginia Department of Transportation

TABLE OF CONTENTS

LIST OF TABLES

LIST OF FIGURES

1. INTRODUCTION

1.1 Motivation

The National Bridge Inspection Standards requires the rating and posting, if needed, of all highway bridges for legal loads and routine permit loads (Morcous et al. 2010). Focusing on the legal load category, the American Association of State Highway and Transportation Officials (AASHTO) Manual for Bridge Evaluation includes three trucks models (AASHTO Type 3, 3S2 and 3-3) to represent the legal load vehicles commonly travelling on nation's highways (Mertz 2015). However, these AASHTO legal trucks are notional load scenarios developed in the 1970s, and do not necessarily represent the more recent developments in the newer truck configurations that operate on highways in the US today. For example, a research study supported by the National Cooperative Highway Research Program (NCHRP) found that the three original AASHTO legal load models do not represent all legal loads (NCHRP Report 2007).

In 2013, the Federal Highway Administration (FHWA) mandated state departments of transportation to rate all bridges within the state inventory for a class of vehicles called specialized hauling vehicles (SHVs) by the end of 2017 for Group 1 bridges (i.e., those bridges whose shortest span is not greater 200 ft and load rating or rating factor is below a certain value) and by the end of 2022 for Group 2 bridges (i.e., all bridges that are not in Group 1), unless state laws preclude SHV use (FHWA 2013). In addition, the 2015 Fixing America's Surface Transportation Act (FAST Act) made certain emergency vehicles (EVs) that have considerably higher axle weight and higher gross weight than standard legal vehicles to be legal on the Interstate System and routes that are within reasonable access to the Interstate (FHWA 2016). These revisions to federal guidelines, especially pertaining to load rating of bridges for SHVs and EVs, presented a challenge to state department of transportations (DOTs) that could drive some of their structures below acceptable rating levels.

Load rating aims to evaluate the safe live load carrying capacity of a bridge, usually defined in terms of a rating factor (RF). The rating factor is a ratio of the capacity of a bridge to the tonnage of a specific vehicle configuration (AASHTO 2015). Bridges constructed to prior standards are compared to present standards, in conjunction with an analysis of the bridge condition, using the Inventory Rating. The Operating Rating is used to evaluate permit overloads on structures. Based

on the current evaluation methods, the operating load capacity of a given bridge system is defined in terms of Rating Factors (RFs) and an equivalent tonnage for a given vehicle configuration that can traverse the bridge (AASHTO 2015). RF values at the inventory level greater than one (1.0) for the expected maximum load indicate that the structure should safely support the expected loads until the next regularly scheduled safety inspection. Otherwise, the bridge will require posting, rehabilitation, or replacement to ensure safety for HL-93 loading. The rating factor for a bridge can be calculated by Equation (1) shown below:

$$RF = \frac{\phi_s \phi_c \phi R - \gamma_d D}{\gamma_L g L (1 + IM)} \qquad (1\text{-}1)$$

where ϕ_s, ϕ_c, ϕ represent the system, condition and resistance factors, respectively; R is the capacity of member; D is the dead load effects due to structural components; L and IM represent live load effect and the dynamic effect, respectively; γ_d is the dead load factor; γ_L is the live load factor; and g is the distribution factor.

The additional live load effects generated by SHVs may adversely affect the load rating of in-service bridges. Although improvement in a bridge's rating factor can be achieved by various means, it is evident from Equation (1) that a reduction in the live load distribution factors (g) would directly lead to an increase in load rating factor. In the AASHTO LRFD specification, the distribution factors can be determined using a set of equations that are functions of the bridge type and its geometrical characteristics. However, several assumptions were made in the development of those distribution factor equations such as: (i) uniform girder spacing, (ii) slab thickness has negligible significant effect on the load distribution, and (iii) HS-20 design vehicle is the representative truck (AASHTO 2002).

To obtain a refined distribution factor that can capture the load distribution behavior of bridges more accurately compared to AASHTO equations, a variety of methods including experimental and numerical approaches have been implemented (Kennedy and Grace et al. 1983, Kim and Nowak 1997, Barr et al. 2001, Eom and Nowak 2001). Although field testing of bridges is the most reliable method for computing actual live load effects (Ebeido and Kennedy 1996, AASHTO

2010, Yost et al. 2005, Nowak et al. 1999), it is expensive and time consuming, and the results are often limited to the bridges investigated. Therefore, numerical modeling represents a viable alternative that could provide a robust approach to obtain reliable live load distribution behavior of bridges (Dicleli and Erhan 2009, Fanous et al. 2011, Puckett et al. 2011, Cai 2005, Harris 2010).

Refined methods of analysis as described in the AASHTO LRFD Bridge Design Specifications (2017), describe a suit of methods capable of accurately describing the behavior of a bridge system. The methods include approaches such as classical plate analysis, finite strip method, finite element analysis, where the analysis methods are capable of including the complex interactions within a structural system that are often simplified in the design process. In recent years, the finite element method and the three-dimensional stiffness method have become the most applicable forms of refined methods of analysis. With advances in computational power, these approaches have allowed for bridges to be represented in their three-dimensional configuration, subjected to variable loading scenarios, and analyzed efficiently, allowing these approaches to become more commonplace in the bridge community.

Should a bridge have an RF value less than 1.0 upon re-rating, there are options for improving the result. In evaluating Equation (1-1), it is evident that opportunities for increasing a bridge's load rating can be derived from reductions in the load distribution factors (g), reductions in the dynamic load allowance (IM), and increases in the bridge capacity (R). There are opportunities for reducing the distribution factors either through refined analysis or live load testing. On the other hand, live load testing provides the only effective method for reducing dynamic load allowance (Barker 2001; Eom and Nowak 2001; Kim and Nowak 1997; Yousif and Hindi 2007). In cases where the refined analysis of the distribution factors does not sufficiently increase the RF, then load tests and perhaps additional strengthening measures may be required to mitigate weight restrictions on these bridges. Nevertheless, this study focuses on a strategy for leveraging Equation (1-1) to improve load ratings using refined methods of analysis.

1.2   Research Objectives

The objective of this research is to evaluate improved estimates of moment and shear demands through refined analysis methods for the bridge classes potentially vulnerable to load ratings under consideration of the new federal regulations and when using conventional, simplified equations for live load demand calculations. In particular, the research focused on the evaluation of live load distribution factors for girder bridges and effective widths for distributing live loads in slab bridges through refined analysis. First, an analysis on the Virginia Department of Transportation (VDOT) bridge inventory is made to identify the class of bridges that are susceptible to load posting due to SHVs and EVs. Three bridge classes (simple span steel girder bridges, reinforced concrete T-beam bridges, and concrete slab bridges) are then selected for this study. In this investigation, a key component in the analysis is the selection and deployment of an appropriate refined method of analysis. These methods of analysis ultimately determine accuracy of the loading and load sharing behavior of the structural system. Therefore, several modeling approaches are evaluated to accurately model girder and slab bridges while remain robust for implementation. Available field-testing results of bridge structures from the literature are used to validate the selected modeling approaches. In this research, a relatively large number of in-service bridges belonging to each of three selected bridge classes are modeled and analyzed to compute the live load demands. First, distribution factors for concrete T-beam and steel girder bridges and effective widths for slab bridges are computed using a common structural analysis software. The distribution factors for girder bridges and effective widths for slab bridges are evaluated for interior and exterior girders under one-lane and two-lanes loaded cases. The effects of SHVs, EVs and the transverse positioning of the vehicle load on the computation of the distribution factors are also investigated. The results are compared with those obtained from the code-specified equations. A statistical machine learning technique is used to evaluate the truck type that governs the distribution factor calculation based on geometric characteristics of a given bridge. Using the data obtained from these numerical simulations, a series of multi-parameter linear regression models are developed to evaluate distribution factor and effective width, respectively, for girder and slab bridges with different geometrical characteristics if a refined method analysis is implemented.

1.3 Dissertation Outline

This dissertation consists of seven sections that are organized as follows:

Section 1: Introduction

This section introduces the motivation for this work, describes the research objectives as well as the organization of the thesis.

Section 2: Literature Review:

This section provides a detailed literature review and current state of practice. It compiles a literature review to document the relevant information related to the assessment of load distribution behavior of bridges using refined analysis and the effects of SHV/EV on bridge load ratings

Section 3: Selection of Bridge Classes:

This section presents a detailed evaluation of VDOT's bridge inventory data to determine the bridge classes that are susceptible to posting due to special hauling vehicles. Based on the results, three bridge classes are selected for their load distribution behavior using refined analysis. For each of these bridge classes, the database of bridges was further analyzed to select representative bridges for each bridge class in subsequent sections.

Section 4: Selection of Refined Analysis Method:

This section evaluates the effectiveness of two refined analysis methods for modeling girder bridges and slab bridges. It also presents the validation of the selected analysis methods with field testing results provided in literature.

Section 5: Evaluation of Distribution Factors for Concrete T-Beam Bridges:

This section focuses on evaluating load distribution behavior of 25 in-service concrete T-beam bridges through refined method of analysis. The effects of vehicle type and transverse position of vehicles were considered in the analysis. The results were comparatively evaluated with those obtained using AASHTO LRFD equations. A support vector machine (SVM) was used to identify the governing truck type based on geometrical properties of bridges.

Section 6: Evaluation of Distribution Factors for Steel Girder Bridges:

This section evaluates live load distribution factors for 21 in-service steel girder bridges considering the impacts of SHVs and EVs on the load distribution behavior. The results were comparatively evaluated with those obtained using AASHTO LRFD equations. The distribution factor of steel girder bridges with various geometrical parameters were predicted using a series of linear regression models that were built using the data from the numerical simulations.

Section 7: Evaluation of Effective Widths for Concrete Slab Bridges:

In this section, refined analysis method was used to compute effective widths of reinforced concrete slab bridges while accounting for the effects of SHVs. Finite element models of 25 in-service concrete slab bridges in Virginia were developed and then analyzed to determine the effective width for interior and exterior girders under different lane loading conditions. A series of linear regression models built using data from the numerical simulations were used to predict the change in effective width of the bridges with various geometrical parameters.

Section 8: Conclusions and Recommendations

This section discusses the main conclusions and makes recommendations for further research.

2. LITERATURE REVIEW

2.1 Introduction

The analytical expressions to determine the load distribution factors in the AASHTO LRFD Specification were developed as a result of NCHRP 12-26 project (Zokaei, 1991) where extensive parametric studies on straight single span bridges were conducted using finite element analysis. The results from the study were considered as a better representation of load distribution in bridge structures compared to "S-over" equations in AASHTO Standard Specification. However, AASHTO LRFD formulas were developed by making a set of assumptions and therefore have some limitations. For instance, the girder spacing was assumed to be uniformly distributed and all girder characteristics were taken to be the same. It was also assumed that the HS-20 design vehicle governs the distribution behavior. In addition, the effects of some important parameters such as cross-frames, diaphragms, parapets, and deck cracking in load distribution were not considered in the development of these expressions.

Since the development of AASHTO LRFD load distribution expressions, a number of studies have been conducted to investigate load distribution behavior of girder bridges and slab bridges through refined analysis. These studies evaluated the effects of various parameters on the load distribution factors and compared their findings with the AASHTO Standard and LRFD approaches. A representative pool of these studies is reviewed in the following sub-sections for girder bridges and slab bridges. These synthesized studies highlight the current state of practice regarding the application of refined methods of analysis to better describe load sharing behavior, but also emphasize the variability of impact of bridge parameters on these same behaviors.

2.2 Load Distribution Behavior of Girder Bridges

Chung et al. (2006) investigated the influence of cross bracings, parapets and deck cracking on load distribution factors of steel girder bridges. They developed 3D finite element models of 9 in-service bridges in Indiana using ABAQUS. Shell elements were used to model the concrete deck, while the steel girders and bracing elements were modeled using beam elements. The composite action between the girder and deck was modeled by rigid links. The models were loaded with AASHTO HS20 design truck to obtain the live load distributions. The study found that when the load distribution factors are calculated using finite element models that considers lateral

bracings, they decrease by up to 11% compared to those computed using finite element models that include only primary members. A decrease up to 25% was observed when only parapets were considered in the models. When both lateral bracing and parapets were added to the models, the obtained load distribution factors were 17-38% less than those obtained using the models with only primary members. On the other hand, considering longitudinal cracks on the concrete deck increased the load distribution factors by 17% while the transverse cracks did not have a considerable effect on the load distribution behavior.

Harris (2010) comparatively evaluated a number of methods used by researchers to determine load distribution factors for girder bridges. The load distribution factors were computed using an approach based on either load fraction method or beam-line method. The finite element model of a bridge validated through the field-testing results was used to determine member response including strains, deflections, and moments, which were then used to determine load distribution factors using variations of load fraction and beam-line methods. The results demonstrated that both of these methods are effective for determining load distribution factors, but proper selection and use of appropriate member response variables is critical.

Catbas et al. (2012) developed 3D finite element models of 40 RC T-beam bridges and evaluated the load distribution factor by analyzing the moment values under HL-93 design truck loads. The models included 3D solid elements for concrete and frame elements for reinforcing bars. The effects of secondary elements such as diaphragms, parapets, and sidewalks were not considered. The study found interior girder moment demands decrease at least 30% when they are computed through finite element analysis rather than AASHTO LRFD equations. The authors proposed a method to compute the load distribution factors using parameters obtained from a simple dynamic test and measured skew angle. Field testing on four in-service T-beam bridges were conducted to evaluate the load distribution factors through both the proposed approach and the detailed field-calibrated finite element models. The rating factors for these bridges were also computed using AASHTO LRFD approach. The average ratio of the load ratings computed by fully calibrated models to AASHTO load ratings was 3.32, while the average ratio of the load rating estimated by the proposed approach to AASHTO load ratings was 1.40. These outcomes demonstrated the potential benefits derived from the proposed approach, which resulted in

improved rating factors while remaining conservative compared to fully calibrated finite element modeling approach.

Nouri and Ahmedi (2012) assessed the effect of skew angle on the load distribution behavior of continuous two-span steel girder bridges. They performed finite element analysis of 72 bridges with varying parameters under AASHTO HS-20 loading in SAP 2000. The models employed shell elements for concrete deck, beam elements for girders and rigid link elements to connect shell and beam elements for representing the composite action between the deck and girders. The results showed that the moment demands for interior and exterior girders decrease up to 33% when the skew angle varied from 0° to 45°. The shear forces at the pier support decreased for interior girders while it increased for exterior girders with increasing skew angle. The study also concluded that the AASHTO LRFD approach overestimates the moment and shear distribution factors up to 45% when the skew angle is over 20°.

Snyder and Beisswenger (2017) studied shear rating factors for prestressed concrete beams using refined analysis in a project funded by Minnesota DOT. They analyzed 50 prestressed concrete bridges through 2D grillage models and computed the live load distribution factors considering the location-based load distribution of each axle along the span. They found an average of 7% decrease in live load distribution factors. Refined analysis increased load ratings for all of the analyzed bridges by an average of 16%.

Dymond et al. (2019) conducted a parametric study to evaluate the shear distribution factors for prestressed concrete girder bridges without any skew. To create shear distribution estimates for nonskewed prestressed concrete girder bridges, a parametric analysis was carried out utilizing a proven three-dimensional (3D) elastic finite-element modeling (FEM) approach. Additional details regarding the FEM may be found in Dymond et al. (2016). Elastic results from testing a full-scale nonskewed laboratory bridge in the University of Minnesota Theodore V. Galambos Structural Engineering Laboratory were utilized to verify the solid element 3D FEM approach as mentioned by Dymond et al. (2016,2018). One approach of verifying the FEM methodology includes measuring girder shear stresses, which were within10% of the findings predicted by the 3D FEM at multiple sites and for different load situations. According to Dymond et al. (2016), analyzing girder displacements, girder end rotations, and bearing pad displacements were additional ways to validate the FEM approach. The outcomes of this study showed that the ratio

of longitudinal stiffness (girder composite longitudinal moment of inertia divided by cube of span length) to transverse stiffness (transverse deck strip moment of inertia divided by cube of beam spacing) plays an important role in shear distributions. They reported that when the stiffness ratio is less than 1.5, the live load shear demands calculated by refined analysis are lower than those computed by AASHTO LRFD approach, while the refined analysis and AASHTO approximation leads to similar results if the stiffness ratio is between 1.5 and 5.0. On the other hand, the refined analysis produced higher shear demands for bridges with a stiffness ratio greater than 5.0.

2.3   Load Distribution Behavior of Slab Bridges

Amer et al. (1999) conducted a parametric study to assess the influence of span length, bridge width, slab thickness and edge beams on the effective width of solid slab bridges. A basic grid analysis approach was used to model 27 slab bridges with varying parameters. The models were loaded with AASHTO HS20 design truck. They concluded that the span length and edge beams are the main parameters that influence the effective width. The effective widths computed by grillage analysis were always higher than those computed with AASHTO LRFD approach. Three bridges were experimentally tested and the effective width for each bridge was computed based on measured strains. Results indicated that the effective width of these bridges computed by grillage analysis were 14% higher on average than those computed by AASHTO equations, while the effective widths based on field tests were 40% higher on average. This indicates that the grillage method is conservative compared to the actual performance.

Mabsout et al. (2004) studied the load distribution behavior of single span, simply supported reinforced concrete slab bridges through parametric analysis. Finite element analyses of 112 bridges with varying span lengths, number of lanes, slab thickness and edge condition were performed using SAP 2000. The models used shell elements to represent the concrete slab. Various loading conditions were considered using the AASHTO design trucks. The maximum longitudinal moments obtained from the models were compared with those computed through AASHTO Standard and LRFD Specifications. They concluded that the AASHTO LRFD Specification overestimates the bending moments for slab bridges.

Jauregui et al. (2007) investigated the load distribution behavior of an in-service RC continuous slab bridge in a project funded by New Mexico DOT. A finite element model of the bridge was developed in SAP 2000 using shell elements to model the slab. A diagnostic load test

was also conducted to compare the bending moments obtained from the numerical model and those calculated from the measured strain data. The measured response demonstrated that the slab stiffness was consistent with the behavior of cracked and gross sections. Furthermore, bending moments calculated from finite element analysis and those deduced from experimental strain data matched each other quite well (using the average of the cracked and gross section modulus). The outcomes of this study showed that the effective width increases by 26% and 22% for positive moment and 13% and 11% for negative moment for the exterior and interior spans, respectively compared to AASHTO LRFD approach.

Davids et al. (2013) conducted refined analysis of 14 in-service slab bridges maintained by Maine DOT. The analyses were performed using a finite element analysis software, SlabRate developed and validated by the researchers. The software employed quadratic plate elements to model the slab. The finite element analyses resulted in an average of 25.5%, 25.7%, and 26.3% increase in rating factors for the HL-93 truck, HL-93 tandem, and AASHTO notional load, respectively compared to the AASHTO LRFD approach.

Three continuous flat slab bridges with three spans each were subjected to stress tests by Saraf (1998), who also computed rating factors in accordance with AASHTO (1994) and the approximation analysis approach outlined in AASHTO (1992). Based on the field data, Saraf (1998) also calibrated three-dimensional shell finite-element models, which were then utilized to compute rating factors. Field testing in conjunction with calibrated FE models produced rating factors for all structures under all loadings that were higher than those anticipated using the equivalent strip approach, leading Saraf (1998) to draw the conclusion that the equivalent strip method is unduly conservative. Three flat slab bridges were subjected to grillage analysis and field load testing by Amer et al. (1999), who came to the conclusion that the equivalent strip widths calculated in accordance with the LRFD standards and the AASHTO standard were conservative.

2.4 Impacts of SHVs and EVs on Bridge Load Rating

SHVs are defined as single unit trucks that have multiple closely-spaced axles, often with lifting or articulating intermediate axles. SHVs are primarily used in construction, waste management, bulk cargo, and commodities hauling industries. While these truck configurations are designed to comply with the Federal Bridge Formula B, the optimization of SHVs produces heavy 4-, 5-, 6-, and 7-axle loads over a short length. As a result, SHVs can produce bending

moment and shear effects on some bridge spans that are substantially larger than those from standard legal-load rating vehicles used to design and assess the bridges, such as the Type 3, 3-3, 3S2, and other state legal load configurations (Sivakumar 2007).

Emergency vehicles also often generate load effects that are larger than those of typical legal loads and may not meet Federal Bridge Formula B. The FAST Act defined EVs as "any vehicle used under emergency conditions to transport personnel and equipment to support the suppression of fires and mitigation of other hazardous situations" (23 U.S.C. §127(r)(2)). This act amended the allowable weight limits for EVs using the Interstate System and roads "within reasonable access to the Interstate System" (FHWA, 2016). However, if states allow EVs to operate without restrictions on off-Interstate roads, then 23 CFR §650.313(c) requires that bridges along these routes must also be load rated and posted as necessary for EVs. In light of the legislation and regulation, FHWA determined that two vehicle configurations, Type EV2 and Type EV3, generally envelope the load effects of typical emergency vehicles. State departments of transportation (DOTs) can use these configurations in following the methods dictated by the AASHTO Manual for Bridge Evaluation (MBE) (2016), with the exceptions that states can assume only a single EV on a bridge at any given moment and can use a lower live load factor compared to typical rating vehicles. Furthermore, FHWA has instructed that bridges meeting certain RF conditions do not need to be rated for the new EV load types until a re-rating is warranted due to changes in conditions or other loadings.

There have been only a few published studies related to the effects of SHVs and/or EVs on bridge load ratings. Islam (2018) discussed a study where 187 in-service bridges owned by Ohio DOT were load rated by either load factor rating or load and resistance factor rating for both Ohio legal trucks and SHVs. The bridges selected for the study included concrete slab bridges, prestressed concrete I-girder and box-girder bridges, and steel girder bridges. The results showed that almost all of the evaluated bridges that had an RF greater than 1.35 for Ohio legal loads also had an RF greater than 1.00 for SHV loads. Gheitasi and Harris (2015) assessed the effect of oversized 11-axle vehicles and the standard design truck on the DFs by developing numerical models of two steel-girder bridges in the state of Michigan. Nonlinear finite element analysis was used in this study to assess the evolution of load distributing mechanisms in two representative in-service structures subjected to overloads. Furthermore, rating factors for the selected structures

were defined using the load and resistance factor rating methodology. The results indicated that the AASHTO LRFD specifications were generally conservative in predicting the DFs and assessing the safety of in-service structures when irregular loading circumstances were present.

Bae and Olivia (2012) developed numerical models for 118 multi-girder bridges and subjected them to 16 different load cases of overload vehicles. The purpose of this study is to provide modified moment and shear load distribution factor equations for vehicles so that their effects on multi-girder bridges can be quickly determined. In developing the equations, various vehicle configurations, the number of bridge spans, bridge skew angles, and diaphragms were taken into account. The study found that the use of AASHTO LRFD equations can overestimate the load effects of oversized vehicles by as high as 25%.

Mott and Diaz (2010) computed the distribution factors for prestressed concrete box beam under short-haul vehicular loading through refined analysis. This research involves calculating the distribution factors of special vehicles such as a concrete mixer, a solid waste truck, and an aerial fire rescue truck analytically and comparing the results to the distribution factors recommended in the AASHTO LRFD bridge design specifications. The researchers found that AASHTO design loads are conservative compared to three specialized vehicle loading considered in that study.

Hayworth et al. (2008) investigated the influence of various specified trucks, including eight legal trucks for the state of Tennessee on the bridge rating factors. To obtain the LRFR ratings, these rating trucks were used on 16 bridges of Tennessee Department of Transportation. The bridges chosen represented four common bridge types: prestressed I-beam bridges, prestressed box beam bridges, cast-in-place T-beam bridges, and steel I-beam bridges. They found that the load rating of bridges with short spans are more likely to be governed by the state legal trucks.

Stawska et al. (2021) evaluated the load effects due to legally overloaded vehicles such as agricultural vehicles on bridge structures in the state of Montana and proposed a method to account the excessive load effects under these vehicles compared with existing legal rating vehicles in bridge load rating. For bridge evaluation procedures, the Monte Carlo simulation technique is used to determine the optimal live load factors. Under grandfather provisions, the proposed calibration of legally overloaded vehicles leads to conclusions and recommendations for bridge posting practices.

3. SELECTION OF BRIDGE CLASSES

3.1 Introduction

According to the 2017 State of the Structures and Bridges Report by the Virginia Department of Transportation's (VDOT) Structure and Bridge Division (VDOT 2017), there are 21,103 bridges and culverts in the Commonwealth, of which, VDOT maintains 19,456. VDOT inspects more than 10,000 of these structures annually, including bridges that are less than 20 ft long and culverts that have openings that are 36 ft^2 or greater, in order to ensure the safe and secure operation of transportation infrastructure in Virginia, as required by the National Bridge Inspection Program (NBIS). In this study, the bridge database was first evaluated to identify the bridge classes that have the highest number of important bridges with a rating factor less than 1. Then, a total of 71 in service bridges were selected from the Virginia Inventory Database to provide a representative sample of bridges for each bridge class. Virginia Department of Transportation provided bridge plans. Several parameters were extracted from the bridge plans and stored in a database. This information was sufficient to perform a refined analysis of the bridges. The database contained information such as bridge type (T-beam, Steel girder, truss, arch or steel-girder), span length, edge to edge width, skew angle, number of girders, girder depth, slab thickness, overhang, curb to curb width, year built, girder eccentricity (distance from the centroid of the girder to the mid-height of the slab), girder moment of inertia, and girder area.

3.2 Bridge Class Selection

To identify the bridge classes to be evaluated in this study, bridges in the VDOT inventory with rating factors (RF) less than 1.0 for all AASHTO SHVs (SU4, SU5, SU6, and SU7) were first identified. The research team obtained the bridge ratings from two different databases: the state database and the districts database. The ratings in the state database have been updated with the ratings from the districts. Because the focus of this investigation was on highway bridges, railroad bridges, pedestrian bridges, and culverts were excluded from the database. For each bridge, the database included ratings for single, semi, SU4, SU5, SU6, and SU7 trucks. The SU ratings were in tons, and the values were normalized for the SU4, SU5, SU6, and SU7 trucks, respectively. To categorize the bridges, the minimum RF based on the SU truck ratings of each bridge was used. Bridges with an RF of 1.0 were classified based on their structural type and material of construction. Using the VA structure number entry, these bridges were also grouped based on route

importance. The bridges were classified into three types: interstate, primary, and secondary. At the time of this analysis, 19% of the bridges in the databases provided had not been rated for SHVs. These bridges without a rating factor for SU trucks were also classified based on structural type and construction material, with the goal of better understanding their primary make-up in comparison to the bridge with RF 1.0. Then, three bridge classes were chosen for evaluation using refined methods of analysis, taking into account the population of bridges affected by SHV ratings, route importance, and distribution of bridges without SHV ratings. Bridge structural characteristics such as span lengths, number of lanes, and skew were examined for the three bridge classes chosen to obtain representative examples to be modeled and analyzed using refined analysis methods.

After applying filters to focus on only highway bridges, the database obtained from the VDOT contained a total of 11,447 bridges. Among those bridges, 1,808 had a rating factor of less than one. There were 2,208 bridges that did not have a rating factor. Figure 3-1 (a) depicts the distribution of RF< 1.0 bridges based on route importance and RF value. The RF values are divided into four categories: (i) 0.3, (ii) 0.3-0.5, (iii) 0.5-0.7, and (iv) 0.7-1.0. It was observed that 81% of bridges with RF <1.0 are located on secondary routes. For those secondary route bridges, 49% had RFs less than 0.7, while the remaining bridges had RFs between 0.7 and 1.0. The vast majority, 89%, of primary route bridges and all interstate bridges with RFs greater than 0.7. Figure 3-1 (b) depicts the structural type distribution of all bridges with an RF< 1.0. The majority of the bridges were classified as girder bridges (74%), followed by slab bridges (22%).
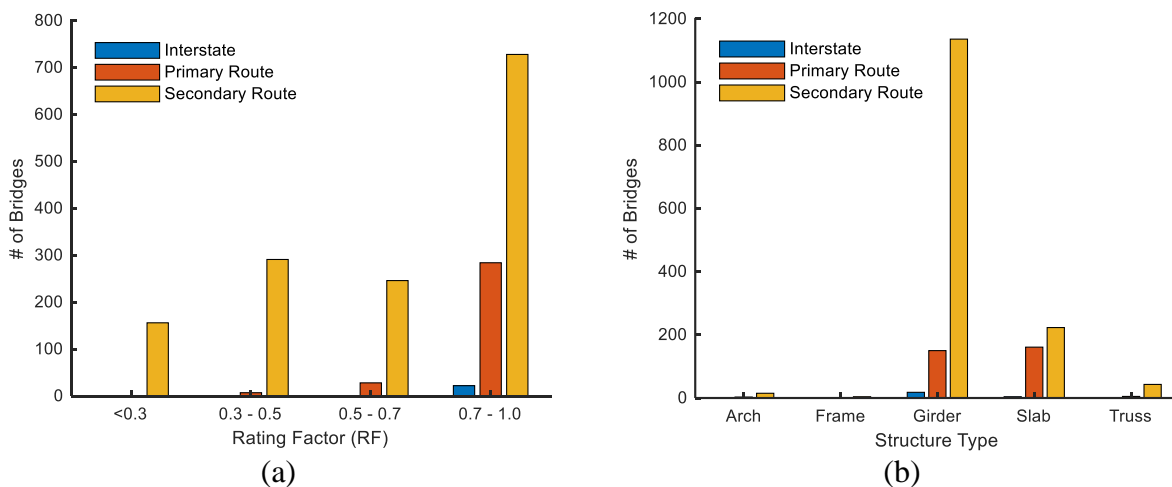
Figure 3-1. Bridges with RF < 1.0 Categorized Based on: (a) rating factor; (b) structure type

Figure 3-2 (a) shows the distribution of slab bridges with a RF < 1.0 based on construction materials and route importance. Almost all of these bridges are concrete slab bridges. There are 4, 161 and 221 concrete bridges with a RF < 1.0 on interstate, primary and secondary routes, respectively. Figure 3-2 (b) shows the distribution of girder bridges with a RF < 1.0 based on construction materials and route importance. Although a large number of these bridges are steel girder bridges with timber (wood) deck, almost all of these bridges are located in secondary routes and were not prioritized for this study. The distribution of concrete and steel girder bridges with concrete decks based on route importance is shown in the inner plot of Figure 3-2 (b). For concrete girder bridges, 50% of the bridges are located on either primary routes or interstates. Similarly, 48% of steel girder bridges are located on either primary routes or interstates.

(a)   (b)
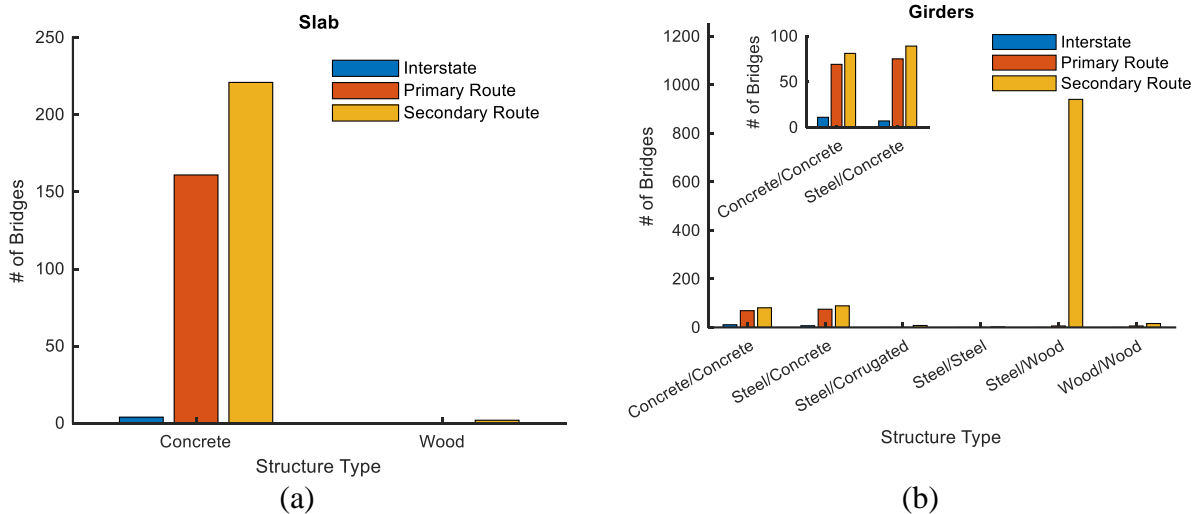
Figure 3-2. Bridges with RF < 1.0 Categorized Based on Construction Material for: (a) slab bridges; (b) girder bridges

Figure 3-3 (a) and (b) show the distribution of concrete and steel girder bridges, respectively with a RF < 1.0 based on superstructure type and route importance. For the concrete girder bridges, 68% of the bridges are reinforced concrete T-beam bridges. The 53% of these T-beam bridges are located on primary routes, while the 45% are on the secondary routes. For steel girder bridges, 69% are simple span girder bridges. About 3% of these simple span steel bridges are located on the interstate routes while the remaining bridges are equally distributed on the primary and secondary routes.

(a)   (b)
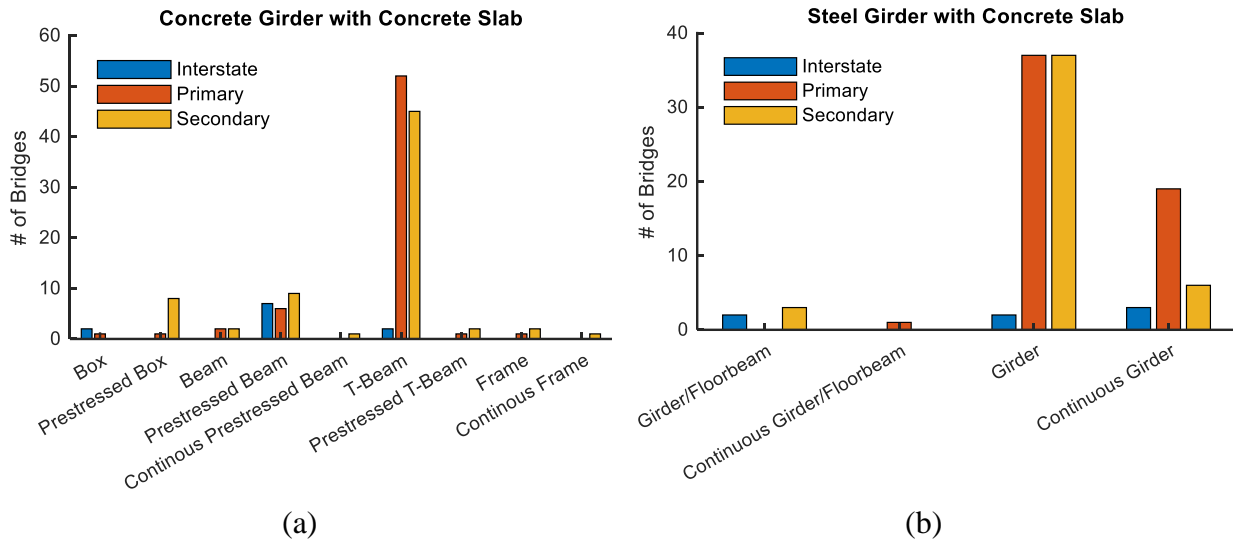
Figure 3-3. Girder Bridges with RF < 1.0 Categorized Based on Superstructure Type: (a) concrete girder bridges; (b) steel girder bridges

Prior to the final selection of bridge types for this study, the distribution of bridges without a rating factor for SHVs was also analyzed. Figure 3-4 illustrates the distribution of bridge types without a rating for SU trucks based on structural type, while Figure 3-5(a) and (b) show the distribution of slab and girder bridges based on construction material. When the bridges with timber deck and/or girder are not considered, it can be seen that concrete slab, concrete girder and steel girder bridges represent the largest share of the population.
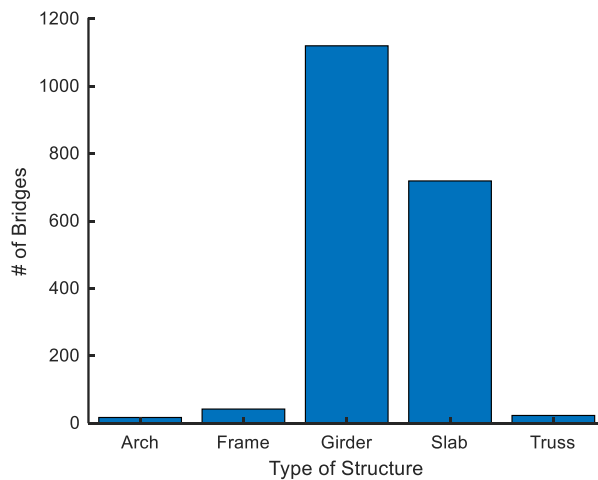
Figure 3-4. Bridges Without a Rating Factor Categorized Based on Structure Type
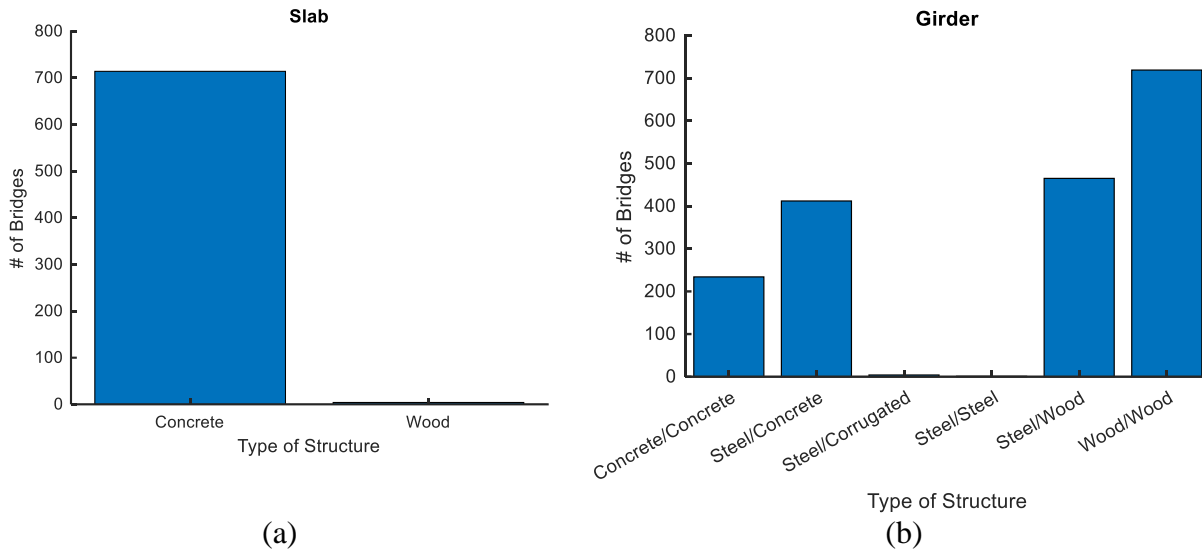
Figure 3-5. Bridges Without a Rating Factor Categorized Based on Construction Material for (a) slab bridges; (b) girder bridges

3.3 Summary

Based on above findings, three bridge classes were selected for the assessment of their load distribution behavior using refined analysis are (1) steel girder bridges, (2) reinforced concrete T-beam bridges slab bridges, and (3) concrete slab bridges. For each of these bridge classes, the database of bridges with a RF < 1.0 was further analyzed to select representative bridges for each bridge class, which will be discussed more in detail in subsequent chapters. The statistics of span length, number of lanes, and skew angle were analyzed for each bridge class. Although it was desirable to initially classify girder bridges also based on girder spacing and slab bridges based on slab thickness, this information was not available in the database.

4. SELECTION OF REFINED ANALYSIS METHOD

4.1 Introduction

In this investigation, a key component in the analysis was the selection and deployment of an appropriate refined method of analysis. These methods of analysis ultimately determine accuracy of the loading and load sharing behavior of the structural system. Considering the computational effort needed to extract the desired response quantities and the complexities in its implementation, a 3D analysis was not explored in this study. Instead, the study focused on the use of 2D methods of analysis that could be efficiently implemented in LARSA 4D (LARSA 4D), VDOT's preferred finite element analysis platform. For the refined analyses of girder bridges, two modeling approaches were evaluated: 1) basic grid analysis, and 2) plate with eccentric beam (PEB) analysis. For the refined analyses of slab bridges, two modeling approaches were evaluated: 1) basic grid analysis, and 2) 2D plate analysis methods. This section provides the description and comparative evaluation of the selected refined methods of analysis.

4.2 Refined Analysis

Depending on the level of refinement, a structural analysis can be described as one-dimensional (1D), two-dimensional (2D) or three-dimensional (3D). The classification of the analysis is not necessarily correlated with the type of elements or geometry considered in the analysis. Following the definitions provided in Adams et al. (2009), an analysis can be described as 1D when the resultant quantities, such as moments, shears, and deflections, are a function of only one spatial dimension. When two or three spatial coordinates are used to describe the results, then the analysis can be described as 2D or 3D analysis, respectively.

A 1D analysis assumes the structure can be modeled using a single series of line elements and with the resultants distributed transversely through empirical equations. This type of analysis cannot explicitly account for geometry and element stiffnesses in the evaluation of load sharing behavior. This 1D analysis approach is the basis of the load sharing behavior (load distribution factors) used for design with the beam line approach within the AASHTO LRFD Bridge Design Specifications (2017). 2D methods of analysis methods are the most commonly used approaches to model slab and slab-on-girder bridges when 1D analysis is not appropriate. For 2D methods, the plane of the deck surface is typically the geometric reference for the analysis with the planar

or line element used to describe the behavior of the bridge system. Using this same approach, a 3D model can effectively be reduced to a 2D analysis (grillage or eccentric beam) while still including the effects of girder eccentricity or transverse components such as cross-frames. 3D methods of analysis require the critical member of the model to be explicitly created, positioned, and connected. For example, in a 3D analysis of a beam-girder bridge, the girder flanges and webs, cross-frames and diaphragms, and bridge deck would be modeled using separate elements.

4.3   Refined Analysis Considered in This Study

4.3.1   Basic Grid (Grillage) Analysis

The basic grid analysis method, which is often also called grillage analysis, involves the modeling of the bridge as a skeletal structure made up of mesh of beams in a single plane. Beam elements are used to model the behavior of the girders in the longitudinal and transverse directions. Properties of the longitudinal grid lines are determined from section properties of the girders and the portion of the slab above them calculated about the centroid of the composite transformed section. Transverse grid lines are added at cross-frame locations and other additional locations with the longitudinal grid to form an idealized mesh. Additional grid patterns can be integrated to allow for refinement of load placement and inclusion of secondary members such as parapets. The basic grid analysis method is simple and easy to implement but has some limitations. This method cannot model physical phenomena such as the shear transfer between girders and deck slab, and warping torsion. These limitations come from the fact that, in grillage analysis, structural members lie in one plane only.

4.3.2   Plate with Eccentric Beam Analysis

The plate with eccentric beam analysis method is an extension of basic grid analysis, where the girders and deck slab are modeled separately. This model is capable of including physical behavior, such as composite action and the eccentricity effect between the slab deck and the girder. Using this modeling approach, it is also possible to capture shear lag effect, which refers to the influence of in-plane shear stiffness on normal stress distribution due to bending. The analysis method utilizes the non-composite section properties of two elements to model composite action by applying the rigid links between the centroid of the girder and the mid-surface of the slab. The girders are modeled using beam elements and the concrete slab deck is modeled as a set of shell elements. By considering at least two shell elements between each line of girders, shear lag effects

can be accounted for. Cross-frames or bracing can be modeled using beam elements that represent the entire cross-frame section.

4.3.3 2D Plate Analysis

The 2D plate analysis method uses a 2D finite element method with plate elements to represent the bridge slab. Plate elements are developed assuming that the thickness of the plate component is small relative to the other two dimensions. The plate is modeled by its middle surface. Each element typically has four corners or nodes. Following general plate theory, plate elements are assumed to have three degrees of freedom at each node; translation perpendicular to the plate and rotations about two perpendicular axes in the plane of the plate. The typical output includes the moments (usually given as moment per unit width of the face of the elements) and the shear in the plate. This form of output is convenient because the moments may be directly used to analyze load sharing behavior within the deck. The main disadvantage of plate elements is that they do not account for the forces in the plane of the plate, resulting in the in-plane stiffness being ignored in the analysis.

4.4 Modeling Validation

The performance of these methods was evaluated by considering important aspects such as the efficiency of model development, accuracy of the results, detail required, and computational effort needed. While computational models are gaining traction as a common tool in structural analysis, validation of modeling approach is still necessary to create confidence in the derived results. To achieve this confidence, the three refined analysis approaches used in this study were validated using the experimental results provided in the literature from the field testing of in-service bridge structures.

The structures analyzed included one steel girder bridge, one reinforced concrete T-beam bridge, and one reinforced concrete slab bridge. All models developed in the validation were created using LARSA 4D, based on the geometric details and loading patterns prescribed in the literature. A comprehensive description of the model development is not presented in this report, but details of the bridge geometries and loading patterns can be found in the original references (Harris et al, 2020, Eom and Nowak, 2001). For the model validation study, the primary objective was to reasonably represent the behavior described in the experiments with the models developed in this study without model tuning or calibration for uncertainties surrounding boundary condition,

constitutive properties, or condition state. Therefore, the models were expected to follow behavior characteristics, but were not expected to match results exactly.

4.4.1 Reinforced Concrete T-beam Bridge

The Flat Creek Bridge carried Route 632 over Flat Creek located in Amelia County, VA. There were five simple spans, each 42.5 ft long, for a total length of 212 ft with no skew. Each span was 24 ft wide and consisted of four longitudinal T-beams. Each exterior T-beam had a vertical stem with a width of 14 in and a depth of 32 in. Each interior T-beam had a vertical rectangular stem with a width of 16 in and a depth of 32 in, and a wide top flange of 7.5 in thick. The wide top flange was the transversely reinforced deck slab (Harris et al., 2020). The strain results of the field load tests were used to verify the refined analysis models. Results for the comparison are illustrated in Figure 4-1. The eccentric beam and grillage models agreed not only in behavior characteristics, but also magnitude of derived response with respect to experimental data. For the same structures, the grillage approach exhibited less agreement with respect to magnitude with apparent higher distributions within the system.
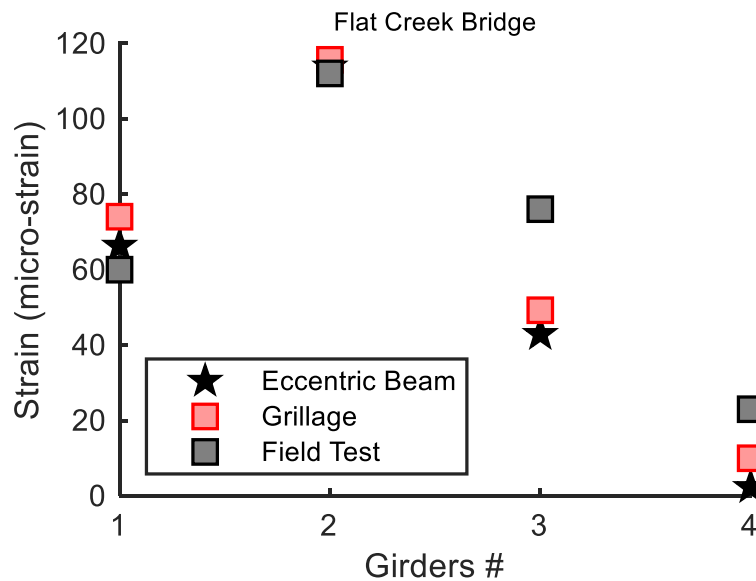
Figure 4-1 Model Validation for RC T-beam Bridge (Flat Creek Bridge)

4.4.2 Steel Girder Bridge

The steel girder bridge selected for validation was located on Stanley Road over I-75 (S11-25032) in Flint, Michigan. The structure consisted of a three-span structure with simple supports and a total length of 285 ft. An 8-in reinforced concrete deck was supported by seven steel plate

girders with a transverse spacing of 7.25 ft. The bridge was part of a comprehensive load testing program conducted by Nowak and Eom (2001) in collaboration with the Michigan DOT. Only the second span of the structure was chosen for validation in this study. This span was 135 ft long with a clear span of 126 ft between pin and hanger connections. The loads applied to the model came from the Nowak and Eom study and were representative of the 11-axle design trucks common to the state of Michigan. For simplicity, only the scenarios of pin–roller and pin–pin were analyzed, with no attempt to calibrate the rotational restraint of the supports, a procedure that was employed by Eom and Nowak (2001). This approach was adopted since the intent of the investigation was to evaluate performance of different methods for determining lateral load distribution rather than an exercise in model calibration. Strain measurement results from this study and a validation study by Harris (2010) were used for model validation.

For the S11 bridge, in addition to field test results of the Eom and Nowak (2001) study, numerical results for the pin–roller scenario provided in the same study was also compared with the modelling approaches (grillage and eccentric beam) in the current study, without any attempt to calibrate the rotational restraint of the supports. This approach was adopted since the intent of the investigation was to judge performance of various methods for determining lateral load distribution instead of an exercise in model calibration.

Figure 4-2 compares the results obtained in this study and those provided in the literature. For this bridge, the grillage and eccentric beam formulations aligned better, but exhibited a departure from the experimental data. This departure is attributed to the effects of boundary conditions, which were shown from the Eom and Nowak (2001) study to exhibit a higher level of restraints than idealized models, thus resulting in lower (that is, more conservative) strain values than the idealized simple support models. Note that the results obtained from grillage and eccentric beam models of the current study aligned well with the numerical results obtained in Eom and Nowak (2001) study, where a pin-roller support assumption was also made.
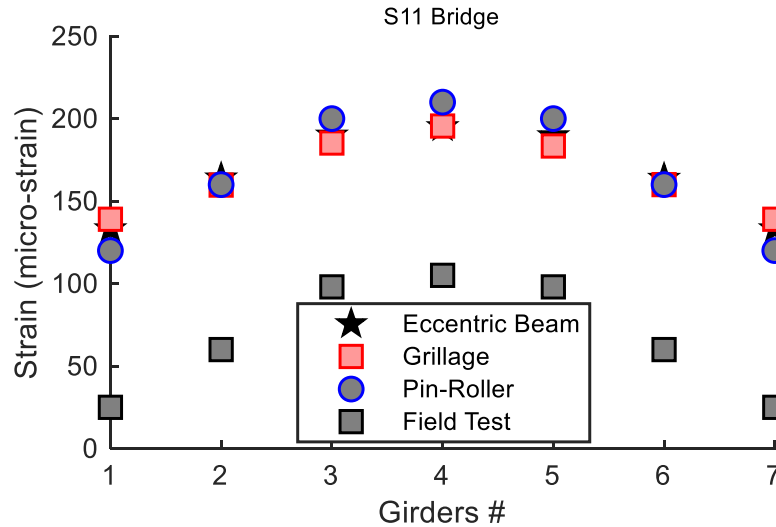
Figure 4-2 Model Validation for Steel Girder Bridge (S11 Bridge)

4.4.3 Reinforced Concrete Slab Bridge

The Smacks Creek Bridge carried Route 628 over Smacks Creek in Amelia County, VA. The superstructure comprised of two 32-ft long, simply supported reinforced concrete slabs that were 21 inches thick and had a 15° skew. The deck had 12-in diameter voids oriented in the direction of traffic, spaced 18 inches apart (Harris et al., 2020). The strain results of the field load tests were used to verify the finite element models shown in Figure 4-3.

When comparing the results, the model is clearly able to describe the behavior characteristics with corresponding relative responses within the system. The 2D plate formulations agrees not only in behavior characteristics, but also magnitude of derived response with respect to experimental data. For the same structures, the grillage approach exhibits less agreement with respect to magnitude with apparent higher distributions within the system. Based on the results derived from this validation and other loading scenarios, the modeling approach was deemed suitable for continued study. While both sets of approaches (2D plate/grillage) proved effective, the 2D plate analysis approach provided an additional benefit due to model development efficiency within the LARSA 4D software package. Note that, for the eccentric beam analysis, LARSA 4D allows generating models automatically with little effort using built-in templates that can also be modified using spreadsheets. On the other hand, the grillage analysis in LARSA 4D requires additional efforts for the placement of grid lines and the calculations of some sectional properties

such as bending and torsional inertias. Therefore, the 2D plate analysis approach was then used for the remainder of the study.
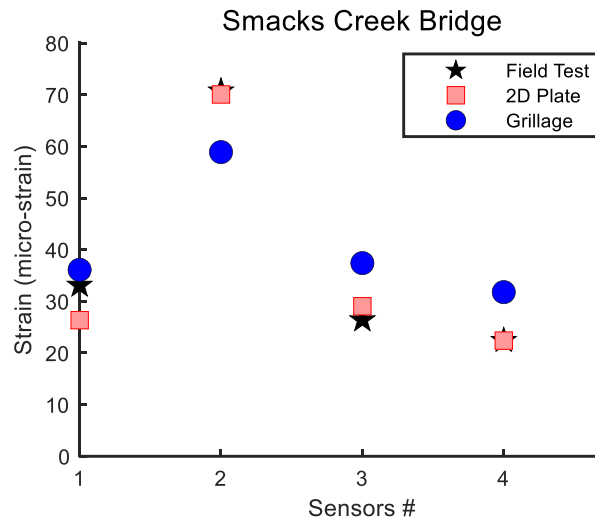
Figure 4-3. Model Validation for Concrete Slab Bridge (Smack Creek Bridge)

4.5   Summary

Based on the results derived from these validations and other loading scenarios, the modeling approaches were both deemed suitable for continued study. While both sets of approaches (eccentric beam/grillage and 2D plate/grillage) proved effective, the eccentric beam and 2D plate analysis approaches provided an additional benefit due to model development efficiency within the LARSA 4D software package. Note that, for the eccentric beam analysis, LARSA 4D allows generating models automatically with little effort using built-in templates that can also be modified using spreadsheets. On the other hand, the grillage analysis in LARSA 4D requires additional efforts for the placement of grid lines and the calculations of some sectional properties, such as bending and torsional inertias. Therefore, the eccentric beam and 2D plate analysis approaches were used for the remainder of the study.

5. EVALUATION OF DISTRIBUTION FACTORS FOR CONCRETE T-BEAM BRIDGES

5.1 Introduction

The objective of this chapter is to leverage the potential improvements in describing load distribution using refined methods of analysis to improve rating factors of concrete T-beam bridges that represent 7% of the total bridges and 23% of the girder type bridges in the state of Virginia. To this end, a total of 25 in-service reinforced concrete T-beam bridges was selected and modeled using a common structural analysis software. The distribution factors for each bridge were evaluated for interior and exterior girders under one lane and two lane loaded cases. The effects of SHVs and the transverse positioning of the truck load on the computation of the distribution factors were also investigated. A statistical machine learning technique was used to evaluate the truck type that governs the distribution factor calculation based on span length and girder spacing of a given bridge. The percent changes in distribution factors derived from the refined analyses of 25 bridges were used to develop multi-parameter linear regression models. Finally, the effects of bridge geometric parameters on the percent changes in distribution factors were assessed.

5.2 Bridge Selection

State DOTs are required to post the weight limits for bridges with a rating factor of less than 1.0 based on the weights of SHVs (Lawson et al. 2018). Therefore, an accurate assessment could potentially improve the rating factors of bridges and prevent posting of critical bridges on interstate and primary routes. Reinforced concrete T-beam bridges, representing 23% of the girder type bridges in the state of Virginia, are the focus of this study. The statistical distributions of T-Beam bridges within the Virginia DOT (VDOT) inventory based on the span length, deck width and skew angle are shown in Figure 5-1. A total of 25 in-service T-beam bridges whose characteristics are also shown in Figure 5-1 were selected for this study. Besides considering the overall inventory characteristics, the bridges located on interstate and primary routes were given a priority in the bridge selection process because they are subjected to high traffic volumes. Furthermore, the bridges with a rating factor between 0.7 and 1.0 were chosen to explore the potential of increasing the rating factor above 1.0 to avoid load posting for these bridges through the computation of a refined distribution factor. Table 5-1 provides the geometrical properties of the selected bridges.
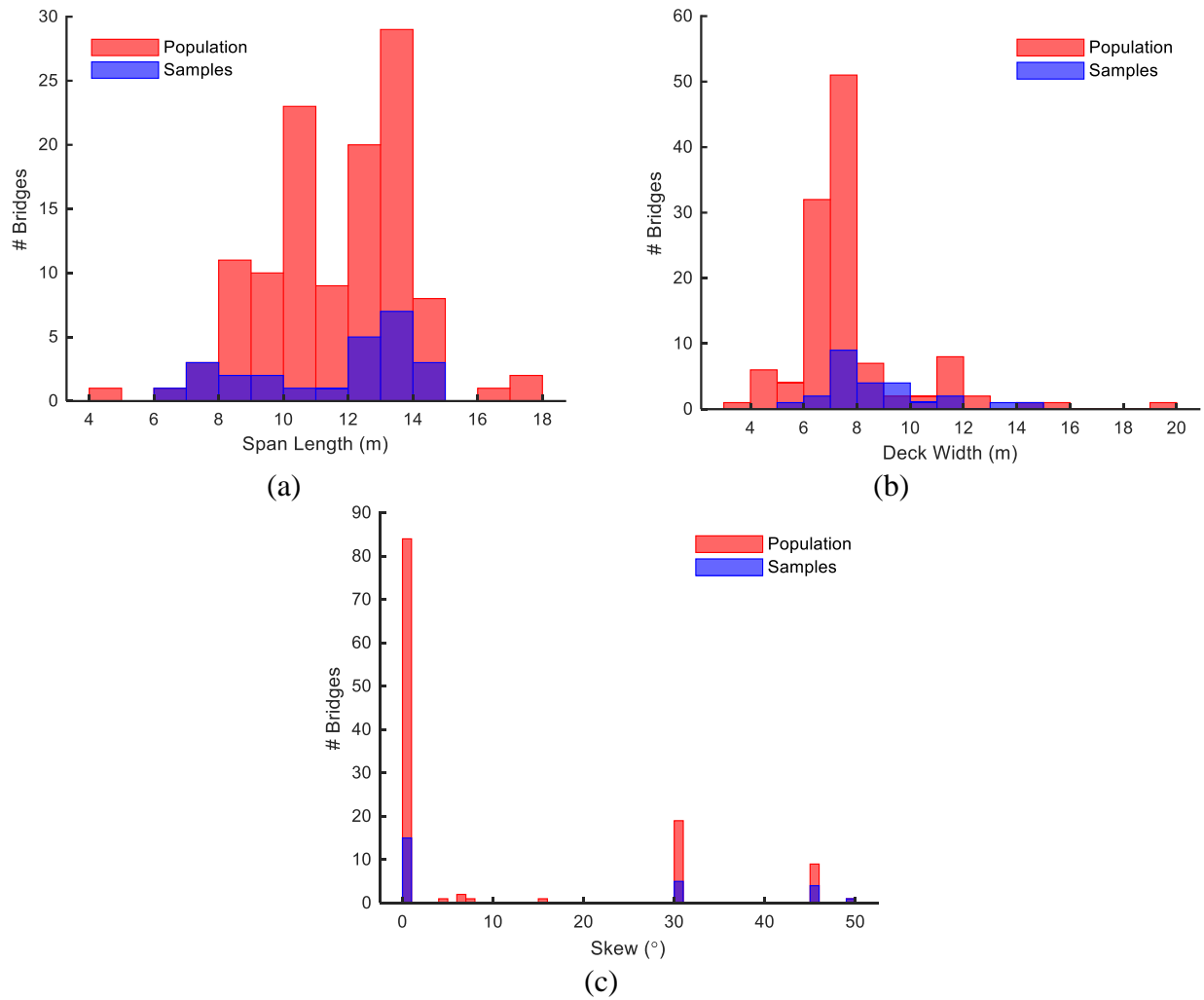
Figure 5-1. T-Beam bridge population in terms of: (a) span length, (b) deck width, and (c) skew

Table 5-1. Reinforced concrete T-beam bridges selected for refined analysis

No	Route	Span Length (m)	Girder Spacing (m)	Overall Section Depth (cm)	Skew Angle (degrees)	Deck Width (m)	Lanes
1	Primary	8.50	1.83	63.50	30	8.29	2
2	Primary	10.39	2.93	90.42	30	9.45	2
3	Primary	14.60	2.41	71.12	50	7.96	2
4	Secondary	7.01	1.83	71.12	0	7.86	2
5	Secondary	12.28	2.19	93.98	0	7.77	2
6	Primary	12.19	1.83	92.20	0	11.22	2
7	Secondary	12.19	2.74	92.46	0	6.22	2
8	Secondary	12.19	2.19	99.06	0	8.50	2
9	Primary	13.41	2.19	99.06	45	9.17	2
10	Primary	13.41	2.19	99.06	45	7.99	2
11	Primary	9.81	3.05	78.99	0	7.74	2
12	Secondary	13.41	2.44	91.19	0	5.82	2
13	Primary	9.75	2.74	79.76	0	6.86	2
14	Primary	8.53	2.19	81.28	30	7.35	2
15	Primary	7.92	1.83	63.50	30	8.63	2
16	Primary	13.11	2.35	114.30	30	7.25	2
17	Primary	7.59	1.55	81.53	0	7.25	4
18	Primary	11.13	2.38	84.58	0	9.54	2
19	Primary	13.99	2.32	100.58	45	8.26	2
20	Primary	14.60	1.98	102.87	0	10.52	2
21	Secondary	6.86	1.74	73.66	0	11.70	2
22	Primary	12.95	2.19	68.07	0	7.92	2
23	Primary	13.11	2.32	106.43	45	9.39	2
24	Primary	13.62	2.38	109.22	0	14.42	2
25	Secondary	14.66	2.44	100.58	0	13.50	2

5.3 Numerical Models and Distribution Factors

5.3.1 Development of Finite Element Models

Finite element models for the selected 25 bridges were developed and validated to obtain the moment and shear effects under different truck loadings. The loadings considered in the analysis include design truck (HS-20), design tandem, and single-unit trucks (SUs) shown in Figure 5-2. The numerical models were developed using LARSA 4D to investigate the effect of the trucks on the distribution factors of the selected bridges subjected to one-lane and two-lanes loading schemes.
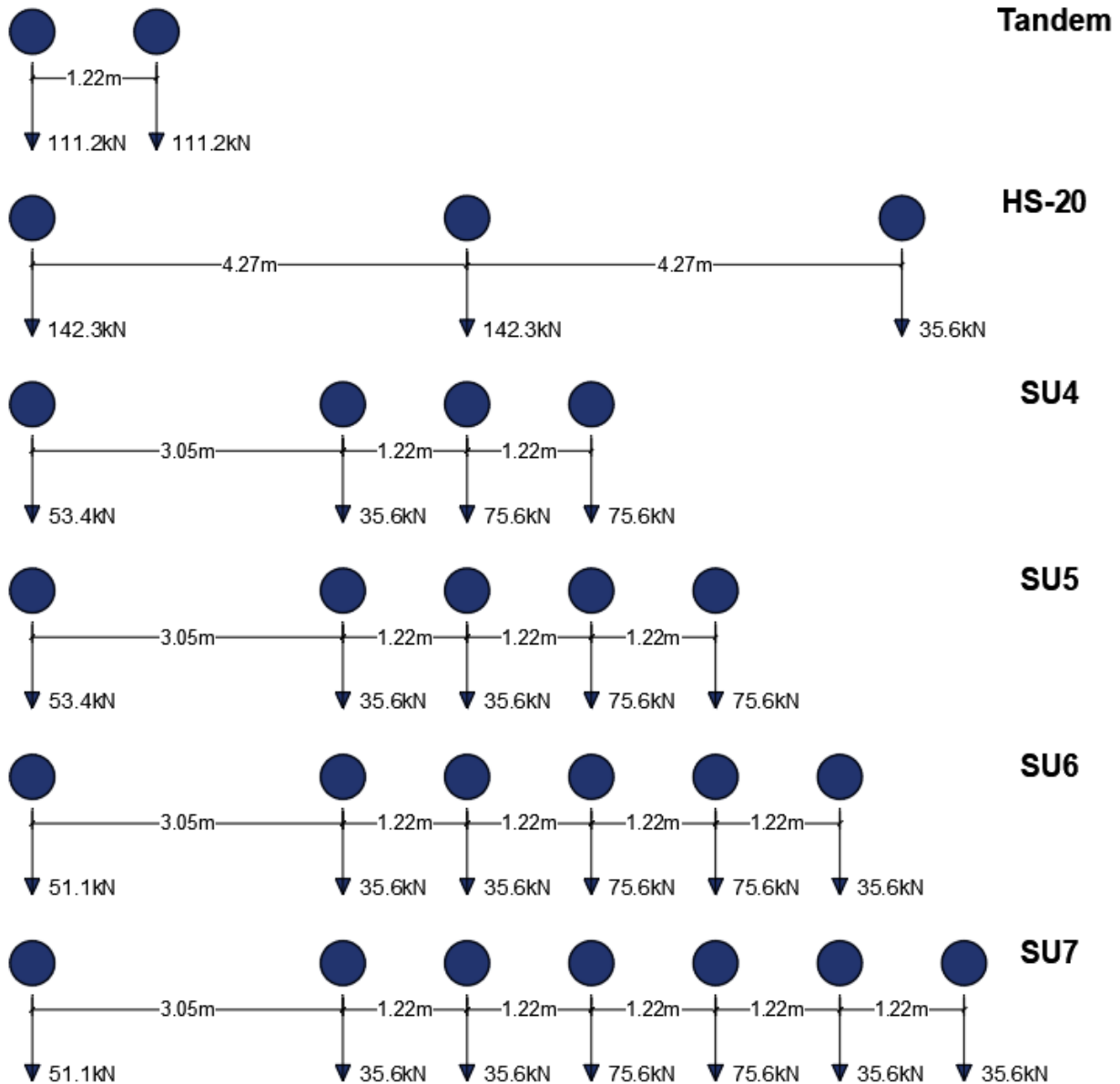
Figure 5-2. Axle loads for design tandem and HS-20, SU4, SU5, SU6, and SU7 trucks

The two-dimensional (2D) numerical models were developed using the plate with eccentric beam approach (Adams et al. 2019). The depth of the bridge was accounted for by locating the deck slab and longitudinal beams at their respective centroids such that the girders were eccentric to the deck plate. Beam elements were used to connect the longitudinal elements transversely at cross frame/diaphragm locations when applicable. Plate elements were used to model the concrete deck over the entire length. All bridges were modeled as simply supported structures with pin-roller boundary conditions. Figure 5-3 illustrates a typical numerical model for T-beam bridges.
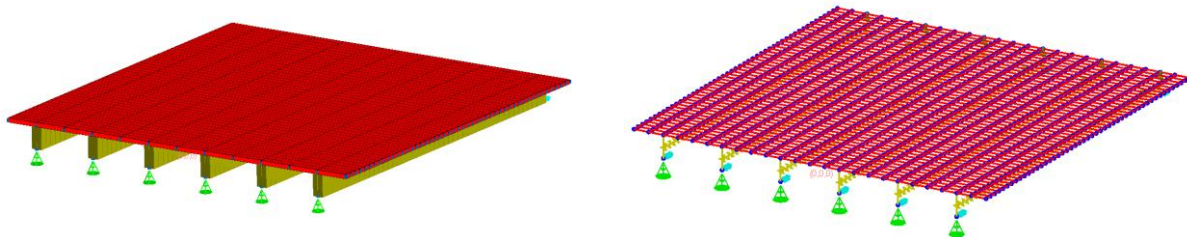
Figure 5-3. Finite element model of typical T-beam bridge

5.3.2 Computation of Distribution Factors

For each vehicle, the wheel loads were modeled as concentrated loads and applied to the nearest nodal coordinate. The loads were positioned longitudinally on the bridge using the influence line approach to generate a maximum response in moment and shear. The transverse position of the load was determined through an iterative approach by systematically moving the loading transversely across the bridge. Numerical simulations of each bridge were conducted under one and two-lane loaded conditions and the load effects and corresponding distribution factors for each case were computed.

The load effects, including shear and moments, were obtained from refined analysis and were used to compute the live load distribution factor, *g*. In particular, the load fraction analysis approach was employed to compute the distribution factors for both moment and shear of each girder of the composite sections (Harris 2010). This method is based on Equation (5-1) shown below, in which $R_{max,j}$ represents the maximum moment or shear of the *jth* girder, N_{trucks} refers to the number of trucks or lanes, and *m* is the multiple presence factor, which is taken as 1.2 and 1.0, respectively, for one lane and two lanes are loaded as specified in the AASHTO (Eom and Nowak 2001; Conner and Huo 2006):

$$g = \frac{R_{max,j}}{\sum_{j=1}^{\#girders} R_{max,j}} \cdot N_{trucks} \cdot m \qquad (5\text{-}1)$$

5.4 Evaluation of Results

5.4.1 Effects of Loading Truck Type

To assess the effect of vehicle type used in the refined analysis on the distribution factors, the distributions factors were obtained for each T-beam bridge under different vehicle loadings and then normalized by the distribution factor obtained under tandem loading. Figure 5-4 and Figure

5-5 illustrate the normalized distribution factors obtained for the moment and shear effects, respectively for the interior and exterior girders under one and two lanes loading conditions. The results are shown for each individual bridge with a solid red circle, while a bar plot illustrate the average of the results obtained from all bridges. It can be seen from Figure 5-4 that the moment effects for the interior girders attains their maximum value for the tandem loading, i.e., producing a normalized distribution factor less than 1.0 for the most bridges. In particular, there is only one bridge for the one lane loaded case where the SU4 truck produced a higher distribution factor. Only for three bridges the moment distribution factor for interior girders are higher than that obtained under tandem loading by 5% or more. The HS-20 truck governs the distribution factor in these cases.

On the other hand, the governing truck for the exterior girder moment effects exhibits more variation for the considered bridges. However, the variations in the distribution factors computed under different trucks are mostly not that significant. For one lane loaded case, only seven bridges have a distribution factor that is 5% or more under other trucks compared to the tandem loading. For these seven bridges, the maximum increase in the distribution factor is 14% when another truck is considered in the analysis rather than tandem loading. Similar results are also observed for two lanes loaded case. However, larger increases in the distribution factor are present for two lanes loading case compared to one lane loading case. An increase more than 30% in the moment distribution factor is observed for four bridges when trucks other than tandem loading are used for the computation of the distribution factor.

Similar trends related to the effects of truck type on the distribution factor are observed for the shear effects. In particular, the maximum shear effects in interior girders are mostly observed for the tandem loading in both one lane and two lanes loading cases and the other trucks are not found to be critical for interior girders. On the other hand, for the exterior girders, other truck loadings produce significant increases in distribution factors compared to the tandem loading. For one lane loaded case, 11 bridges are governed by other trucks with a maximum increase in distribution factor of 119% produced by SU5. Similarly, in the case of two lane loaded case for exterior girders, 16 bridges governed by other trucks with a maximum increase of 100% in distribution factor observed for SU7 truck.
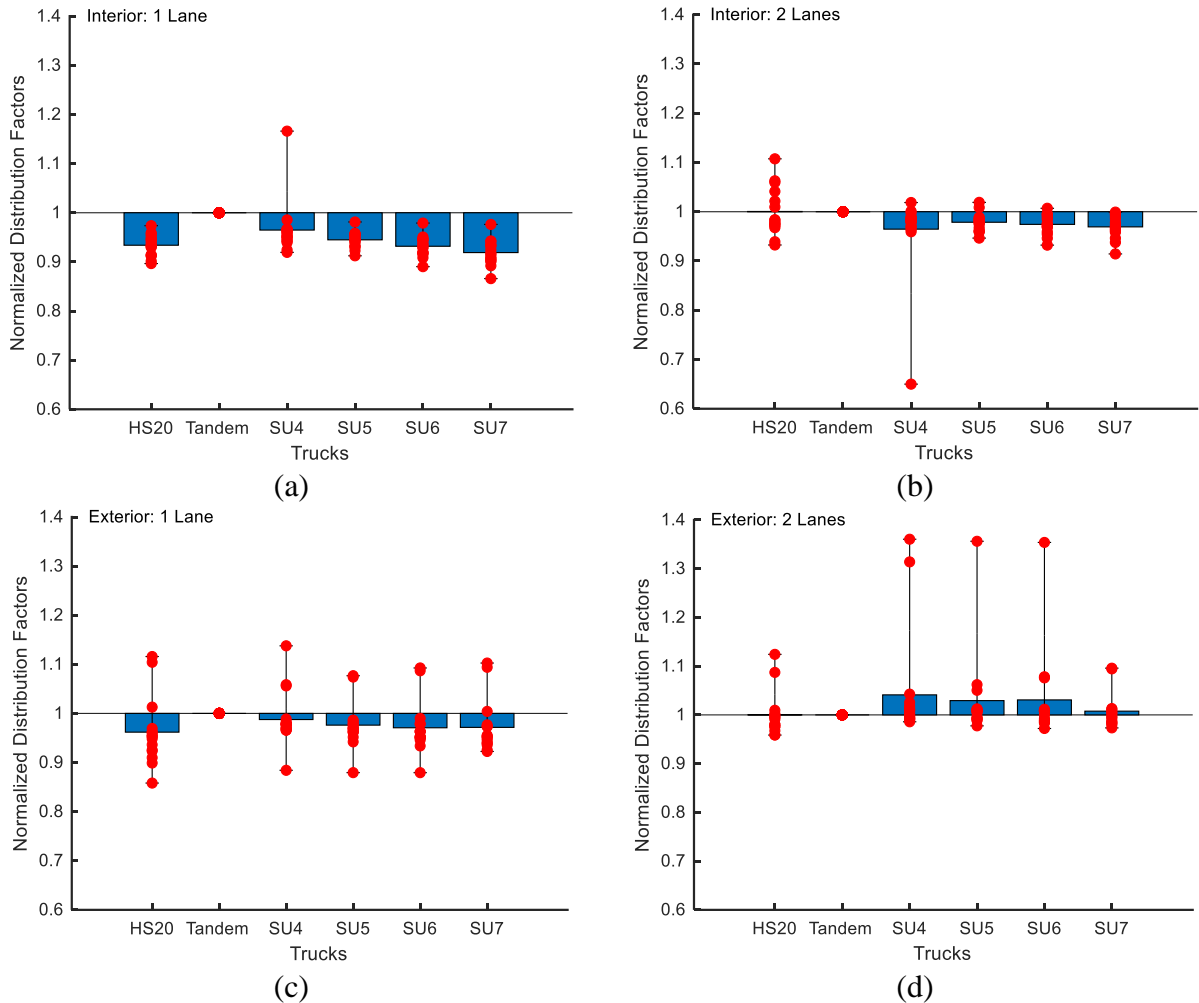
Figure 5-4. Normalized moment distribution factors for: (a) interior girder one lane, (b) interior girder two lanes, (c) exterior girder one lane, (d) exterior girder two lanes loaded cases.
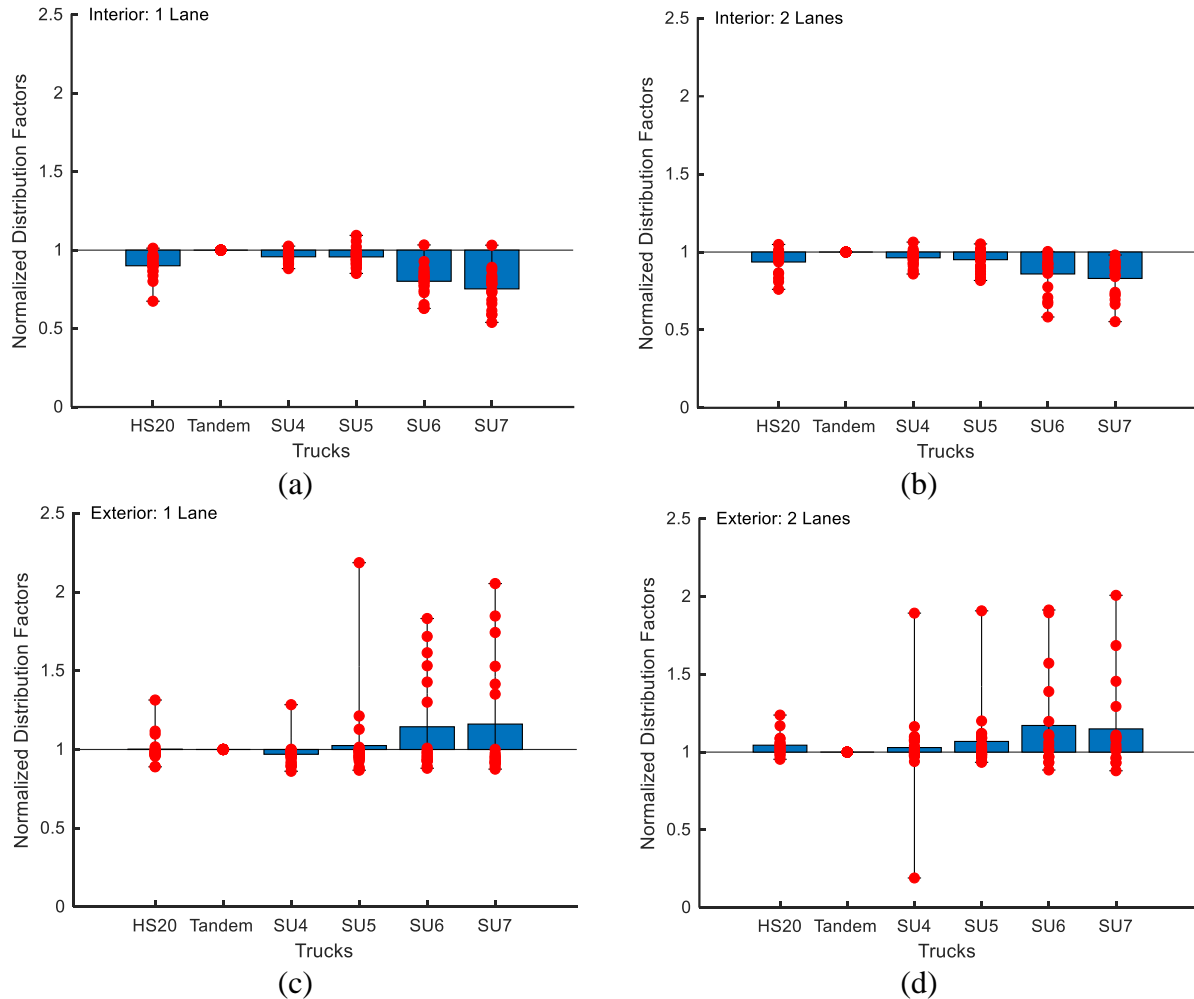
Figure 5-5. Normalized shear distribution factors for: (a) interior girder one lane, (b) interior girder two lanes, (c) exterior girder one lane, (d) exterior girder two lanes loaded cases.

5.4.2 Classifying Governing Truck Based on Bridge Geometry

To identify the critical truck type that would result in a maximum distribution factor for exterior and interior girders based on span length and girder spacing of a given bridge, a multi class support vector machine (SVM) analysis was applied. SVM is a statistical analysis method that is used to group observations and generate heat maps to predict future observations. The span length and girder spacing were selected as two parameters for the classification since they typically have the highest effect on the distribution factors. However, a standard support vector machine is designed only for binary classification problems. To solve a multi-classification problem, SVM must decompose the problem into several binary problems (Angulo et al. 2003). This approach can accommodate any number of groups or classes embedded in a dataset. This method has

advantages in solving high-dimensional pattern recognition, and nonlinear and small sample events.

Using built-in commands in statistical analysis software "R" (R Development Core Team 2005), the distribution factor results obtained from finite element analyses with the respective applied loads were used to develop a categorizing model that had a 90% accuracy. In the development of the categorization model, 80% of the observations were used for training the model, while the remaining 20% of the observations were used for testing the model and validating its accuracy.

Figure 5-6 shows the simulation results on the multi-classification of the governing truck type for moment distribution factors. In these plots, the "x" marks represent support vectors, or points that directly impact the classification line, while the marks "o" denote the points that do not impact the computation of classification line (i.e., lines or hyperplanes between the different classes). For the moment distribution factors of interior girders subjected to one-lane loading, the bridges with a span length from 13 m to 14.6 m and a girder spacing from 1.6 m to 2.2 m are governed by the SU4 vehicle as shown in Figure 5-6(a). The SU4 also governs bridges with a span length from 10 m to 12 m and a girder spacing from 2.8 m to 3.0 m. For bridges that are outside of that range, tandem loading poses the critical effect. For the moment distribution factors of interior girders subjected to two lanes, either HS 20 or tandem loading governs as shown in Figure 5-6(b).

The moment distribution factors of exterior girders subjected to one lane loading are mostly governed by tandem or HS20 truck as can be seen from Figure 5-6(c). Only for a small region limited by a span length from 10 m to 12 m and a girder spacing from 2.8 m to 3.0 m, the SU4 governed the case. Figure 5-6(d) shows that four truck types dominated the moment distribution factors of exterior girders subjected to two-lanes loadings. The bridges with a span length of 10 m to 14 m and a girder spacing from 1.6 m to 2.2 m were governed by the SU7 truck, while the HS 20 governed bridges with a span length from 9.0 m to 12.0 m and a girder spacing from 2.2 m to 2.6 m. Likewise, the moment distribution factors of exterior girders for bridges with a span length between 10.0 m and 14.7 m and a girder spacing between 2.6 m and 3.0 m were controlled by the SU4. The SU4 also governed bridges with a span length from 14 m to 15 m and a girder spacing from 2.2 m to 3.0 m. In other words, the bridges with longer span lengths were governed by the SUs trucks for the exterior girders subjected to two-lanes loadings.
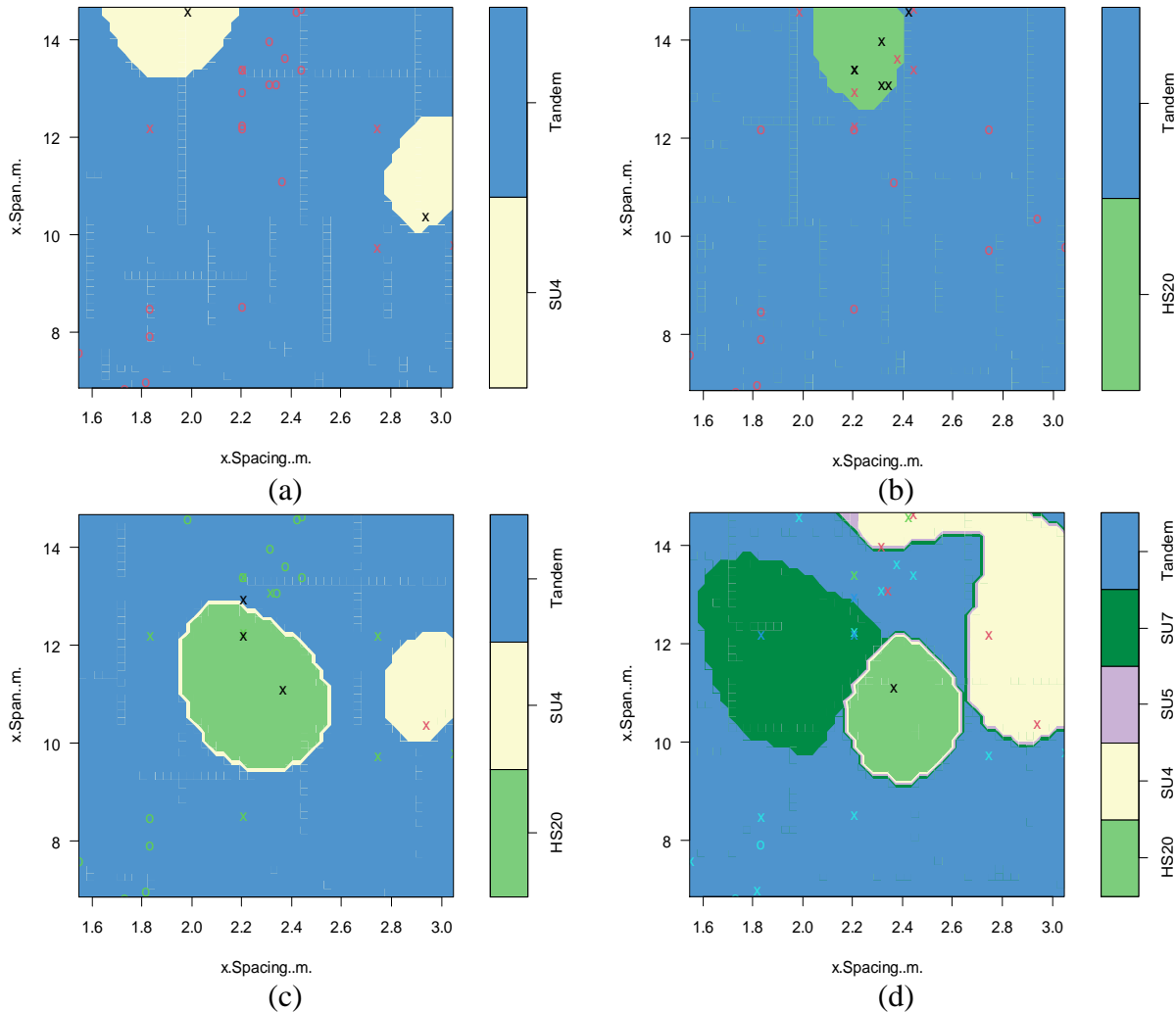
Figure 5-6. Governing truck types for moment distribution factor based on T-Beam bridge geometry for: (a) interior girder one lane, (b) interior girder two lanes, (c) exterior girder one lane, (d) exterior girder two lanes loaded cases.

Figure 5-7 8 illustrates the simulation results on the multi-classification of the governing truck type for shear distribution factors. For the shear distribution factors of interior girders subjected to one-lane loading, the bridges with a span length from 7 m to 7.5 m and a girder spacing from 1.8 m to 2.2 m were governed by the SU4 vehicle as shown in Figure 5-7(a). The results from SU4 and SU6 were also plotted even though they have a negligible impact. For bridges that were outside of that range, tandem loading posed the critical effect. For the shear distribution factors of interior girders subjected to two-lanes loading, tandem loading mostly governed as shown in Figure 5-7(b). Only for small region of a span length between 7.0 m and 10.0 m and a girder spacing between 2.8 m and 3.0 m, the SU5 governed.

The shear distribution factors of exterior girders subjected to one-lane loading were governed by the tandem truck for about half of the region, while the SU trucks governed much of the rest of the cases, as can be seen from Figure 5-7(c The SU5 governed two regions; one is bound by a span length of 7 and 8 m and a girder spacing from 1.7 m to 2.3 m and another one is bound by a span length of 13.0 m to 14.7 m associated with a girder spacing from 1.6 m to 2.2 m. The SU7 governed the region of span length of 13 m to 14.7 m and a girder spacing of 2.0 to 2.4 m. Also, the SU4 governed the region of span length of 7.5 m to 11 m and a girder spacing of 2.5 m to 2.9 m. In addition, the SU6 governed the small region limited by a span length between 9 m and 12 m and a girder spacing between 2.8 m and 3.0 m. In other words, for bridges with a relatively shorter span lengths, the SU trucks governed when the girder spacing is large. For bridges with a relatively longer and shorter span lengths, the SU trucks governed for smaller girder spacings. Figure 5-7(d) shows that SU trucks dominated the shear distribution factors of exterior girders subjected to two-lanes loadings. For bridges with short span lengths with a spacing of 1.6 m to 2.4 m, the SU trucks governed the case, as well as for girders with a spacing of 2.5 m or higher. For bridges with a relatively longer span lengths, the SUs truck governed for girder spacing between 1.8 m to 2.5 m.
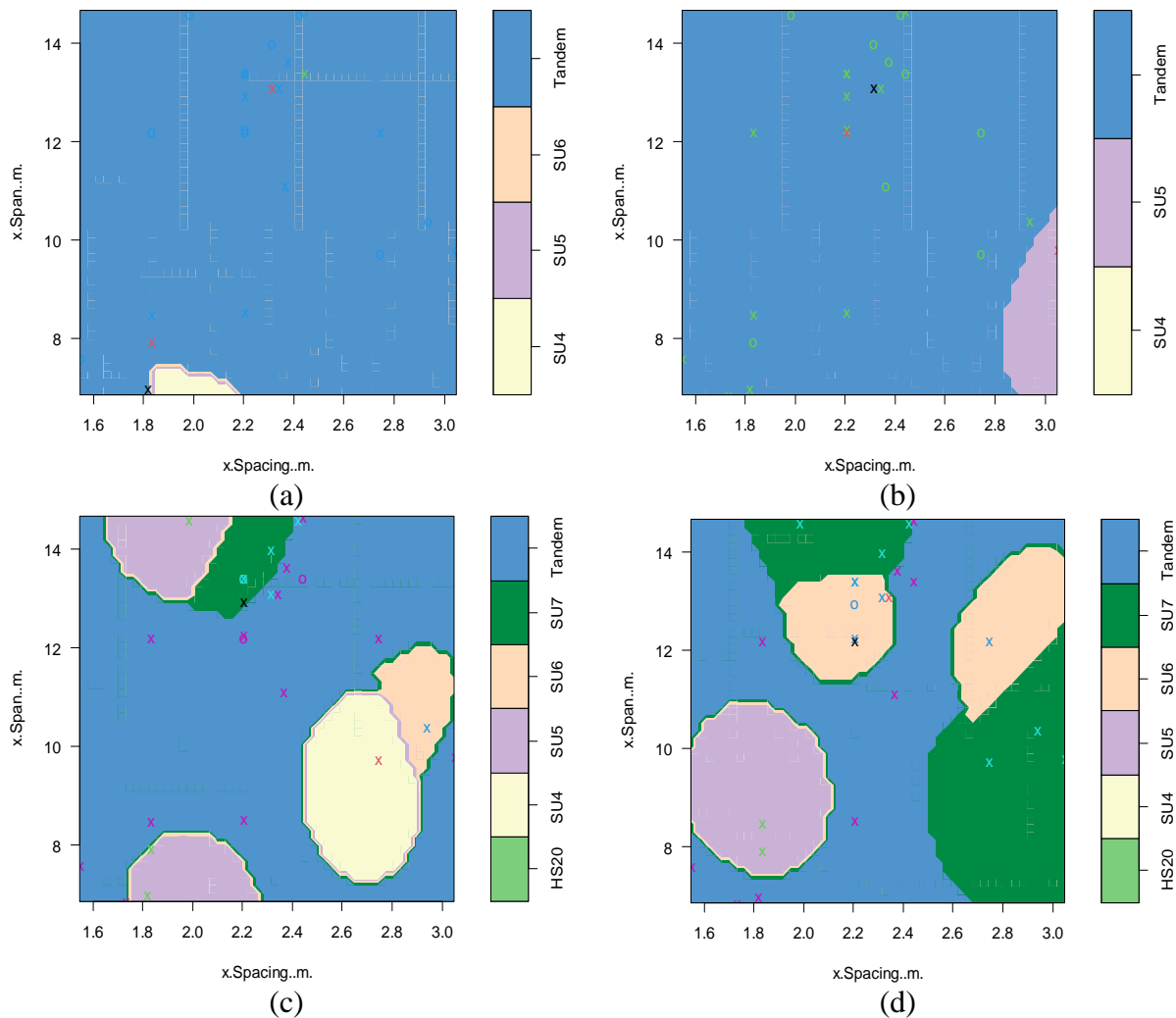
Figure 5-7. Governing truck types for shear distribution factor based on T-Beam bridge geometry for: (a) interior girder one lane, (b) interior girder two lanes, (c) exterior girder one lane, (d) exterior girder two lanes loaded cases.

Overall, for interior girders under one lane or two lanes loaded cases, design truck or tandem governs the moment and shear distribution factors for most of the T-beam bridges analyzed in this study. However, for exterior girders, especially under two lane loaded case, the SHVs also governs the moment and shear distribution factors for bridges with different span length and girder spacings.

5.4.3 *Effect of Transverse Load Positioning*

To investigate the effect of the transverse trucks position on the distribution factors of moment and shear for T-beam bridges, the trucks were placed at three distinctive transverse positions that would potentially maximize the applied moments and shear for interior and exterior girders. These three positions, also shown in Figure 5-8, are: (i) Side: the first wheel is placed at 0.61 m (2 ft) from the parapet, (ii) Quarter: the truck center is positioned at quarter of the clear width of the bridge, and (iii) Middle: the truck center is positioned at half of the width of the bridge. To evaluate the effects of different trucks on the governing transverse load position, the analyses were conducted using the design tandem, HS-20 and SU trucks at each of three positions. In addition, both one lane and two lane loaded cases were considered. Therefore, a total of 36 loading cases (6 different trucks × 3 positions × 2 two lane load cases) were applied on a given bridge and the moment and shear effects were computed. These computations were carried out on all 25 bridges.

| (a) | (b) |
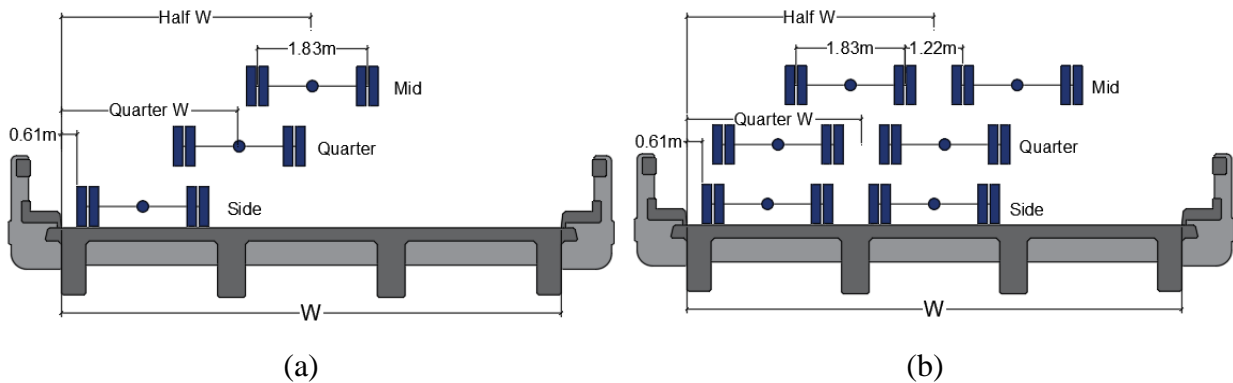
Figure 5-8 Truck transverse positions for: (a) One lane loaded and (b) two lane loaded cases.

Figure 5-9 illustrates the calculated distribution factors for moment and shear for one of the bridges (Bridge #24) for both one lane and two lanes loaded cases. It can be seen that the highest moment and shear distribution factor for the exterior girders for this particular bridge occurs when the load was placed at the side position. For the interior girders, all of three loading positions, i.e., the side, quarter or middle positions, lead to similar peak distribution factors. For side position, this peak value of the distribution factor generally occurs in girder 2, while for other two loading position, the peak value is mostly observed in interior girder 3. In addition, for the loading at each of three transverse positions, the trends in the distribution factor are similar for different truck types.
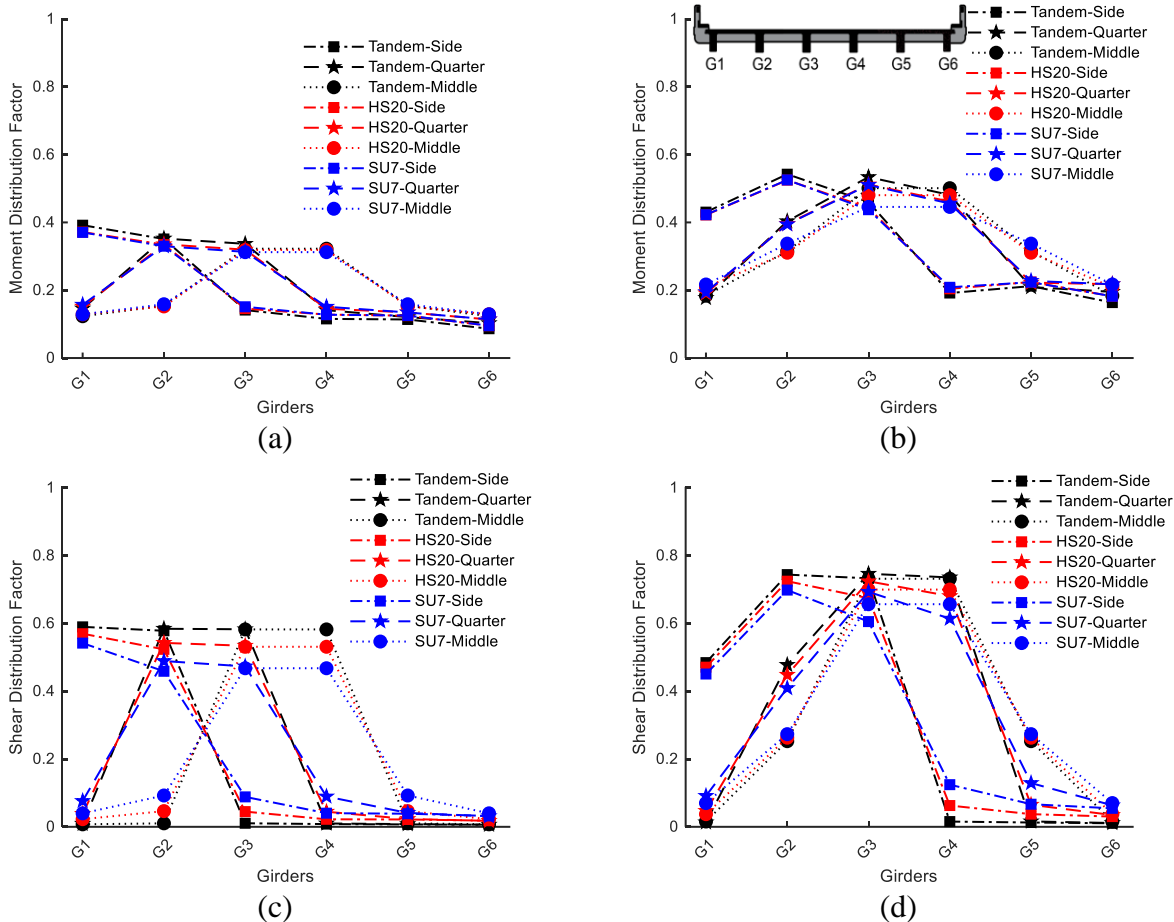
Figure 5-9. Distribution factors considering different transverse truck position and truck type: (a) moment - one lane, (b) moment - two lanes, (c) shear – one lane, and (d) shear – two lane loaded cases.

The governing transverse truck position for each load effect were identified for all bridges and the results are summarized in Figure 5-10 and Figure 5-11 below for moment and shear effects, respectively. In these figures, the number of bridge analysis cases for governing transverse load position was provided under each of six different truck types considered in the analyses. In general, the maximum distribution factors for moment and shear of exterior girders occur with the loading at the side position. Also, for the interior girders under two lanes loaded scenario, a maximum moment or shear distribution factor occurs for about half of the bridges when the trucks are placed at side position. However, for interior girders under one lane loading, the quarter position governs the moment distribution factors for most of the bridges and governs for shear distribution factors for about a half of the bridges. Nevertheless, as illustrated in Figure 5-9, the distribution factors obtained for other two positions are quite close to those obtained for the quarter position for the

interior girders. Therefore, the side position, i.e., the placement of trucks at 2-feet from the parapet, can be used as transverse loading position while evaluating the distribution factors for both exterior and interior girders.
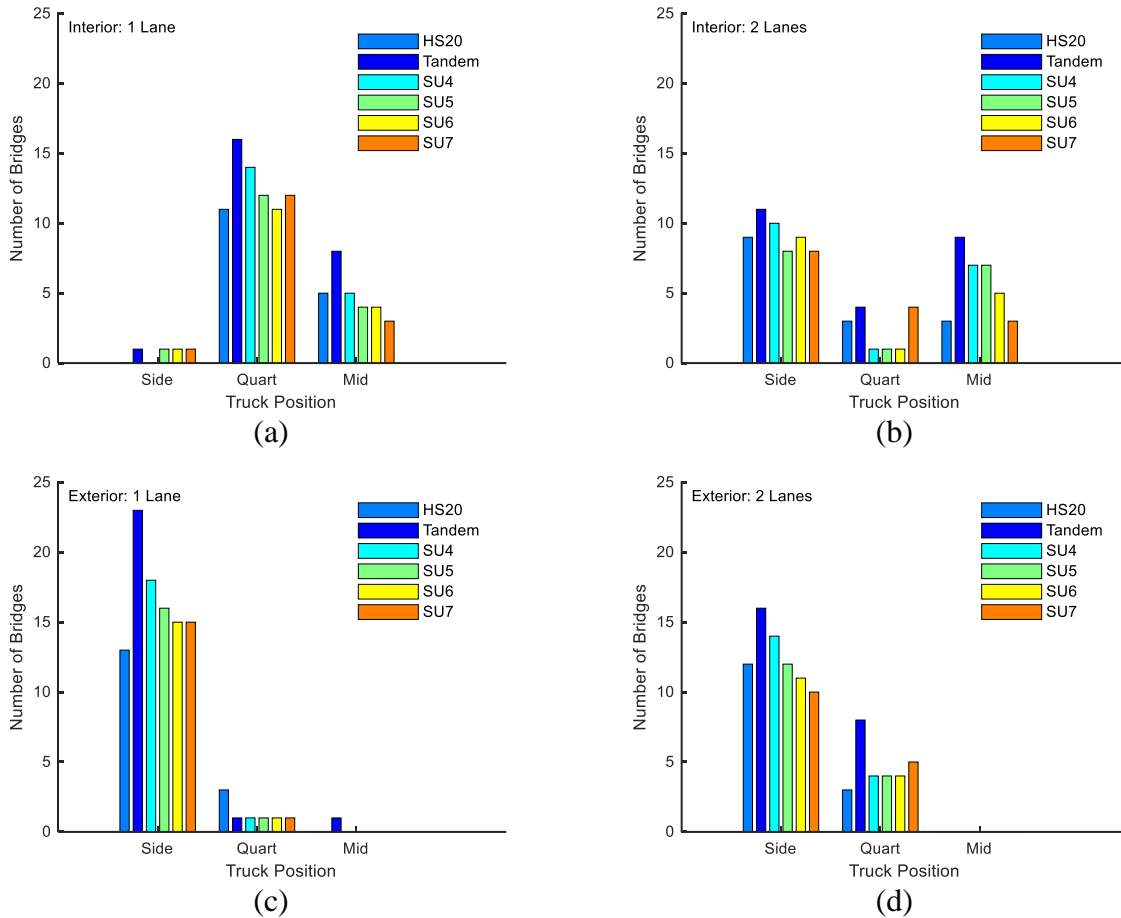
Figure 5-10. Governing transverse truck position for moment distribution factors: (a) interior girder one lane, (b) interior girder two lanes, (c) exterior girder one lane, (d) exterior girder two lanes loaded cases.
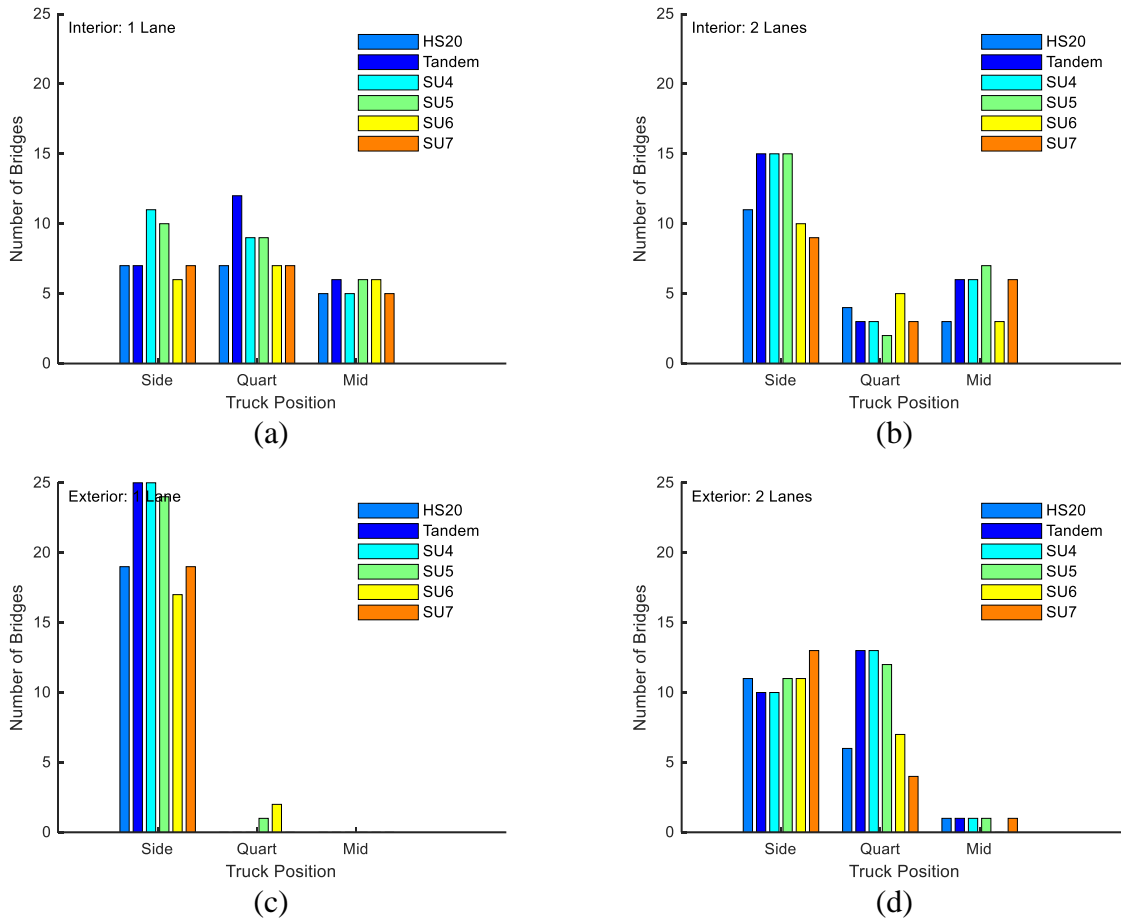
Figure 5-11. Governing transverse truck position for shear distribution factors: (a) interior girder one lane, (b) interior girder two lanes, (c) exterior girder one lane, (d) exterior girder two lanes loaded cases.

5.5   Comparison with AASHTO LRFD Distribution Factors

5.5.1   *Percent Change in Distribution Factors Relative to AASHTO Equations*

In this section, the moment and shear distribution factors for the exterior and interior girders computed through FE analyses as described above are compared to those calculated using the AASHTO LRFD load distribution factor equations (Zokaie 2000). Percent change between distribution factor computed from the AASHTO LRFD design reference (DF_{AASHTO}) and that obtained from FE model (DF_{model}) is computed as:

$$\Delta DF\,(\%) = \frac{DF_{model} - DF_{AASHTO}}{DF_{AASHTO}} \cdot 100 \qquad (5\text{-}2)$$

where ΔDF is the percent change in the *distribution factor* when a refined analysis is conducted to compute them rather than AASHTO LRFD equations. For the distribution factor computed

through refined analysis, the truck that led to highest distribution factor, i.e., the worst case for the rating factor improvement, was compared with the AASHTO LRFD design reference. Note that a negative value for ΔDF suggests the DF_{model} is smaller than DF_{AASHTO} and a given bridge is more effective in distributing the loading than originally predicted through AASHTO LRFD equations. Therefore, for such a case, there will be an increase in the load rating relative to the AASHTO LRFD design basis.

The computed percent changes in distribution factors for moment and shear for the 25 reinforced concrete T-beam bridges are presented in Figure 5-12 and Figure 5-13, respectively. In these figures, the percent change in distribution factors for each bridge are shown for both the design truck or tandem (square red markers) and the governing SU truck (blue circle markers). For a given bridge, the marker is filled for the overall governing truck, e.g., a solid red marker indicates the design truck or tandem provides the higher percent change distribution factor compared to SU trucks. For the moment distribution factors, design truck or tandem governs almost all the cases except exterior girder two lane loading for some bridges. The computation of shear distribution factors is governed by design truck or tandem for interior girders under both one lane and two lanes loadings, while the SU trucks mostly governs the distribution factors for exterior girders under both one lane and two lanes loadings. It can be also seen that for the cases where the design truck or tandem governs, the results obtained for the SU trucks are quite close to those obtained from the design truck or tandem. On the other hand, when the SU trucks govern (i.e., cases such as moment/exterior girders/two lanes; shear/exterior girders/one lane; shear/exterior girders/two lanes), the difference between the results obtained for the design truck or tandem and SU trucks is more significant.
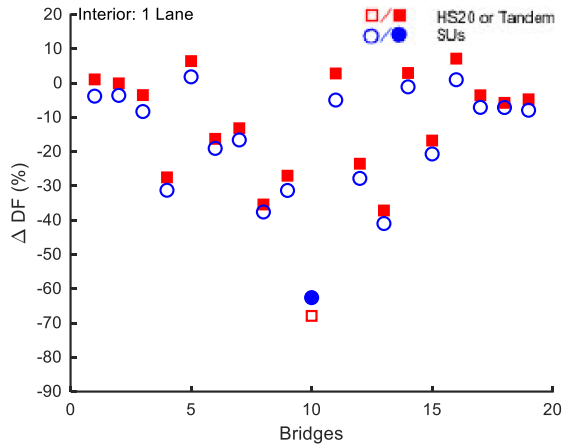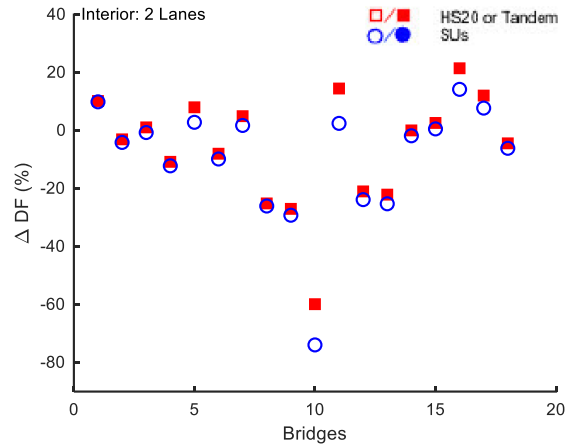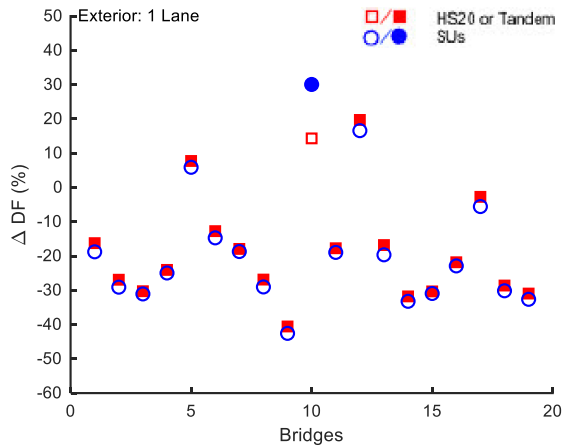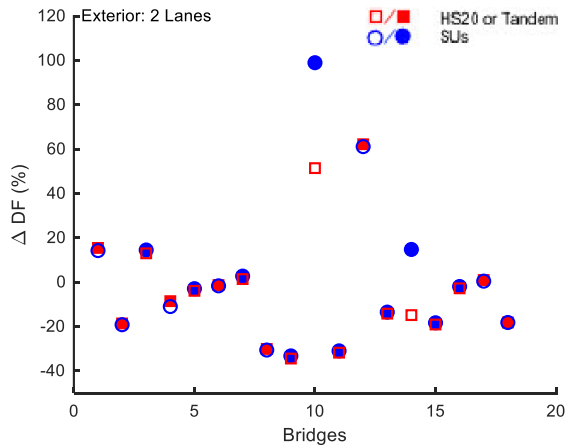
Figure 5-12: Comparison of percent change in moment distribution factors relative to AASHTO LRFD equations: (a) interior girder one lane, (b) interior girder two lanes, (c) exterior girder one lane, (d) exterior girder two lanes loaded cases.
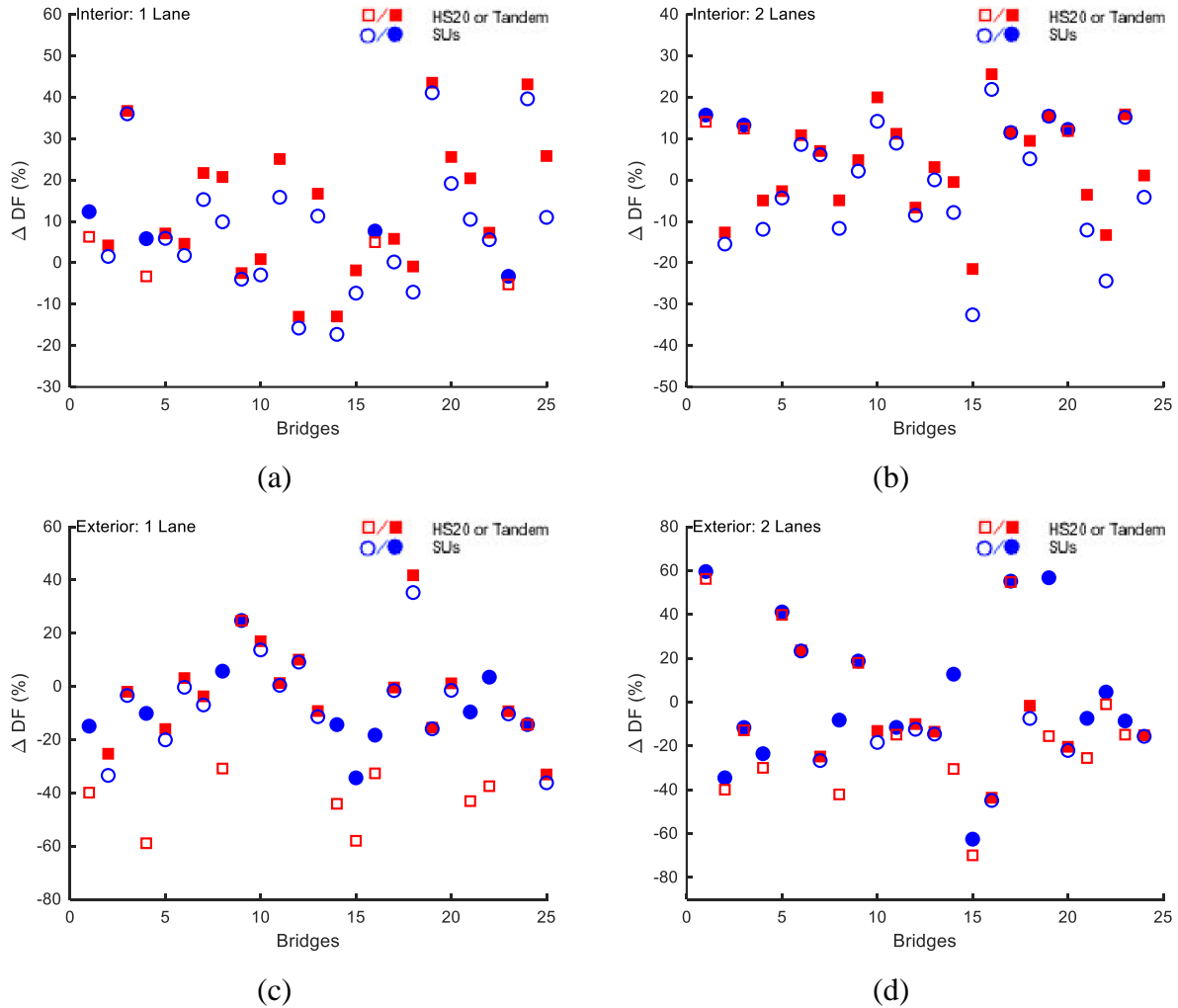
Figure 5-13: Comparison of percent change in shear distribution factor relative to AASHTO LRFD equations: (a) interior girder one lane, (b) interior girder two lanes, (c) exterior girder one lane, (d) exterior girder two lanes loaded cases.

The percent changes in distribution factors considering overall governing truck among design truck, tandem and SU trucks for the 25 reinforced concrete T-beam bridges are presented in Table 5-2. In general, the refined analysis produced lower moment distribution factors than those of AASHTO LRFD for interior and exterior girders. Similarly, for shear in exterior girders, the distribution factors computed by refined analysis were lower than those calculated using AASHTO equations. However, the distribution factors for shear in interior girders determined through refined analysis were higher than those computed from AASHTO LRFD equations.

The results indicate that AASHTO LRFD design equations can be conservative in the calculations of moment distribution factors for interior and exterior girders (DePolo and Linzell

2008; Barr et al. 2007; Yoo et al. 2013; Huang 2004; Huang 2008; Zokaie et al. 1991). Therefore, employing a refined method of analysis can lead to lower moment distribution factors, which, in turn, enhances the rating factors. Furthermore, the AASHTO design equations tend to overestimate the shear distribution factor for exterior girders while underestimate it for interior girders for most of the concrete T-beam bridges analyzed here.

Table 5-2. Percent change in distribution factor relative to AASHTO LRFD equations

No	Interior Moment		Exterior Moment		Interior Shear		Exterior Shear	
	One lane	Two Lanes	One lane	Two lanes	One lane	Two lanes	One lane	Two lanes
1	-11%	6%	-46%	-43%	4%	-13%	-25%	-35%
2	-63%	-60%	30%	99%	-13%	-1%	-14%	13%
3	3%	14%	-18%	-31%	-2%	-22%	-34%	-63%
4	20%	20%	-42%	-63%	8%	26%	-18%	-44%
5	-24%	-21%	20%	62%	6%	12%	0%	55%
6	-37%	-22%	-17%	-13%	-1%	9%	42%	-2%
7	3%	0%	-32%	15%	43%	15%	-15%	57%
8	-17%	3%	-30%	-18%	26%	12%	1%	-20%
9	7%	21%	-22%	-2%	20%	-4%	-10%	-7%
10	-4%	12%	-3%	1%	7%	-13%	4%	5%
11	0%	-3%	-27%	-19%	37%	13%	-2%	-12%
12	-6%	18%	-29%	-19%	-3%	0%	-9%	0%
13	-5%	-4%	-31%	-18%	43%	16%	-14%	-9%
14	-11%	9%	-37%	-16%	26%	1%	-33%	-15%
15	-31%	-11%	-24%	-8%	6%	-5%	-10%	-24%
16	-4%	1%	-30%	15%	7%	-3%	-16%	41%
17	-31%	-12%	-32%	0%	5%	11%	3%	24%
18	-28%	-11%	-24%	-9%	22%	7%	-4%	-25%
19	6%	8%	8%	-3%	21%	-5%	6%	-8%
20	-19%	-8%	-13%	-1%	-4%	4%	25%	19%
21	-50%	-38%	76%	69%	1%	20%	17%	-13%
22	-13%	5%	-18%	3%	25%	11%	1%	-12%
23	1%	10%	-16%	15%	12%	16%	-15%	60%
24	-35%	-25%	-27%	-30%	-13%	-7%	10%	-10%
25	-27%	-27%	-41%	-33%	17%	3%	-9%	-14%

5.5.2 Prediction Equations for the Change of Distribution Factors

The results obtained from the refined analyses of the selected bridges provide a foundation for evaluating the geometric parameters driving load distribution behavior and developing linear regression models based on these parameters. To this end, multi-parameter linear regression models were developed to predict the percent change in distribution factor for T-beam bridges using four parameters that describe the geometrical characteristics of the bridges.

Regression models for the change in distribution factors were developed using the statistical analysis software "R" (Team 2013). The outcome is a presentation of the best-fitting models with various sizes up to the full parameter model. Models were created to predict the percent change in shear and moment distribution factors for interior and exterior girders considering one and two-lanes loaded cases. The geometric characteristics of bridges considered in the model development include span length, girder spacing, number of girders, skew angle, moment of inertia of girders, slab thickness, girder depth, and overhang of the deck. Only the most significant four parameters were selected to develop the prediction models in each case. The choice for the four parameters was based on the possibility of preparing look-up tables for VDOT using the results from prediction models if up to four parameters are used to describe a selected bridge. To improve the accuracy of the prediction models, the regression equations were established considering the interaction among the selected four parameters. In addition, 80% of the results from refined analysis were used as a training set, while the remaining 20% were split evenly and used for testing and validation of the model. In multiple regression, the core concept of validation is to add additional observations to the regression equation and determine R_c^2, the coefficient of determination for this new data. The model is validated if the R_c^2 is satisfactory. The coefficient of determination is employed in the validation because it is a well-known metric in regression analysis and provides a method for estimating expected shrinkage in R^2 (Herzberg, 1969). Finding the points predicted by the equation for each sample item and comparing the predicted values with the actual values constitutes the calculation.

The developed regression models for the prediction of the change in distribution factors for moment and shear distribution factors are shown in Table 5-3 and Table 5-4, respectively. In these tables, the regression equations in these two tables do not include the terms that have two parameters interacting with each other. The entire equations that include these interacting parameters are in the Appendix.

Table 5-3. Prediction equations for changes in moment distribution factors

Girder/Loading	R^2	R_c^2	Prediction Equations for Moment ΔDF (%)
Interior/One-lane	0.82	0.78	$\Delta DF_{M\text{-}int\text{-}1L} = -3879 + 257.28L + 217.16t_s + 62.28d + 754O_v$ where $10 < L < 13$; $17 < t_s < 23$; $60 < d < 74$; $0.6 < O_v < 1$
Interior/Two-lanes	0.76	0.72	$\Delta DF_{M\text{-}int\text{-}2L} = -3704 + 188L + 222.48t_s + 64.27d + 828O_v$ where $10 < L < 13$; $17 < t_s < 23$; $60 < d < 74$; $0.6 < O_v < 1$
Exterior/One-lane	0.76	0.71	$\Delta DF_{M\text{-}ext\text{-}1L} = 4244 - 1116.2L - 1094S + 19.74d + 38.31O_v$ where $10 < L < 13$; $2 < S < 3$; $60 < d < 74$; $0.6 < O_v < 1$
Exterior/Two-lanes	0.81	0.75	$\Delta DF_{M\text{-}ext\text{-}2L} = 154.8 - 5.67L - 3.40d + 19.21\theta - 23.23O_v$ where $10 < L < 13$; $60 < d < 74$; $0 < \theta < 45$; $0.6 < O_v < 1$

L: span length (m); S: girder spacing (m); N_b: number of girders; θ: skew in the bridge (degrees); I: moment of inertia of girders (cm^4); t_s: slab thickness (cm); d: girder depth (cm); O_v: overhang (m).

Table 5-4. Prediction equations for changes in shear distribution factors

Girder/Loading	R^2	R_c^2	Prediction Equations for Shear ΔDF (%)
Interior/One-lane	0.78	0.75	$\Delta DF_{S\text{-}int\text{-}1L} = -579.08 - 139.26L + 37.74t_s + 193.52N_b + 1347.5O_v$ where $10 < L < 13$; $17 < t_s < 23$; $3 < N_b < 5$; $0.6 < O_v < 1$
Interior/Two-lanes	0.72	0.70	$\Delta DF_{S\text{-}int\text{-}2L} = 120 - 2.87L - 104.86S - 22.67\theta - 68.72N_b$ where $10 < L < 13$; $2 < S < 3$; $0 < \theta < 45$; $3 < N_b < 5$
Exterior/One-lane	0.71	0.69	$\Delta DF_{S\text{-}ext\text{-}1L} = 1482 - 167.37L - 776S - 10.94d - 239.41O_v$ where $10 < L < 13$; $2 < S < 3$; $60 < d < 74$; $0.6 < O_v < 1$
Exterior/Two-lanes	0.75	0.71	$\Delta DF_{S\text{-}ext\text{-}2L} = -127.5 + 66.88S + 97.97 \times 10^{-4}I - 63.55\theta + 3.09N_b$ where $2 < S < 3$; $7.5 \times 10^9 < I < 12.5 \times 10$; $0 < \theta < 45^9$; $3 < N_b < 5$

L: span length (m); S: girder spacing (m); N_b: number of girders; θ: skew in the bridge (degrees); I: moment of inertia of girders (cm^4); t_s: slab thickness (cm); d: girder depth (cm); O_v: overhang (m).

5.5.3 Validation of Prediction Equations

To validate the prediction equations, the changes in distribution factor for moment and shear were computed using the developed regression models and compared to those obtained from the refined analysis as shown in Figure 5-14 and Figure 5-15. The solid black line in the plots indicates no difference between the two calculations. The dashed lines represent the limits of 10% error between the regression model and the refined analysis. The blue circle markers represent the findings for the bridges within the parameter ranges of the regression model, as given in Table 5-3 and Table 5-4. On the other hand, the red square markers represent those bridges with parameters

that were outside the parameter range of model. In all cases, the corresponding bridge number is provided next to the markers in the figures. The results indicated that the developed prediction equations provided a reasonable estimate for the load distribution under both one-lane and two-lanes loaded cases. For both moment and shear distribution factors, the errors in the ΔDFs predicted from regression models were less than 10% for most of the bridges. The results also show that the developed regression models satisfactorily predicted the ΔDFs for many bridges with some parameters that were outside of the parameter ranges of the model. They can be used as screening tool to identify bridge structures that are prone to posting yet have a high potential for rating factor improvement through refined study.
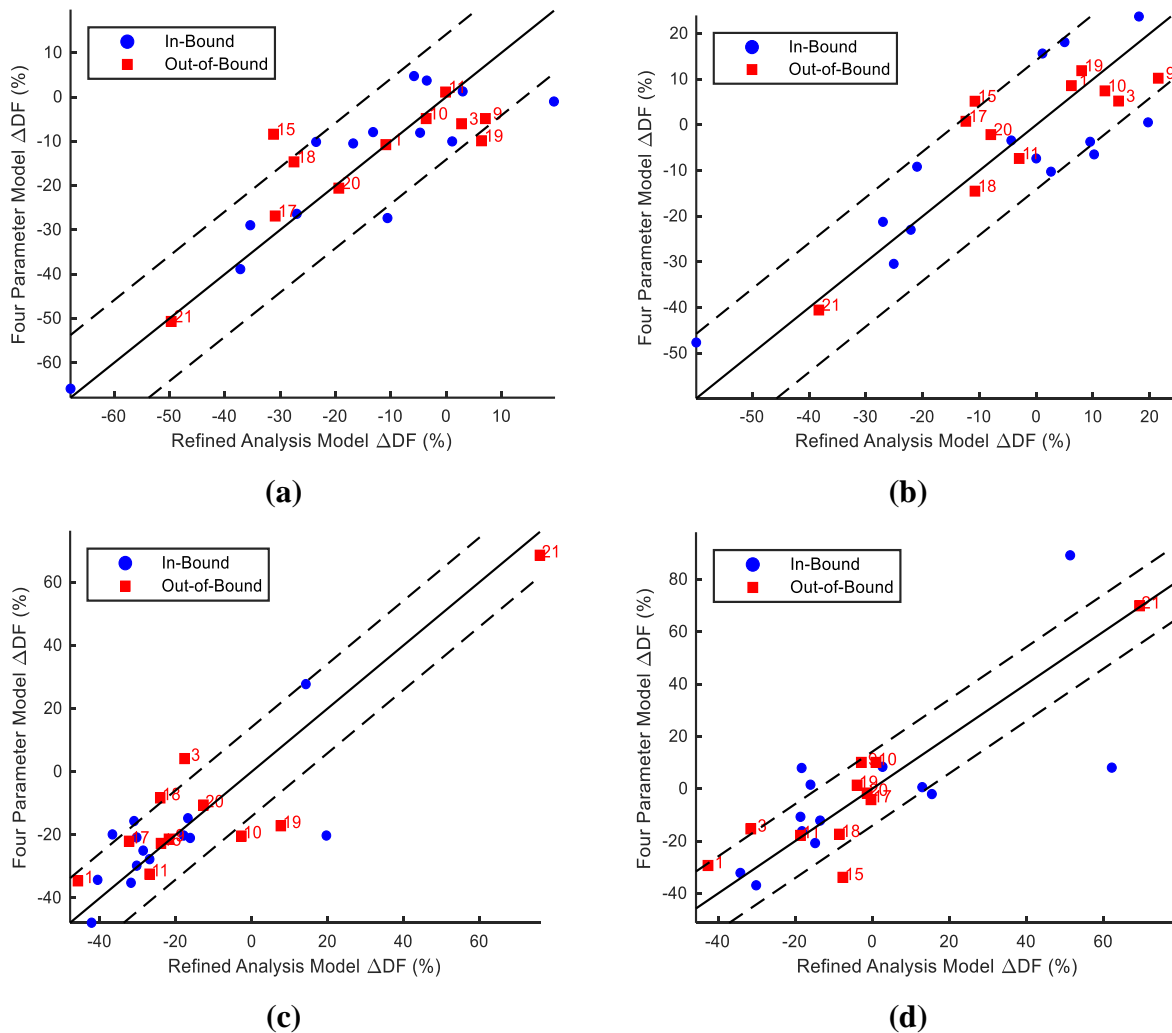
Figure 5-14. Predicted change versus actual refinement in moment distribution factors for: (a) interior girder one lane, (b) interior girder two lanes, (c) exterior girder one lane, (d) exterior girder two lanes loaded cases.
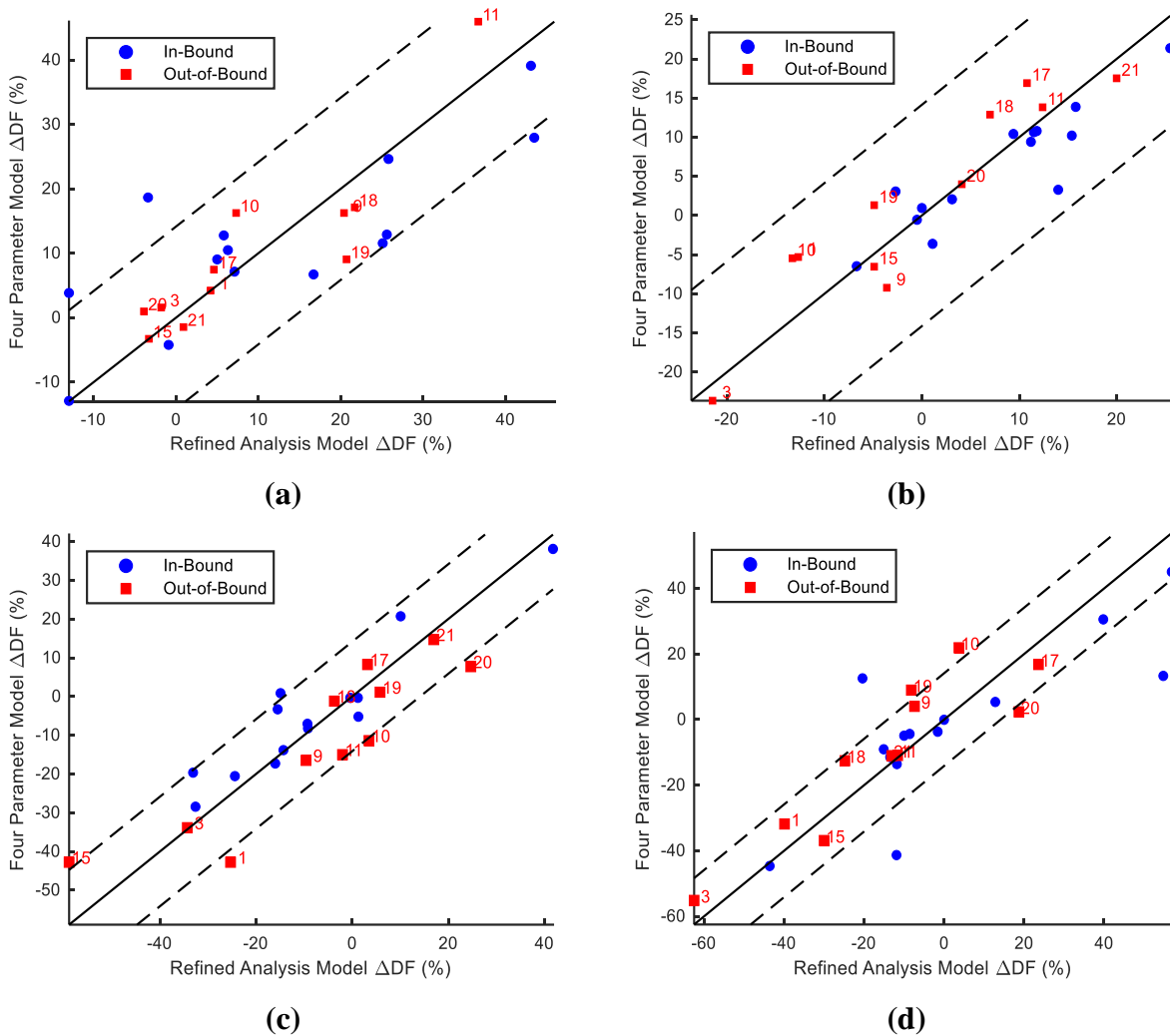
Figure 5-15. Predicted change versus actual refinement in shear distribution factors for: (a) interior girder one lane, (b) interior girder two lanes, (c) exterior girder one lane, (d) exterior girder two lanes loaded cases.

5.5.4   *Effects of Geometrical Parameters*

In this section, the effects of bridge geometrical characteristics on the obtained results for the ΔDFs is evaluated. To this end, the contour plots were created using the develop regression models within their parameter limits to illustrate the variation of ΔDFs with the two most significant parameters for each of the regression models. The obtained results are presented in Figure 5-16 and Figure 5-17 for moment and shear effects, respectively.

For interior girders subjected to one and two lanes loaded cases, the two most significant parameters for the percent change in moment distribution factors are the girder depth and span length. It can be seen from Figure 5-16 (a)-(b) that as the girder depth increases with a lower span

length, the reduction of the moment distribution factors could be larger through refined analysis. Note that in the AASHTO LRFD equations to compute interior moment distribution factors, the moment of inertia of the girder, which depends on girder geometry including girder depth, is considered within the longitudinal stiffness parameter. However, the findings indicate that for shorter span bridges, the girder depth has more significant role on the distribution factor than that is estimated by the AASHTO equations.

For exterior girders subjected to one-lane loading, the two most significant parameters for percent change in moment distribution factors were the girder spacing and span length. For this case, a simultaneous increase in the girder spacing and span length decrease the percent change in the distribution factor through refined analysis compared to AASHTO LRFD equations as can be seen in Figure 5-16(c). Note that AASHTO LRFD uses the lever rule on some scenarios to compute the moment distribution factor for exterior girders. This method is very conservative and applies to those bridges whose parameters are outside the limits of applicability of the AASHTO LRFD equations to compute the distribution factors.

For the case of exterior girder under two lanes loaded shown in Figure 5-16(d), the two significant parameters for percent change in moment distribution factors are the girder depth and skew. A reduction in distribution factor was observed when any of these two parameters became larger. The reason for such a difference could be the fact that AASHTO specifications on distribution factors for two-lane loading relies on the distribution factors of the interior girders rather than an independent analysis and does not consider the skew effect if the skew angle equals or less than 30°.
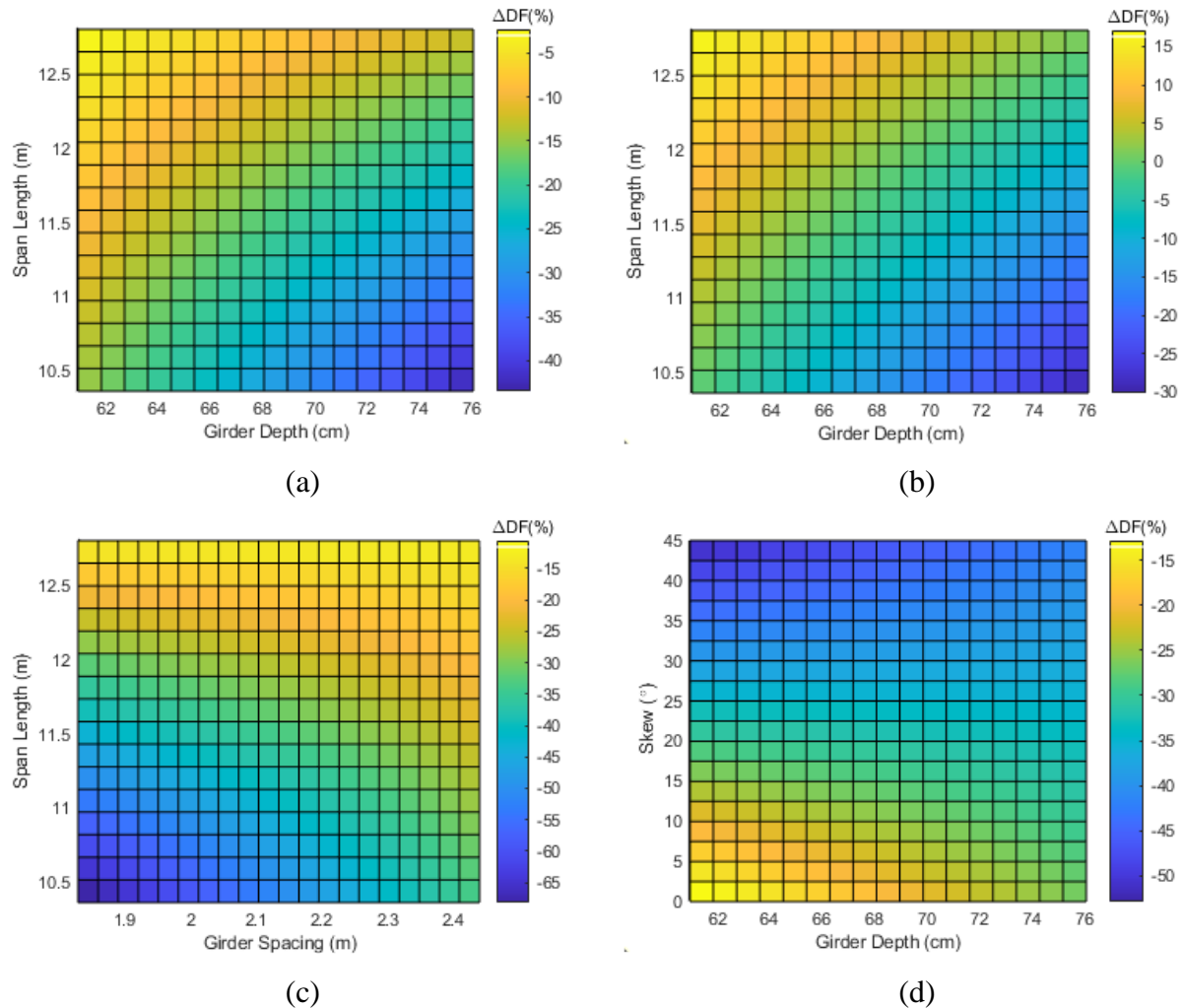
Figure 5-16. Contour plots for predicted change in moment distribution factors based on bridge's geometry for: (a) interior girder one lane, (b) interior girder two lanes, (c) exterior girder one lane, (d) exterior girder two lanes loaded cases.

The important bridge parameters affecting the percent change in shear distribution factors includes skew, span length, number of girders, overhang, slab thickness and girder spacing as shown in Figure 5-17. For interior girders that are subjected to one lane loading, two dominant parameters are the number of slab thickness and overhang. It can be seen from Figure 5-17(a) for bridges with larger overhangs and lower slab thickness, that the change in distribution factors obtained from refined analysis would be larger than those obtained from AASHTO equations. For interior girders subjected to two-lanes loading, the skew angle and number of girders are the most effective parameters. The contour plot in Figure 5-17(b) suggests that a reduction in the shear distribution factor is observed for bridges with fewer girders regardless of the skew. Note that the shear distribution factor equations from the AASHTO LRFD consider the spacing as the only

parameter in computing the distribution factor for one- and two-lanes loadings. However, various parameters such as girder spacing, slab thickness, overhang, and number of girders influence the load distribution for the shear of interior girders and these factors are considered in finite element modeling.

For exterior girders subjected to one lane loaded, the span length and girders spacing are the significant factors. As can be seen in Figure 5-17(c), a reduction in distribution factor was observed when these two parameters were either simultaneously high or simultaneously low. The fact that AASHTO LRFD applies the lever rule, which is a conservative approach as mentioned above, in some cases for the calculation of exterior shear girder under one lane loading could be the cause for the difference between the computed distribution factors. For exterior girders subjected to two-lanes loaded, the skew and girders spacing were the significant parameters. It can be seen in Figure 5-17(d) that a reduction in shear distribution factor for exterior girders is associated with high values in both parameters, i.e. girder spacing < 2.3 m, the refined analysis could yield higher DFs for shear in exterior girders with 2 lanes loaded, regardless of the skew.
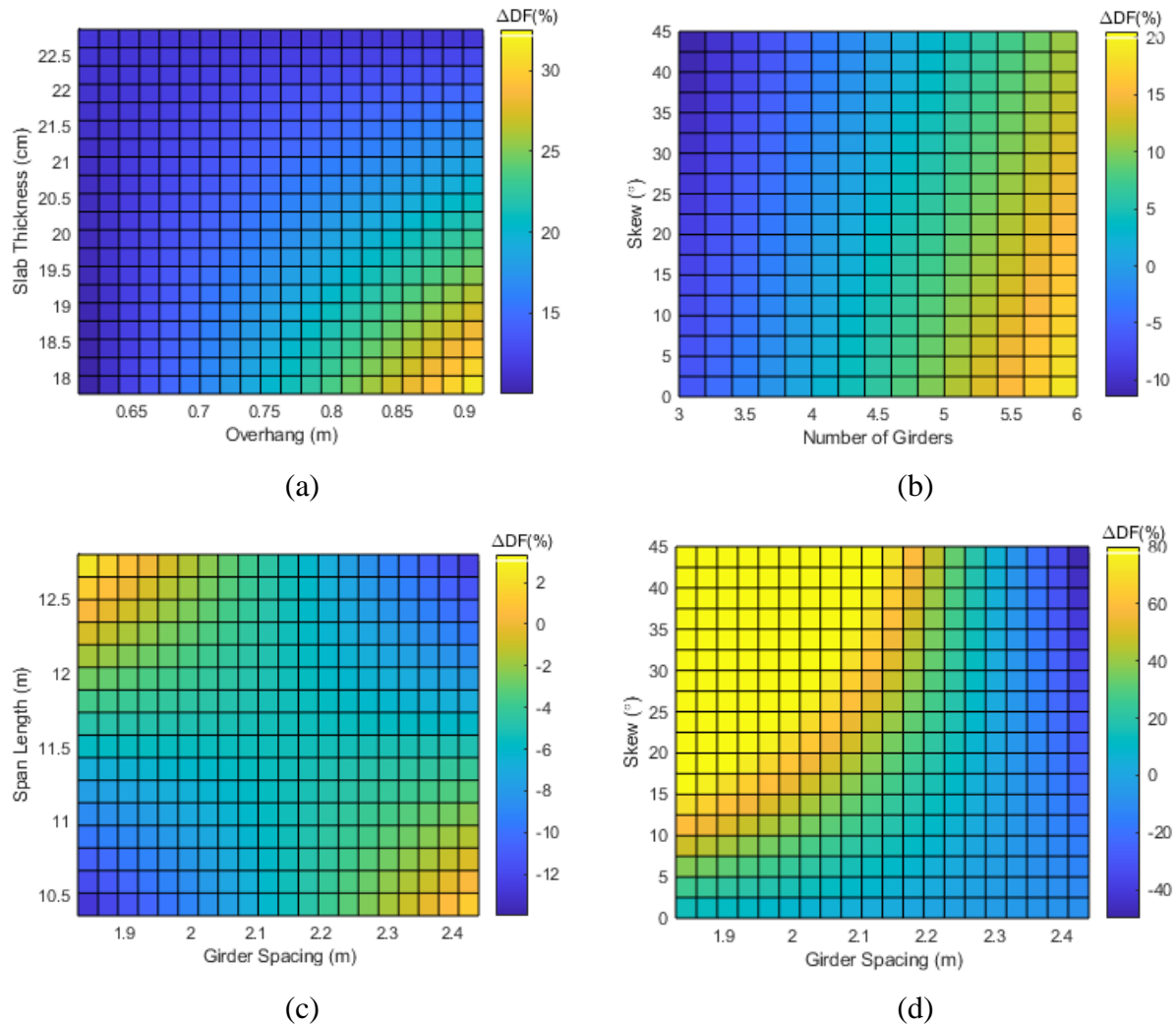
Figure 5-17. Contour plots for predicted refinement in shear distribution factors based on bridge's geometry for: (a) interior girder one lane, (b) interior girder two lanes, (c) exterior girder one lane, (d) exterior girder two lanes loaded cases.

5.5.5 *Effects on Rating Factor*

As shown in Equation 1, the distribution factors and load rating factors are inversely proportional, i.e., a decrease in the distribution factors lead to an increase in rating factor. Taking all the variables except the distribution factor in the load rating equation shown in Equation 1 as the same, the percent change in the rating factor (ΔRF) computed from refined analysis and AASHTO LRFD Specifications can be obtained as:

$$\Delta RF\,(\%) = \frac{RF_{model} - RF_{AASHTO}}{RF_{AASHTO}} \cdot 100 = \left(\frac{RF_{model}}{RF_{AASHTO}} - 1\right) \cdot 100 \qquad \textbf{(3)}$$

or

$$\Delta RF\,(\%) = \left(\frac{DF_{AASHTO}}{DF_{model}} - 1\right) \cdot 100 \qquad \textbf{(4)}$$

where RF_{model} and RF_{AASHTO} denote the rating factor computed using refined analysis and AASHTO LRFD Specifications, respectively. As a result, equation (5) can be used to evaluate the change in the rating factor when the load distribution factor is computed through refined analysis instead of AASHTO equations.

5.6   Summary

The FHWA mandates that state transportation departments to rate all bridges in their inventory for a class of vehicles known as special hauling vehicles (SHVs) by the end of 2017 for Group 1 bridges and by the end of 2022 for Group 2 bridges, unless state laws prohibit SHV use. Virginia DOT's list of bridges that are vulnerable to load posting owing to SHVs is largely made up of reinforced concrete T-beam bridges. Given the importance of the route, reinforced concrete T-beam bridges were among the chosen bridge type for the refined assessments in this study. This study investigated by how much the rating factor of reinforced concrete T-beam bridges could change, especially under special hauling vehicles, by computing the distribution factors using a refined method of analysis. The selection and implementation of a suitable refined technique of analysis was a critical component of this investigation. The finite element models for 25 in-service T-beam bridges were developed and the live load distribution factors were evaluated. The effects of loading truck type and transverse positioning of the truck on the computation of distribution factors using refined analysis were evaluated. A comparison was made for the distribution factors computed by the refined analysis and AASHTO LRFD equation. Furthermore, regression models were developed to predict the percent change in distribution factors should a refined analysis be conducted based on bridge geometry. Below are the conclusions that are based on the results of this study:

- The design truck or tandem loading tends to govern the moment and shear distribution factors for interior girders. However, for exterior girders, SU trucks generally give the larger distribution factor, especially for two-lanes loaded scenarios.

- Because the distribution factors computed for interior girders using the SU trucks in refined analysis are very close to those obtained from the design truck and tandem, and because the SU trucks govern the distribution factors for exterior girders, only SU trucks need to be considered in refined analyses of reinforced concrete T-beam bridges to obtain both moment and shear distribution factor.

- The transverse positioning of the trucks can have an impact on the load distribution factors for interior girders, but generally, not for exterior girders, where the largest distribution factors tend to occur when the trucks are positioned close to the edge of the bridge.

- Except for the interior shear and moment distribution factors with two-lanes loaded, the moment and shear distribution factors obtained from the refined analysis, are lower for most reinforced concrete T-beam bridges than those computed through the conventional AASHTO LRFD approach. Depending on the distribution factor, 64% to 84% of the bridges had lower factors determined through refined analysis compared to the AASHTO LRFD-based equations.

- Given certain bridge geometrical characteristics, the developed regression models can predict the percent change in distribution factors using refined analysis. The coefficient of determination for that prediction is at least 0.74.

- Considering the ability of the prediction equations in detecting percent change in distribution factors, these equations can be used as screening tool to make a decision about whether a refined analysis can improve ratings for a particular bridge or not.

6.   EVALUATION OF LOAD DISTRIBUTION FACTORS FOR STEEL GIRDER BRIDGES

6.1   Introduction

Steel girder bridges account for 31% of all bridges in the state of Virginia and some of these bridges may experience a lower load rating when they are rated with SHVs or EVs. For such bridges, refined method of analysis can be leveraged for possible improvements in characterizing load distribution behavior and potentially improving rating factors. This study evaluates the load distribution factors for steel girder bridges through refined analysis considering SHVs and EVs. A total of 21 in-service steel girder bridges were chosen and modeled using standard structural analysis software. The moment and shear DFs calculated from refined analysis were compared with those computed using AASHTO LRFD equations. In addition, a set of equations were developed through regression analysis to predict the DFs of refined analysis.

6.2   Bridge Selection

About 75% of the slab-on-girder bridges in the state of Virginia are steel girder bridges, which are the focus of this study. The statistical distributions of steel girder bridges in the Virginia Department of Transportation (VDOT) inventory are shown in Figure 6-1 considering deck width, span length, and skew angle. The study included a total of 21 operational steel girder bridges, whose features are also depicted in Figure 6-1. The characteristics of the entire inventory were taken into account when choosing the bridges, and those along the interstates and primary routes were given preference as they are subjected to high traffic volumes. A refined DF was computed for the bridges with a rating factor less than 1.0 but greater than 0.7 to investigate the possibility of improving the rating factor for vulnerable bridges. The chosen bridges' geometrical characteristics are shown in Table 6-1.
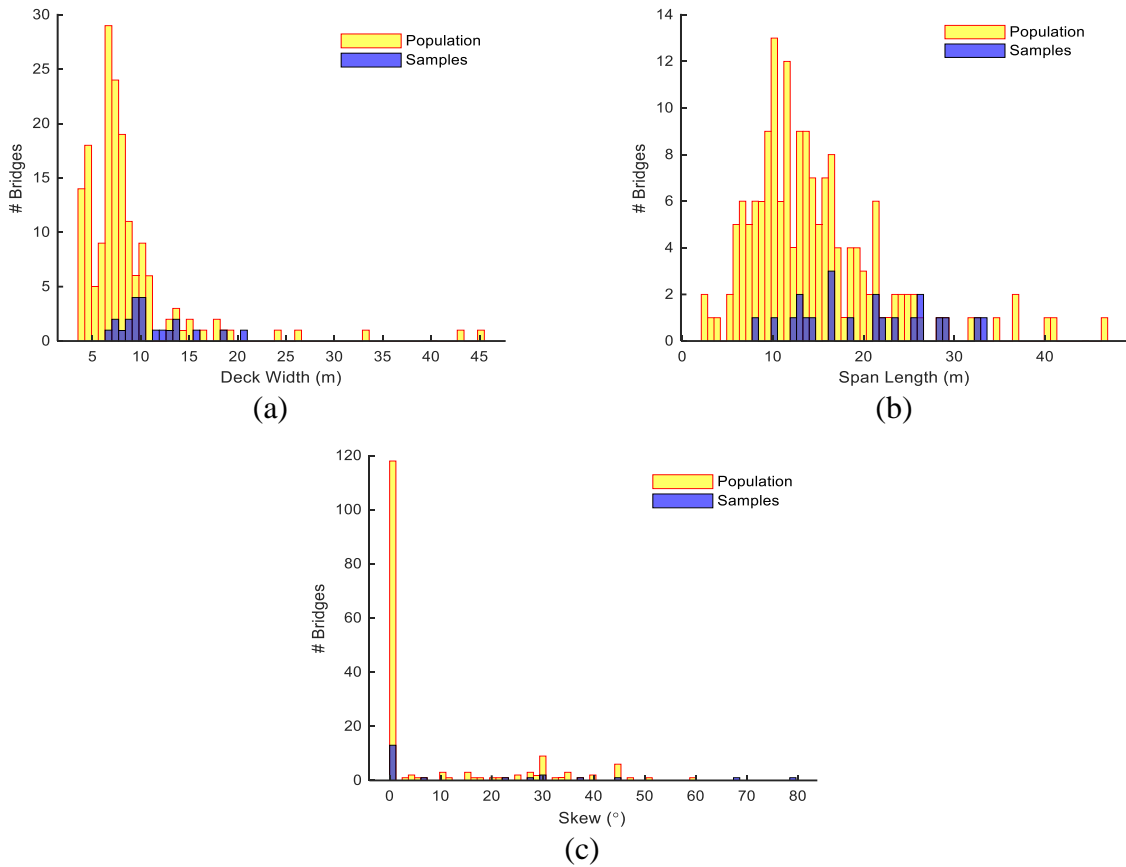
Figure 6-1. Steel girder bridge population based on: (a) deck width, (b) span length, and (c) skew

Table 6-1. Selected steel girder bridges for this study

No	Route	Span Length (m)	Girder Spacing (m)	Overall Section Depth (cm)	Number of Girders	Skew Angle (degrees)	Deck Width (m)	Lanes
1	Primary	11.69	2.34	93.14	4	30	8.86	2
2	Primary	28.19	2.54	113.32	4	0	9.47	2
3	Primary	14.78	2.06	103.00	5	0	10.06	2
4	Primary	18.59	3.05	180.98	5	0	13.09	3
5	Primary	16.69	2.19	103.48	7	23	7.57	2
6	Secondary	29.26	1.93	102.36	4	0	7.53	1
7	Primary	31.85	2.74	112.01	7	37	18.75	4
8	Primary	7.62	1.75	70.80	5	0	8.84	2
9	Interstate	13.79	2.74	88.70	6	28	13.41	3
10	Interstate	16.46	2.35	102.26	5	7	11.43	2
11	Primary	22.10	1.98	108.84	7	79	12.50	2
12	Primary	23.14	2.21	108.84	6	68	13.72	3
13	Primary	12.95	2.29	93.55	4	45	9.70	2
14	Primary	33.53	2.74	165.10	4	0	10.16	2
15	Primary	16.76	2.06	102.36	5	0	10.08	2
16	Primary	9.91	2.35	87.45	4	0	7.88	2
17	Primary	21.34	1.91	108.84	5	0	9.47	2
18	Primary	25.91	2.06	113.92	6	0	9.14	2
19	Secondary	32.46	2.41	165.10	9	0	20.99	5
20	Primary	13.03	1.32	71.73	5	0	6.71	1
21	Primary	21.62	2.02	110.11	5	0	10.06	2

6.3 Refined Analysis: Model Development and Computation of Distribution Factors

6.3.1 Development of Finite Element Models

The first step of the refined analysis involves creating a reliable FE model of a bridge structure, which then can be analyzed to evaluate load distribution behavior of bridges. Here, two-dimensional FE models of the selected steel girder bridges were developed by employing the plate with eccentric beam (PEB) modeling approach. All numerical models were created using LARSA 4D. In PEB modeling, the girders and deck slab of bridges were modelled separately. The girders were modeled using beam elements that are located along the centroids of longitudinal girder lines. The concrete deck was modeled with plate elements from edge to edge throughout its whole length. In order to account for the depth of the structure, the longitudinal girders were eccentric and deck slab as they are both modeled at their corresponding centroids. Beam elements were also employed to link the longitudinal elements transversely at crosswise frame/diaphragm positions if present. Figure 6-2 depicts a standard model for a steel girder bridge. All of the bridges were simply supported, and pin-roller supports were used to model the boundary conditions of each bridge.
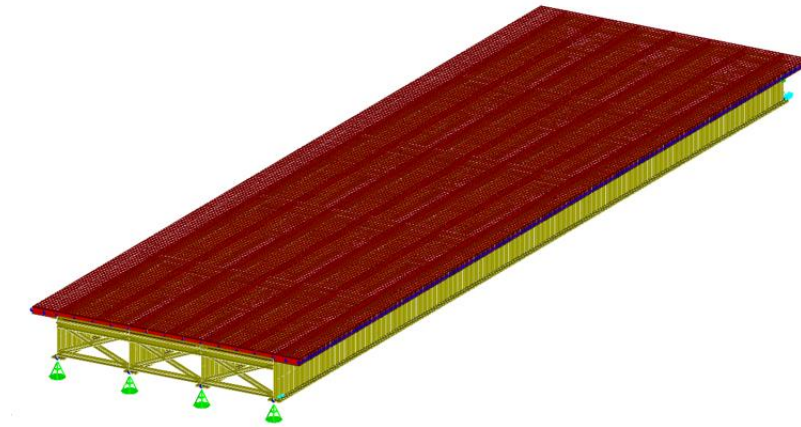
Figure 6-2. Standard FE model of a steel girder bridge

To evaluate the load distribution behavior, the selected bridges were subjected to one-lane and two-lane loadings using various vehicle types. The vehicle loadings considered in the analysis are design truck (HS-20), design tandem, single-unit trucks (SUs) and emergency vehicles (EVs) as shown in Figure 6-3.
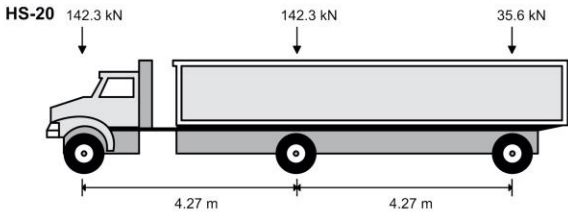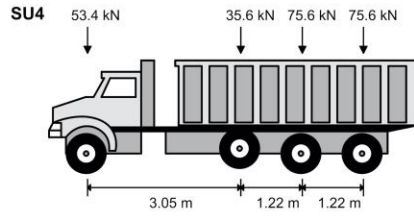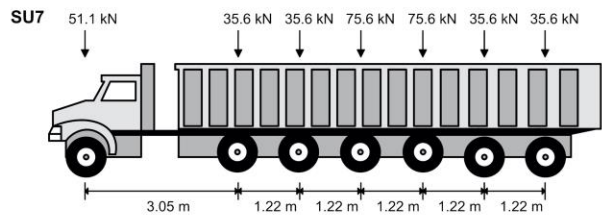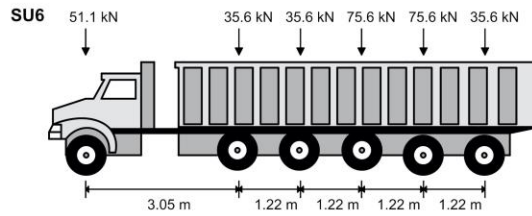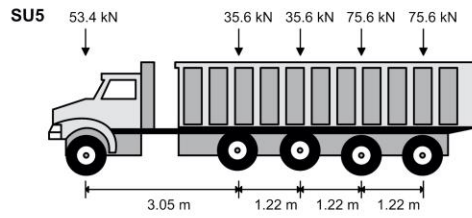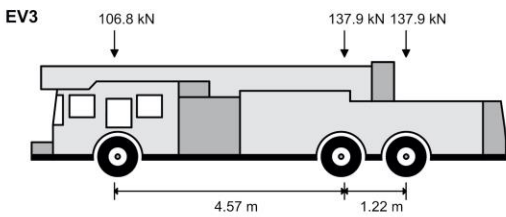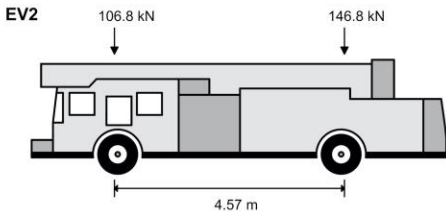
Figure 6-3. Axle loads for design tandem and HS-20, SU4, SU5, SU6, SU7, EV2 and EV3 trucks

6.3.2   Computation of Distribution Factors

The created FE models were used to calculate the moment and shear effects for the 21 bridges that were chosen under various vehicle loadings. The live load distribution factor (DF), or *g,* was then computed using these load effects. The DFs for each girder were calculated using the load fraction analysis method (Harris 2010). This approach is described by Equation (5-1) below, where $R_{max, j}$ denotes the maximum moment or shear of the jth girder, N_{trucks} is the number of trucks or lanes, and *m* is the multiple presence factor, which is taken as 1.2 and 1.0, respectively, for one and two lanes loaded as specified in AASHTO (Eom and Nowak 2001, Conner and Huo 2006):

$$g = \frac{R_{max,j}}{\sum_{j=1}^{\#girders} R_{max,j}} \cdot N_{trucks} \cdot m \tag{6-1}$$

6.4 Evaluation of Results

6.4.1 Effects of Loading Truck Type

The load DFs for each steel girder bridge under various vehicle loadings were determined using the developed FE models. Both moment and shear load DFs were calculated under one-lane loaded and two-lane loaded cases. The results are presented for interior and exterior girders separately in the following discussions. To facilitate the assessment of the influence of vehicle type on DFs, the DFs computed for different vehicle loading are compared to the DFs calculated for tandem loading.

Figure 6-4 compares the moment DFs obtained from HS 20, SU trucks, and EV trucks with those obtained using tandem for the interior and exterior girders under one and two lanes loading conditions. Similarly, Figure 6-5 provides this comparison for the shear DFs. The results for each individual bridge are shown with a marker, providing the value of the DF from the tandem loading in the x-axis and that of other trucks in the y-axis. If the marker falls on the 1:1 line, which is the solid black line, this indicates that the DF obtained from the tandem and other truck loadings are the same. However, if the marker falls above 1:1 line then the other truck types result in higher load DFs.

Figure 6-4(a) shows that the moment DFs for the interior girders for the one lane loaded case attain their maximum value mostly for the tandem loading. When HS20 truck is used instead of tandem in the refined analysis, the obtained DFs are always slightly lower for this case. When SU or EV trucks are used in the analysis, there are four and eight bridges for which the SU and EV trucks, respectively produced a higher DF than the tandem loading. However, the difference between the calculated DFs is not significant and below 10% except for one bridge (bridge #11) where the DF is calculated to be 21% higher when the EV2 or EV3 truck are used. Similarly, for two lanes loaded case presented in Figure 6-4(b), the tandem loading results in the largest DFs for most of the analyzed structures. There are only four bridges where the moment DF is higher by 5% or more than that obtained under tandem loading.

Figure 6-4(c) and (d) compares the moment DFs for the exterior girders under one lane and two lane loaded cases, respectively. Similar to interior girders, the difference between the DFs obtained from the tandem loading and other vehicles are not significant for most of the bridge cases. However, there are a few bridges where the HS20, SU or EV trucks produced considerably larger DFs for the one lane loaded case. In particular, for Bridge #17, the moment DF for the exterior girder under one lane loaded is at least 216% higher when the HS20, SU or EV trucks are used in the refined analysis rather than tandem truck. For three other bridges, there are increases in the DFs between 6% and 15% for one lane loaded case when the trucks other than tandem are considered in the analysis. For two lanes loaded case, the tandem loading governs the calculation of DFs for the exterior girders. There are two bridges for which the moment DF increases by 10% and 15% when the other trucks are used. It should be also noted that the SU trucks produced considerably lower DFs compared to the tandem loading for a few bridge cases.

(a)

(b)
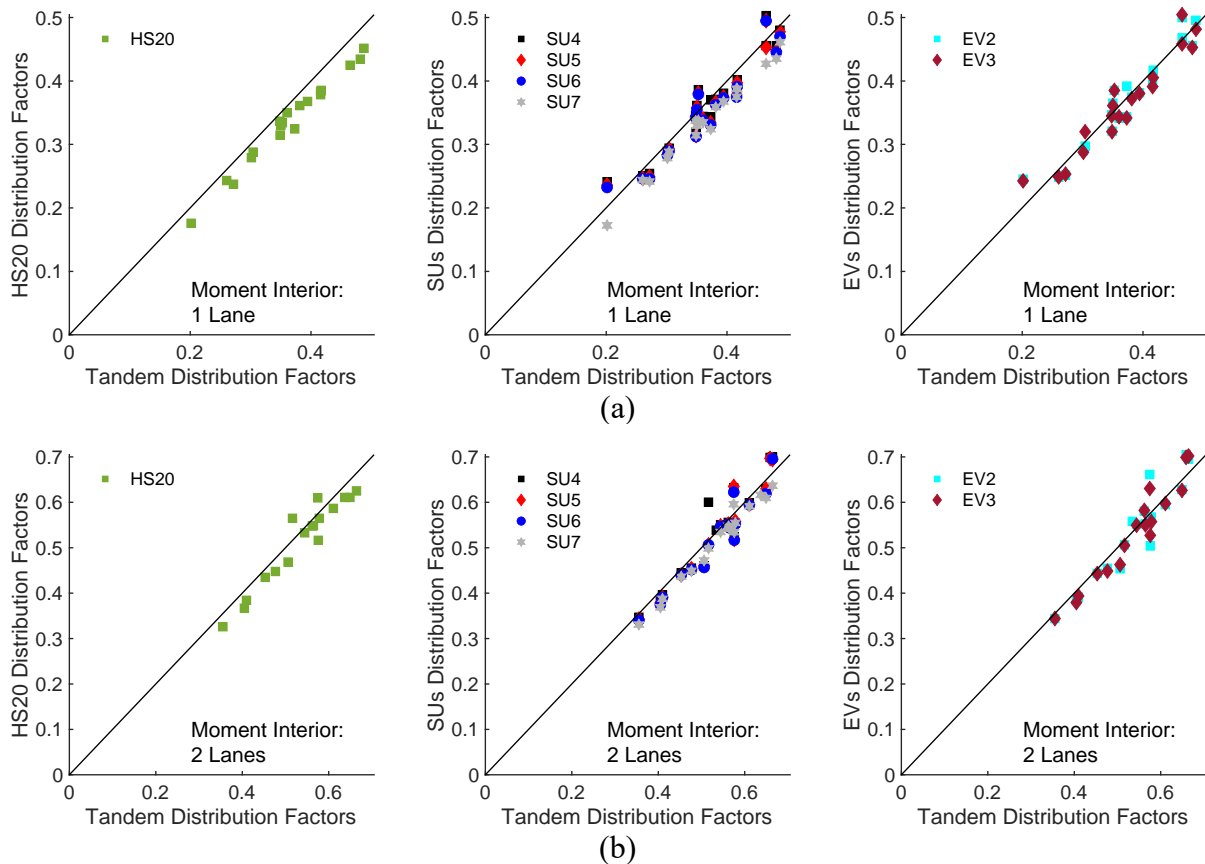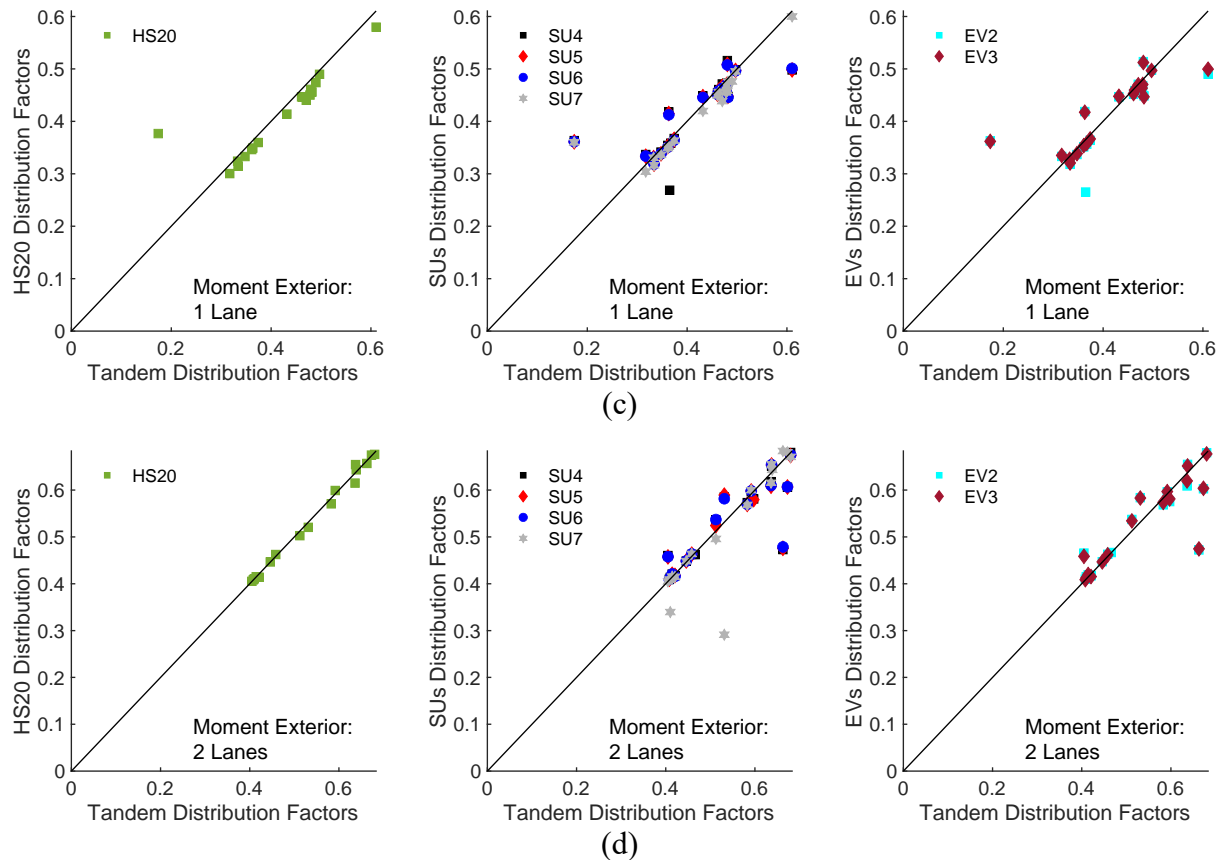
Figure 6-4. Comparison of moment DFs for tandem and other trucks: interior girders (a) one lane and (b) two lanes, and exterior girders (c) one lane and (d) two lanes loaded cases.

Figure 6-5(a) and (b) compares the shear DFs of interior girders for the one lane and two lanes loaded cases, respectively. Other truck types are not found to be significant for interior girders, with tandem loading often producing the largest shear effects in both one- and two-lane loading scenarios. However, these trucks produce significant increases in shear DFs for the exterior girders when compared to tandem loading for some cases as shown in Figure 6-5(c) and (d). For one-lane loaded case, for 17 bridges out of 21, the HS-20, SU, or EV trucks govern the computation of shear DF for the exterior girders. For five of these 17 bridges controlled by these trucks (HS-20, SU, or EV), the shear DFs for exterior girders are higher by 20% or more compared with those obtained under tandem loading. These increase ranges from 25% to 107%. For two-lane loaded case, the shear DF for exterior girders for 16 bridges were governed by SU or EV trucks rather than tandem loading. However, for most of these bridges, there is only slight increase in the shear DF. The increase in the shear DFs is more than 5% for only five bridges, with a maximum increase of 31%. The higher increases in shear DFs observed for exterior girders compared to interior girders can

be attributed to the fact that the truck positioning that causes the worst shear effects is typically when the truck wheels are at the support. As a result, the bridge girders closest to the truck wheels carry a greater share of the load.

In general, the design truck or tandem mostly governed the moment DFs for both interior and exterior girders and shear DFs for interior girders. However, the shear DFs for external girders on bridges with various girder spacings and span lengths, for both one and two lanes loaded cases, were controlled by the EV and the SUs.

(a)

(b)
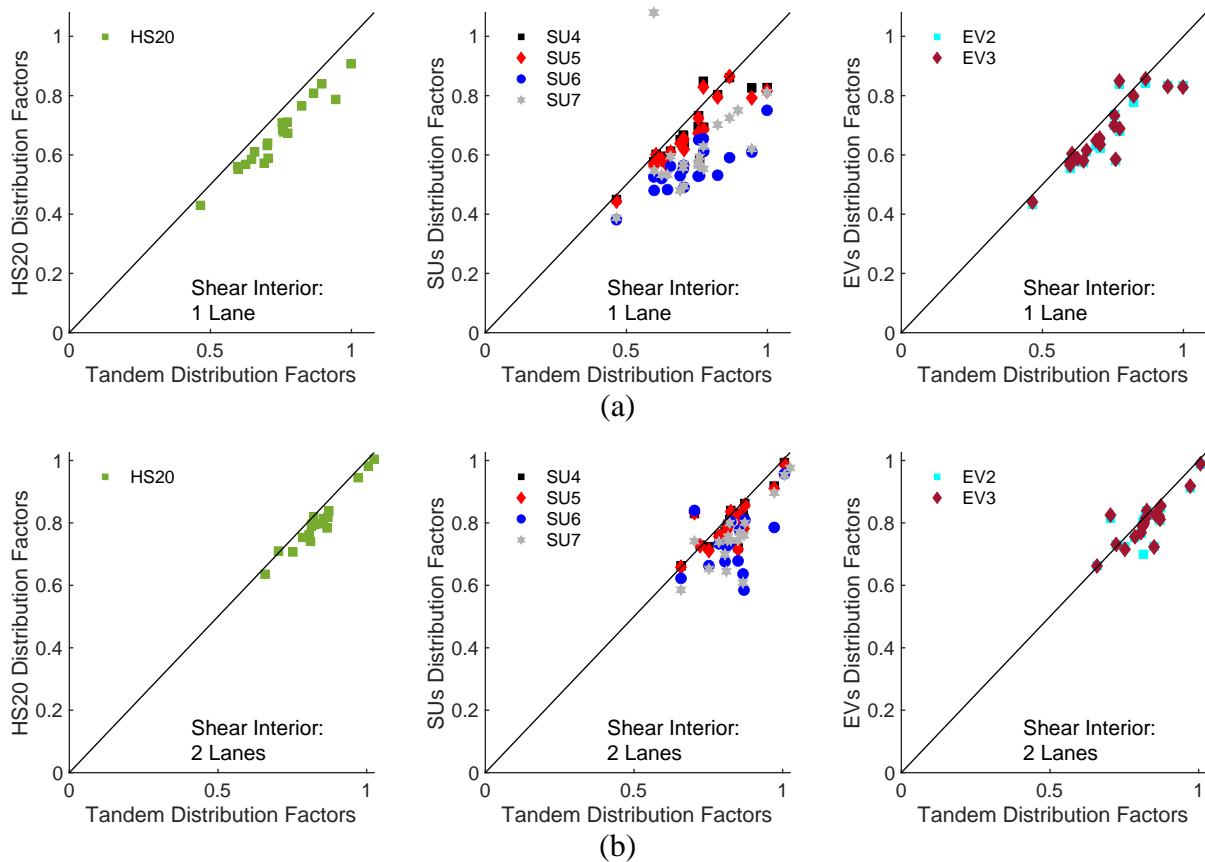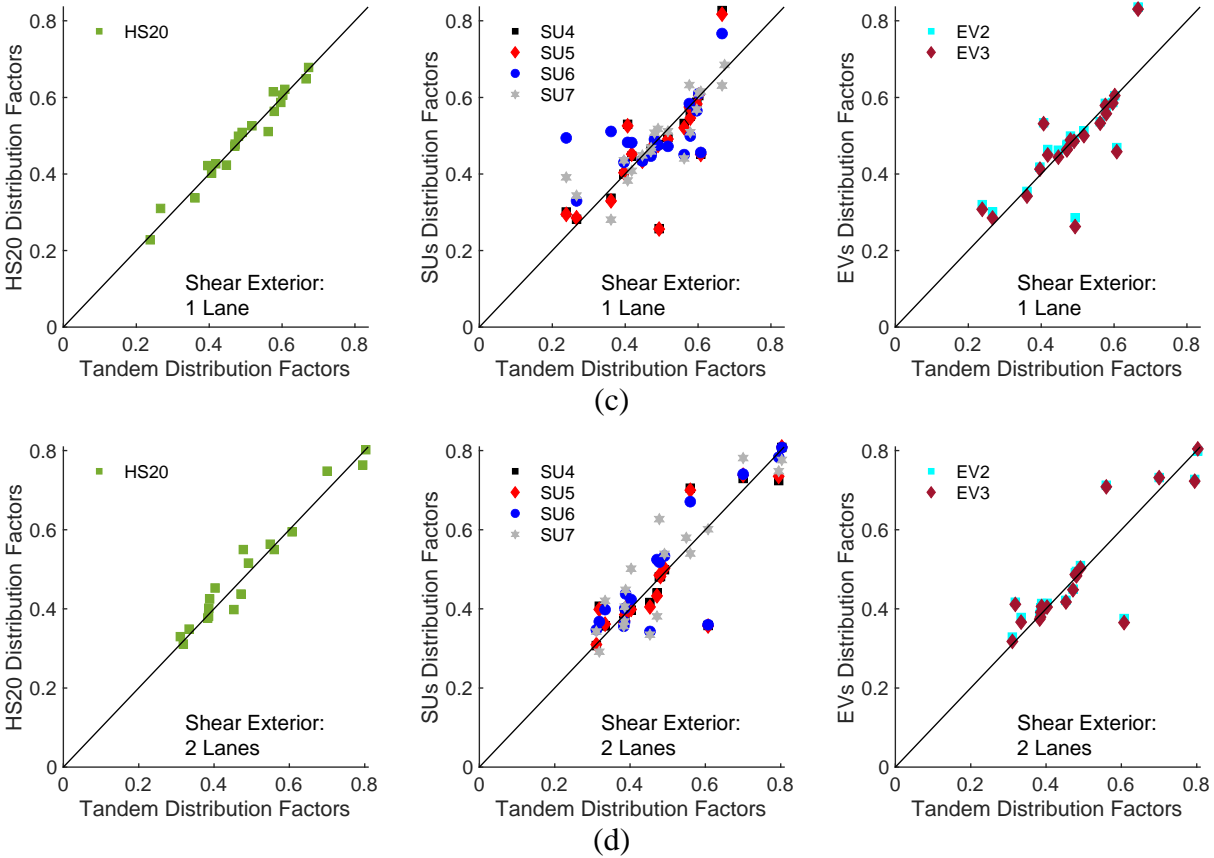
Figure 6-5. Comparison of shear DFs for tandem and other trucks: interior girders (a) one lane and (b) two lanes, and exterior girders (c) one lane and (d) two lanes loaded cases.

6.4.2   Relation between bridge parameters and governing truck loading

To obtain an understanding on the relationship between the bridge design parameters and the truck loading governing the calculation of the DF, the DFs calculated for each bridge under different truck loadings are compared in this section. This comparison was carried out only for the shear effects of the exterior girders. This is due to the fact that the tandem truck governs the DFs for moment effects of both interior and exterior girders as well as the shear effects of the interior girders as discussed in the previous section.

To facilitate the comparison, a parameter called *DF Ratio* is defined as:

$$DF\ Ratio = \frac{[DF]_{SUs\ or\ EVs}}{[DF]_{HS20\ or\ Tandem}} \tag{3}$$

which is the ratio of the governing (largest) shear DF obtained from SU trucks and EVs to the governing shear DF obtained from HS20 or tandem loading. This ratio is calculated for each bridge and is plotted against bridge span length for one lane and two lanes loaded cases in Figure 6-6(a) and (b) and plotted against girder spacing in Figure 6-6(c) and (d). The span length and girder spacing were selected as bridge design parameters as they typically play an important role in load distribution behavior of girder bridges. A *DF Ratio* higher than one indicates that the computation of the DF for this bridge is governed by the SU trucks or EVs. As shown in Figure 6-6, most of the bridges has a DF Ratio greater than one for the shear effects on exterior girder for both one- and two-lane loaded cases. As can be seen from Figure 6-6(a), the *DF Ratio* attains higher values for bridges with relatively short span length for one-lane loaded case. This indicates that the SU trucks or EVs can be more critical for shear effects of short span bridges. On the other hand, there is no clear relationship between girder spacing and the *DF Ratio* for both one-lane and two-lane loaded cases. Note that the DF Ratio values for bridges 6 and 20 are set to be zero for the two lanes cases as shown in Figure 6-6 (b) and (d) because these bridges only have one lane as shown in Table 6-1.
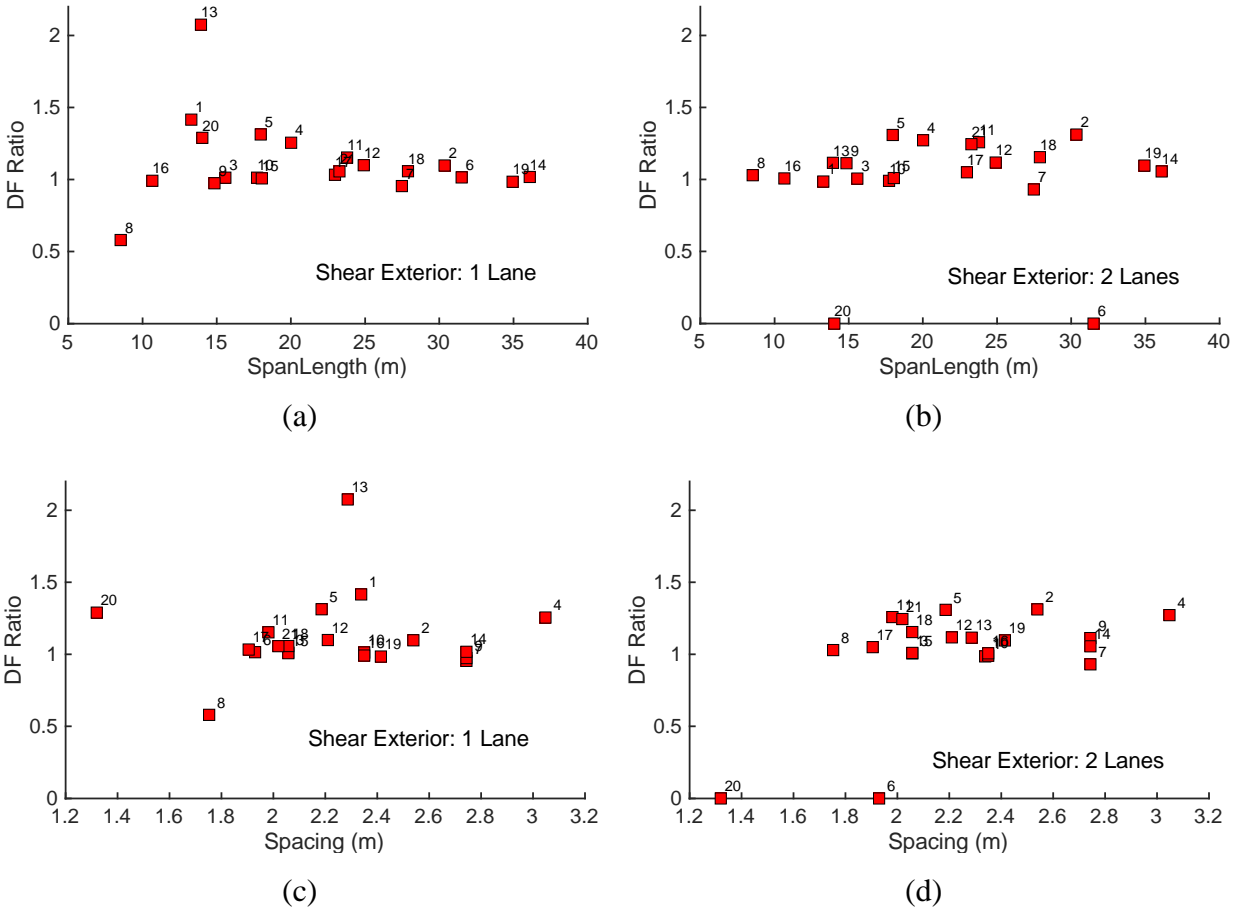
Figure 6-6. *DF Ratio* vs bridge span length for (a) one lane and (b) two lanes loaded cases; and *DF Ratio* vs girder spacing for (c) one lane and (d) two lanes loaded cases.

6.4.3   Effect of Transverse Truck Position

To evaluate the impact of truck position in transverse direction of a bridge on moment and shear DFs, as shown in Figure 6-7, the trucks were positioned in three transverse locations that may have the potential to maximize the girder load effects. The first position is called as "Side" where the closest wheel of truck is 0.61 m (2 ft) away from the parapet. The second position is called "Quarter" where the center of truck is positioned at a quarter of the bridge's clear width. The third position of truck is called "Middle" where the center of truck is positioned at half of the bridge's width. In the analyses, the trucks were positioned at each of three locations described. To assess the impact of different trucks, four vehicle loading (design tandem, HS-20, SU, and EV trucks) were considered. Additionally, the analyses were conducted for both one lane and two lanes loaded cases. As a result, the moment and shear effects were calculated for a total of 48 loading cases on a given bridge. These calculations were performed on all 21 bridges.

(a)

(b)
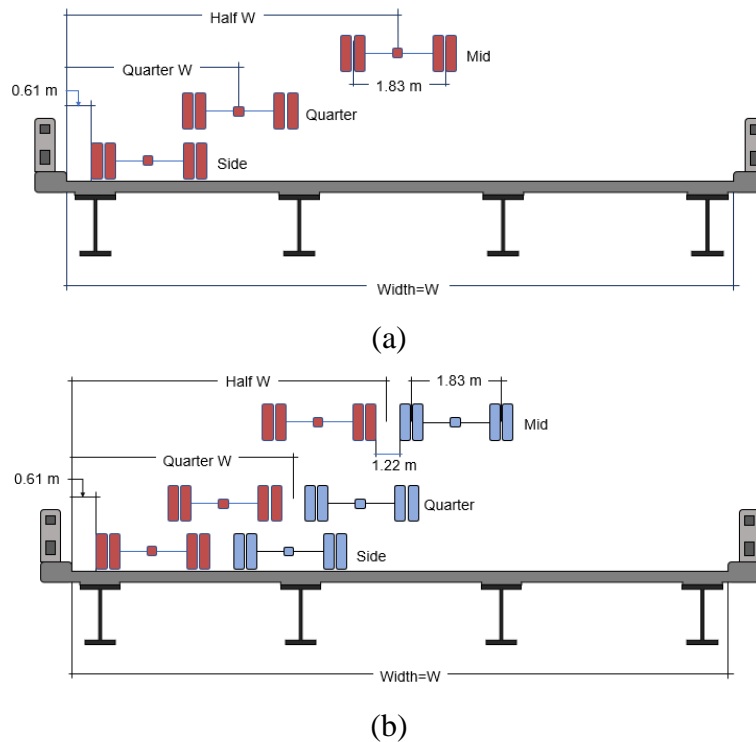
Figure 6-7. Transverse positions of vehicle loading for: (a) one lane loaded and (b) two lanes loaded cases.

Since the results obtained from different truck loadings were similar, only the results obtained from the tandem loading are presented and discussed here. The governing transverse truck position was determined for all bridges, and the results are presented in Figure 6-8 for moment effects and in Figure 6-9 for shear effects. A solid marker indicates the governing truck position for the DF calculation. For the interior girders, the moment DFs are governed by the side position for eight bridges, by the quarter position for ten bridges and by the middle position for three bridges for one lane loaded cases. For the bridges where the quarter or middle position governs the DF computation, the DFs are on average 7% and 4% higher than the side position. The two-lane loaded case for interior moment DFs shows similar outcomes. For exterior girders, the DF calculation is governed by the side position for almost all bridges for one lane loaded case and for most of the cases two-lane loaded cases.

For shear effects, similar observations for the positioning of the truck are made. As shown in Figure 6-9(a) and (b), the quarter position governs shear DFs for interior girders for about half of

the bridges, but with only a difference of 2% and 4% on average for one-lane and two-lane loadings, respectively, when compared to the side position. For the exterior girders, the side position again governs the calculation of DF.

Although for interior girders, the truck positioning other than side position governs several bridge cases, the difference between the DF computed using that particular truck positioning and those obtained from the side positioning is not considerable for both shear and moment effects. Since the side positioning also governs the DF computation for most bridges for exterior girders, the side positioning can be used to compute the moment and shear DFs for both interior and exterior girders.
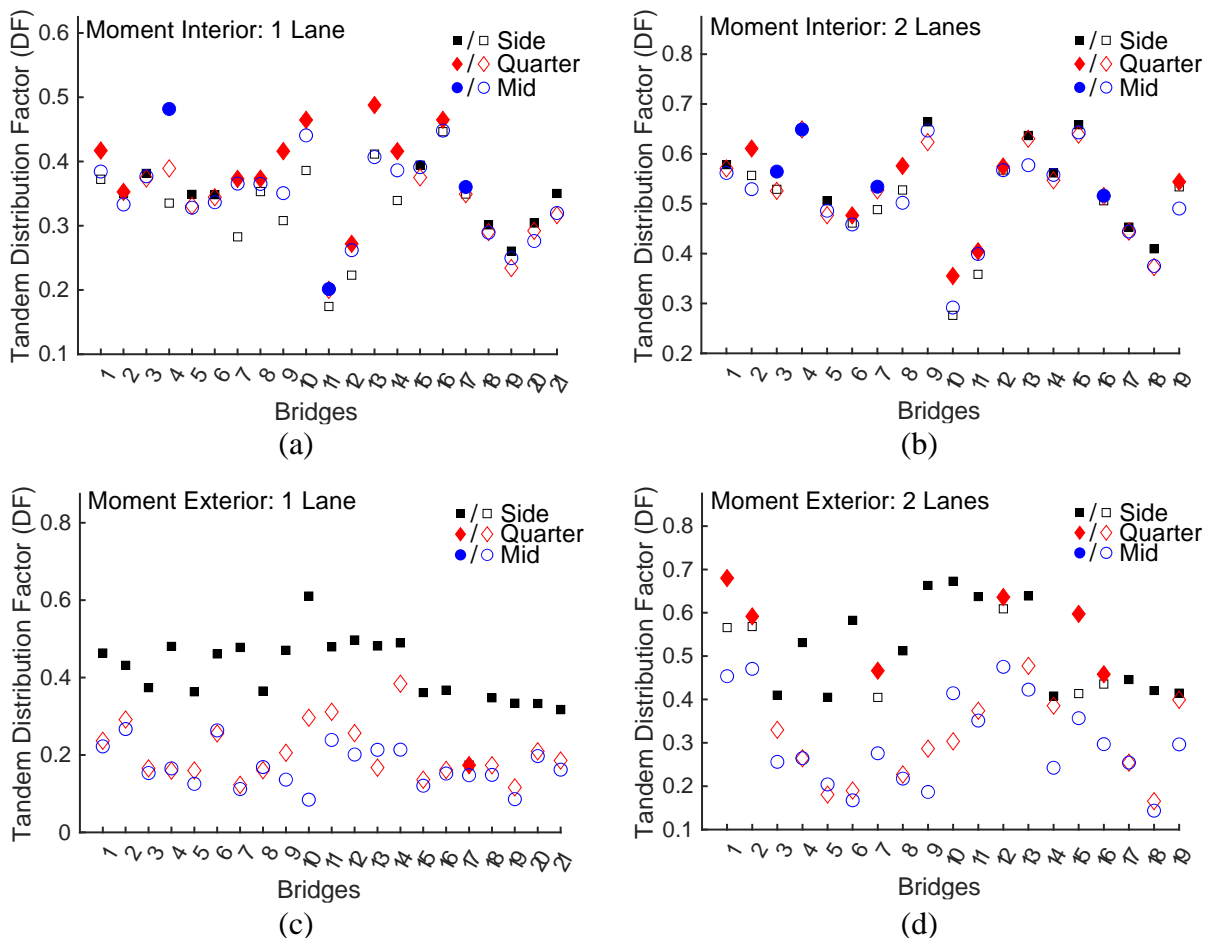
Figure 6-8. Comparison of moment DFs from different transverse trucks position: interior girders (a) one lane and (b) two lanes loaded cases, and exterior girder (c) one lane and (d) two lanes loaded cases.
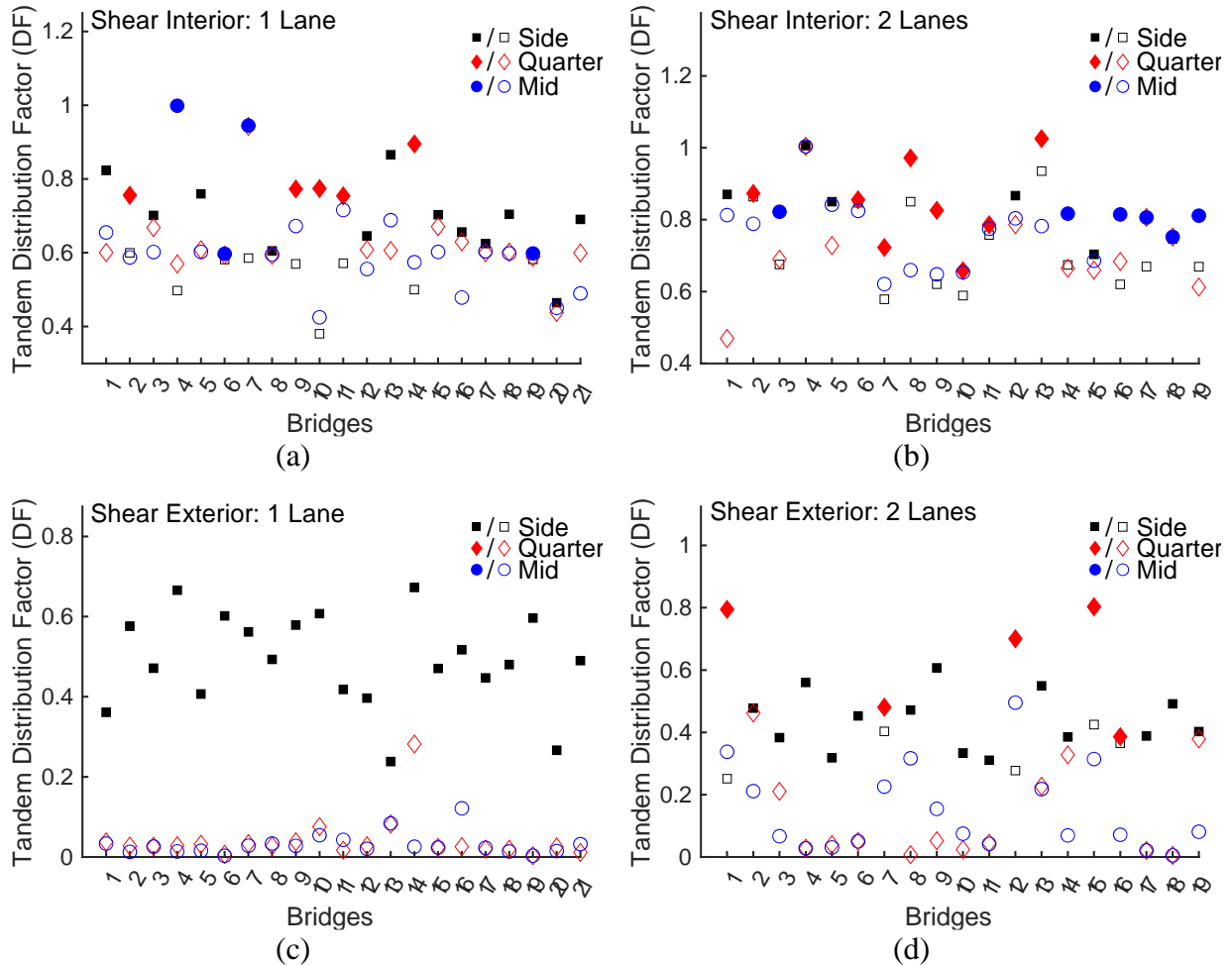
Figure 6-9. Comparison of shear DFs from different transverse trucks position: interior girders (a) one lane and (b) two lanes loaded cases, and exterior girder (c) one lane and (d) two lanes loaded cases.

6.5 Comparison with AASHTO LRFD Distribution Factors

The DFs calculated for the exterior and interior girders through FE analyses as described above are compared to those computed by the AASHTO LRFD equations (Zokaie 2000). Figure 6-10 and Figure 6-11 show the DFs of each of the truck category (HS20/tandem, SUs and EVs) compared to the AASHTO LRFD for moment and shear effects on interior and exterior girders, respectively, under one- and two-lane loading conditions. The results are given for each individual bridge with a marker, and the solid black 1:1 line indicates that the DF derived from both AASHTO LRFD equations and refined analysis using each truck category are identical, while any data point below this unit line indicates the DF computed with AASHTO equations is higher.

Figure 6-10(a)-(d) show that the moment DFs for the interior and exterior girders for the one- and two-lane loaded cases obtained through AASHTO LRFD equations are higher than the DFs computed through refined method of analysis for almost all bridges. Table 6-2 provides the average of the difference between the DFs computed using the AASHTO LRFD equations and the refined analysis using a select vehicle loading (HS20/tandem, SUs and EVs) for all bridges. A negative value in the table indicates a higher distribution factor computed using AASHTO equations. AASHTO LRFD equations results in an average of 17% and 20% higher values for interior girder moment DFs for one lane and two lane loaded cases, respectively compared with those obtained from the refined analysis using tandem or HS20 trucks. For the exterior girders, the same differences in the moment DFs are 39% and 28%. Note that when the SU trucks are used in the analysis, the average differences between the DFs obtained AASHTO LRFD equations and refined analyses are very similar to the results of tandem/HS20 truck loading case. On the other hand, when the EVs are used in the analysis, the average differences increase, indicating that the tandem/HS20 or SU trucks produce more critical DF values than the EVs.

(a)

(b)

Figure 6-10: Comparison of moment DF computed through refined analysis versus code equations: interior girders (a) one lane and (b) two lanes loaded cases, and exterior girder (c) one lane and (d) two lanes loaded cases.

Table 6-2. Average of percent difference between the DFs computed from AASHTO LRFD and those from refined analyses

	One lane loaded				Two-lane loaded			
	Interior girder		Exterior girder		Interior girder		Exterior girder	
	Moment	Shear	Moment	Shear	Moment	Shear	Moment	Shear
HS20/Tandem	-17%	7%	-39%	-28%	-20%	-7%	-28%	-33%
SU	-18%	4%	-40%	-24%	-20%	-9%	-27%	-29%
EVs	-21%	-6%	-43%	-32%	-25%	-14%	-32%	-37%

For shear effects, the AASHTO LRFD equations are found to be conservative for the calculation of DFs for exterior girders for both one-lane and two-lanes loaded cases as shown in Figure 6-11(c) and (d). Compared with the results obtained from the refined analysis, the AASHTO LRFD equations results in higher values ranging from 24% to 32% for different truck categories for one-lane loaded case and from 29% to 37% for two lanes loaded case. The lowest differences between the AASHTO LRFD equations and refined analysis are observed for the SU trucks, indicating that they can be more critical than the design truck or EVs in computing the shear DFs for exterior girders. For the interior girders, the AASHTO LRFD equations are still found to be conservative for two lanes loaded case but with a lower difference between the DFs obtained from AASHTO equations and refined analyses. The one lane loaded case of interior girders, the refined analyses result in an average of 7% and 4% higher values than the DFs calculated from the AASHTO LRFD equations when tandem/HS20 and the SUs are used, respectively.

(a)

(b)
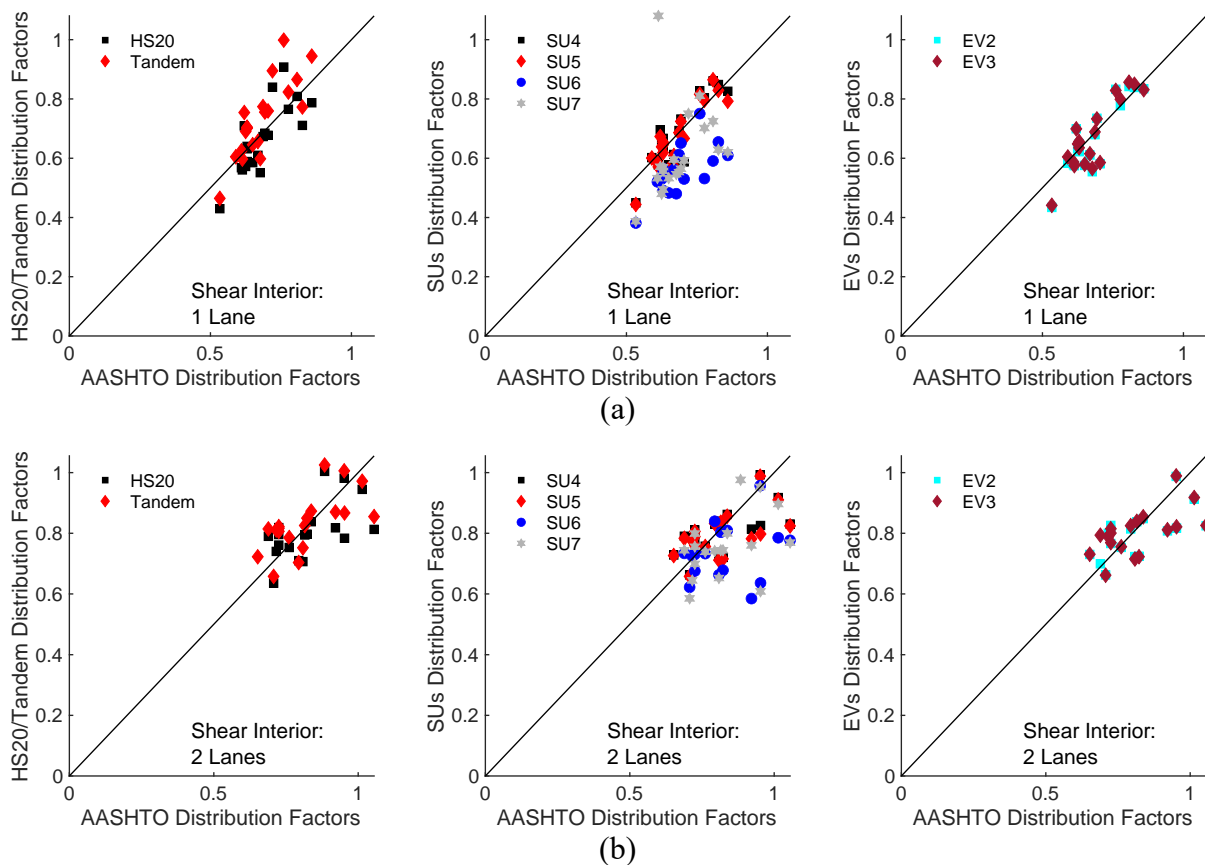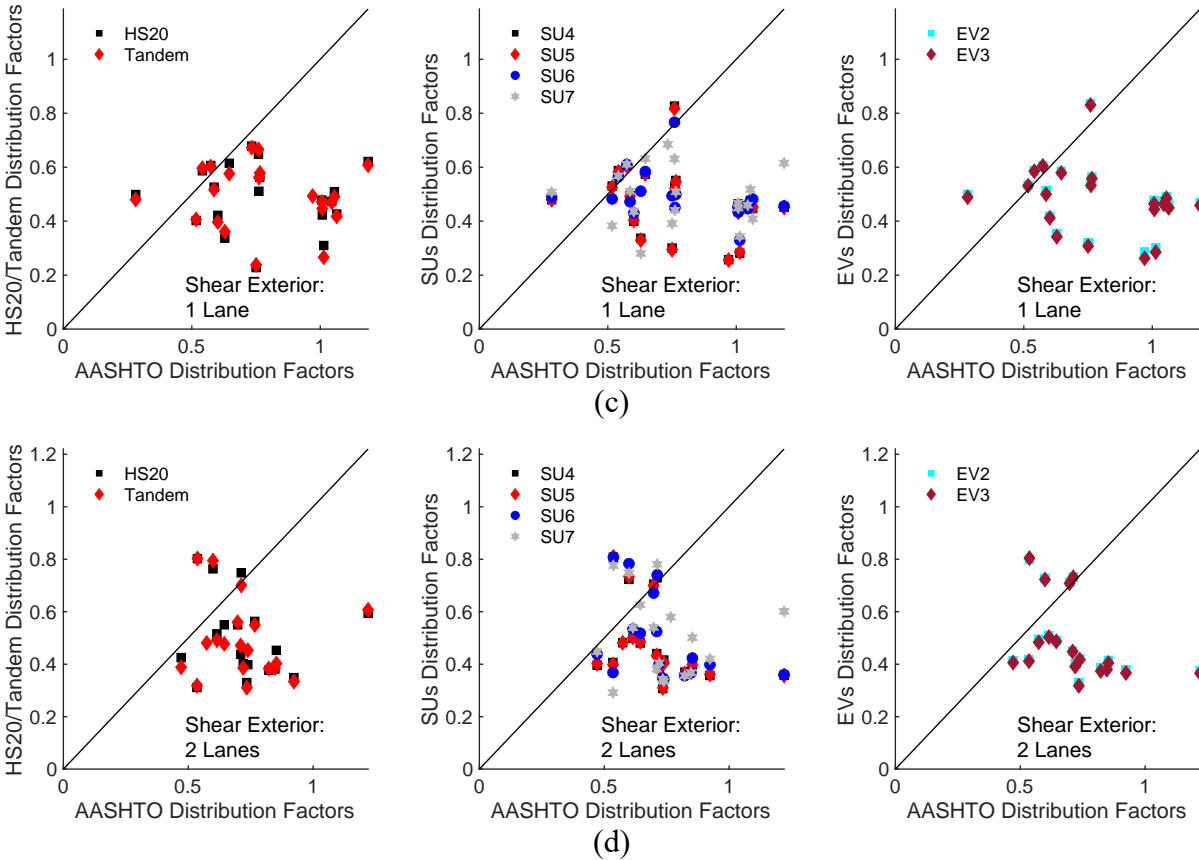
Figure 6-11: Comparison of shear DF computed through refined analysis versus code equations: interior girders (a) one lane and (b) two lanes loaded cases, and exterior girder (c) one lane and (d) two lanes loaded cases.

Since the load rating factors and DFs are inversely proportional, as described in Equation 1, a decrease in the DFs will result in an increase in the rating factor. Therefore, one can easily obtain an understanding on the effect of DF on the bridge load rating when the DF is determined using refined method of analysis rather than AASHTO calculations.

6.6   Prediction Equations for Distribution Factors

6.6.1   Regression Equations

The DFs derived from refined analyses of the selected bridges were used to assess the geometric factors impacting load distribution behavior and to create linear regression models based on these factors. As a result, linear regression models were created to predict the DFs for steel girder bridges using four key factors that define the geometric characteristics of bridges. The statistical analysis software "R" was used to create regression models for the DFs (Team, R. C.

2013). Models were developed to predict shear and moment DFs for interior and exterior girders under one and two lane loaded conditions. The girder spacing, span length, skew angle, number of girders, moment of inertia of the girders, girder depth, slab thickness, and deck overhang are some of the geometric properties of the bridge that were taken into account when developing the models. In each case, only the four most important parameters were chosen to develop the prediction models. To improve the precision of the prediction models, the interaction between the four factors that were chosen was taken into account while creating the regression equations. The remaining 20% were utilized for model testing and validation, while the remaining 80% of the improved analytical findings were employed as a training set. Table 6-3 and Table **6-4** demonstrate the generated regression models for predicting the DFs for moment and shear DFs, as well as the coefficient of determination or R-squared (R^2) (Herzberg 1969). In these tables, the regression equations in these two tables do not include the terms that have two parameters interacting with each other. The entire equations that include these interacting parameters are in the Appendix. In the tables, the bounds of each parameter for which the regression equations are developed are also provided.

Table 6-3. Prediction equations for moment DFs

Girder/Loading	R^2	Prediction Equations for Moment DF
Interior/One Lane	0.84	$DF_{M\text{-}int\text{-}1L} = 0.364 - 0.005L + 0.115S - 0.001\theta - 0.025N_b$
		where $13 < L < 26$; $1.9 < S < 2.7$; $0 < \theta < 45$; $4 < N_b < 6$
Interior/Two Lanes	0.76	$DF_{M\text{-}int\text{-}2L} = -0.508 - 0.061L + 0.584S + 0.019\theta + 5.911O_v$
		where $13 < L < 26$; $1.9 < S < 2.7$; $0 < \theta < 45^9$; $0.15 < O_v < 0.31$
Exterior/One Lane	0.70	$DF_{M\text{-}ext\text{-}1L} = 0.843 + 0.271S - 0.055t_s - 0.005\theta - 0.057N_b$
		where $1.9 < S < 2.7$; $17 < t_s < 23$; $0 < \theta < 45$; $4 < N_b < 6$
Exterior/Two Lanes	0.84	$DF_{M\text{-}ext\text{-}2L} = -0.313 - 0.060L + 0.479S + 0.025\theta + 3.710O_v$
		where $13 < L < 26$; $1.9 < S < 2.7$; $0 < \theta < 45$; $0.15 < O_v < 0.31$

L: span length (m); S: girder spacing (m); N_b: number of girders; θ: skew in the bridge (degrees); I: moment of inertia of girders (cm^4); t_s: slab thickness (cm); d: girder depth (cm); O_v: overhang (m).

Table 6-4. Prediction equations for shear DFs

Girder/Loading	R^2	Prediction Equations for Shear DF
Interior/One Lane	0.73	$DF_{S\text{-}int\text{-}1L} = 3.25 + 6.769 \times 10^{-3}L - 1.51S - 0.078t_s - 0.054N_b$
		where $13 < L < 26$; $17 < t_s < 23$; $4 < N_b < 6$; $0.6 < O_v < 1$
Interior/Two Lanes	0.90	$DF_{S\text{-}int\text{-}2L} = -3.80 - 0.162L + 1.624S + 0.063d + 0.418N_b$
		where $13 < L < 26$; $1.9 < S < 2.7$; $72 < d < 91$; $4 < N_b < 6$
Exterior/One Lane	0.85	$DF_{S\text{-}ext\text{-}1L} = 0.03 + 0.19S + 1.672 \times 10^{-3}d - 0.001\theta - 0.224O_v$
		where $13 < L < 26$; $1.9 < S < 2.7$; $72 < d < 91$; $0.15 < O_v < 0.31$
Exterior/Two Lanes	0.70	$DF_{S\text{-}ext\text{-}2L} = -3.854 - 0.290L + 0.238t_s + 0.121d - 0.250N_b$
		where $13 < L < 26$; $17 < t_s < 23$; $72 < d < 91$; $4 < N_b < 6$

L: span length (m); S: girder spacing (m); N_b: number of girders; θ: skew in the bridge (degrees); I: moment of inertia of girders (cm^4); t_s: slab thickness (cm); d: girder depth (cm); O_v: overhang (m).

The developed regression models were used to compute the moment and shear DFS. The results were compared to those derived from the refined analysis to validate the prediction equations as shown in Figure 6-12 and Figure 6-13. In addition to solid black 1:1 line, the 10% error limits between the refined analysis and regression model results are also shown in the figures as dashed lines. The blue circle markers illustrate the results for bridges with parameters that are within the regression model's parameter ranges, whereas the red star markers represent bridges with characteristics that are outside bounds of the models. The number next to the marker indicates the bridge number given in Table 6-1. The findings show that the developed prediction equations provide an acceptable estimate of the load distribution. For most bridges, the prediction errors of regression models are less than 10% for both the moment and shear DFs. The findings also show that the constructed regression models can accurately predict the DFs for bridges with the parameters outside of the model's parameter ranges.
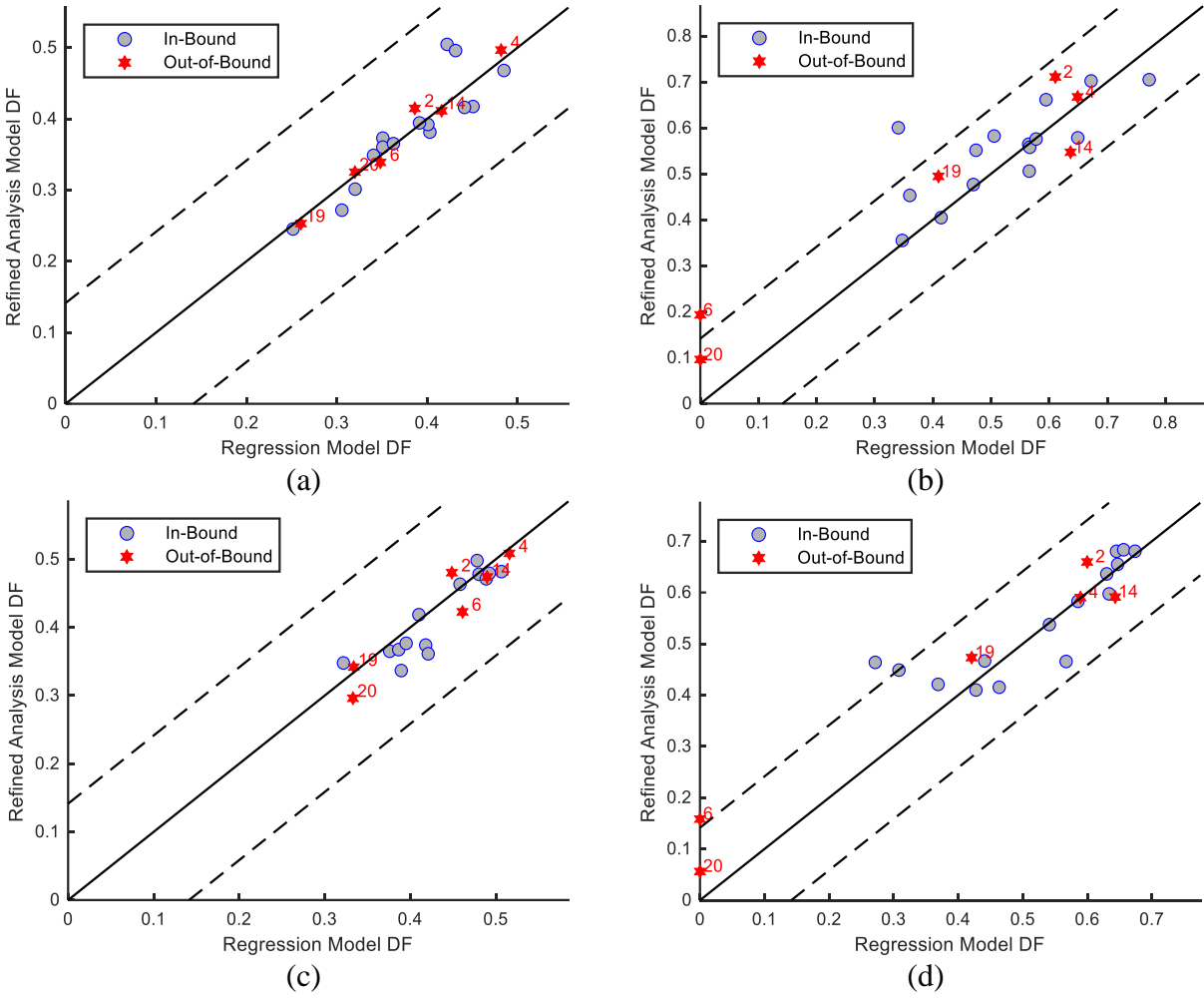
Figure 6-12. Comparison between moment DFs from refined analysis and regression model for: interior girders (a) one lane and (b) two lanes loaded cases, and exterior girder (c) one lane and (d) two lanes loaded cases.

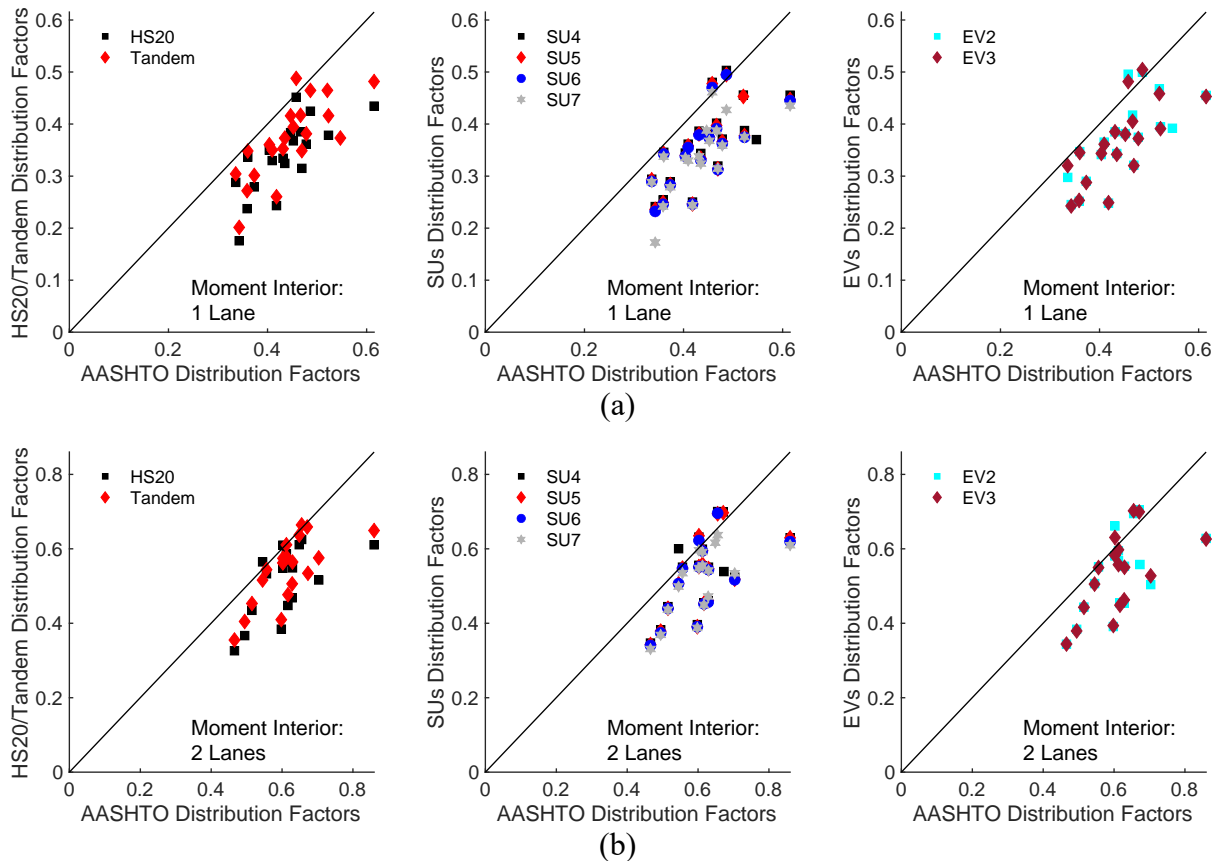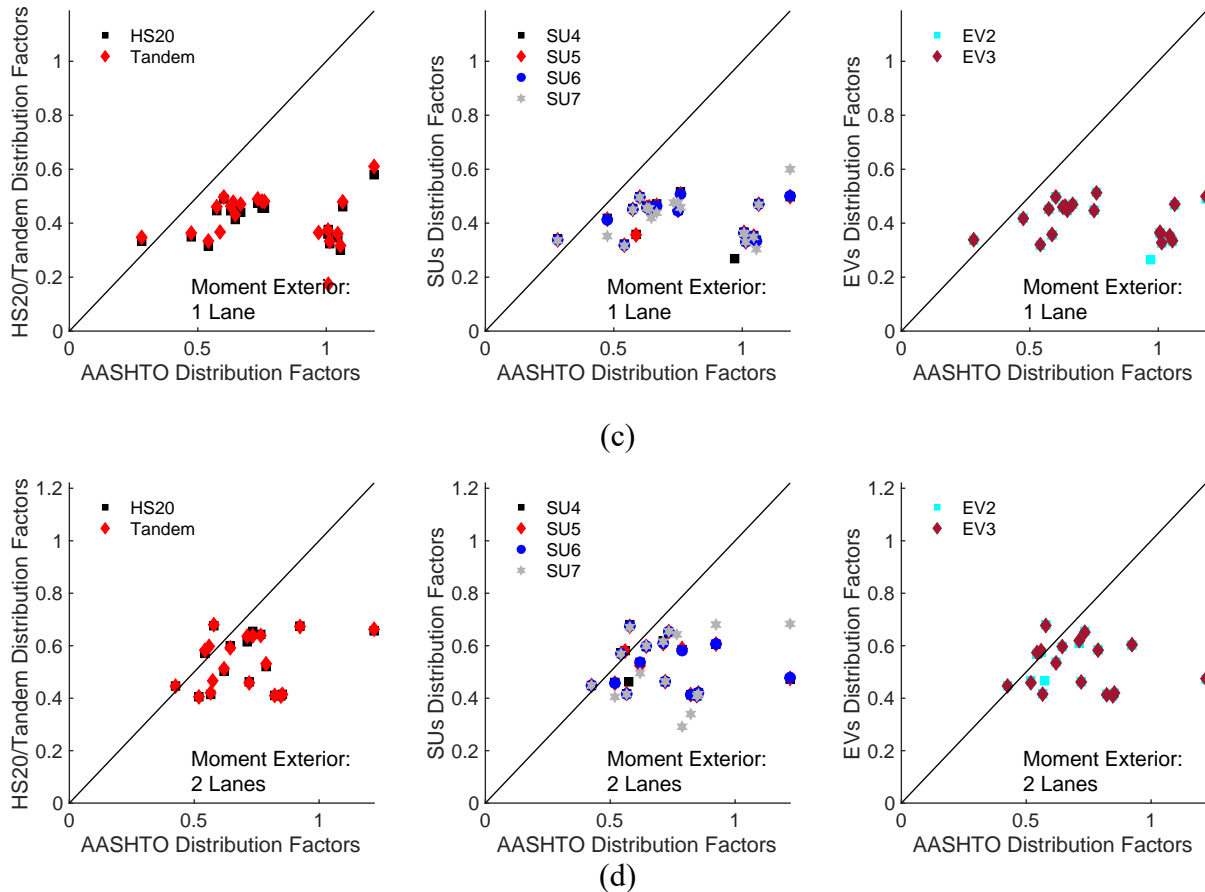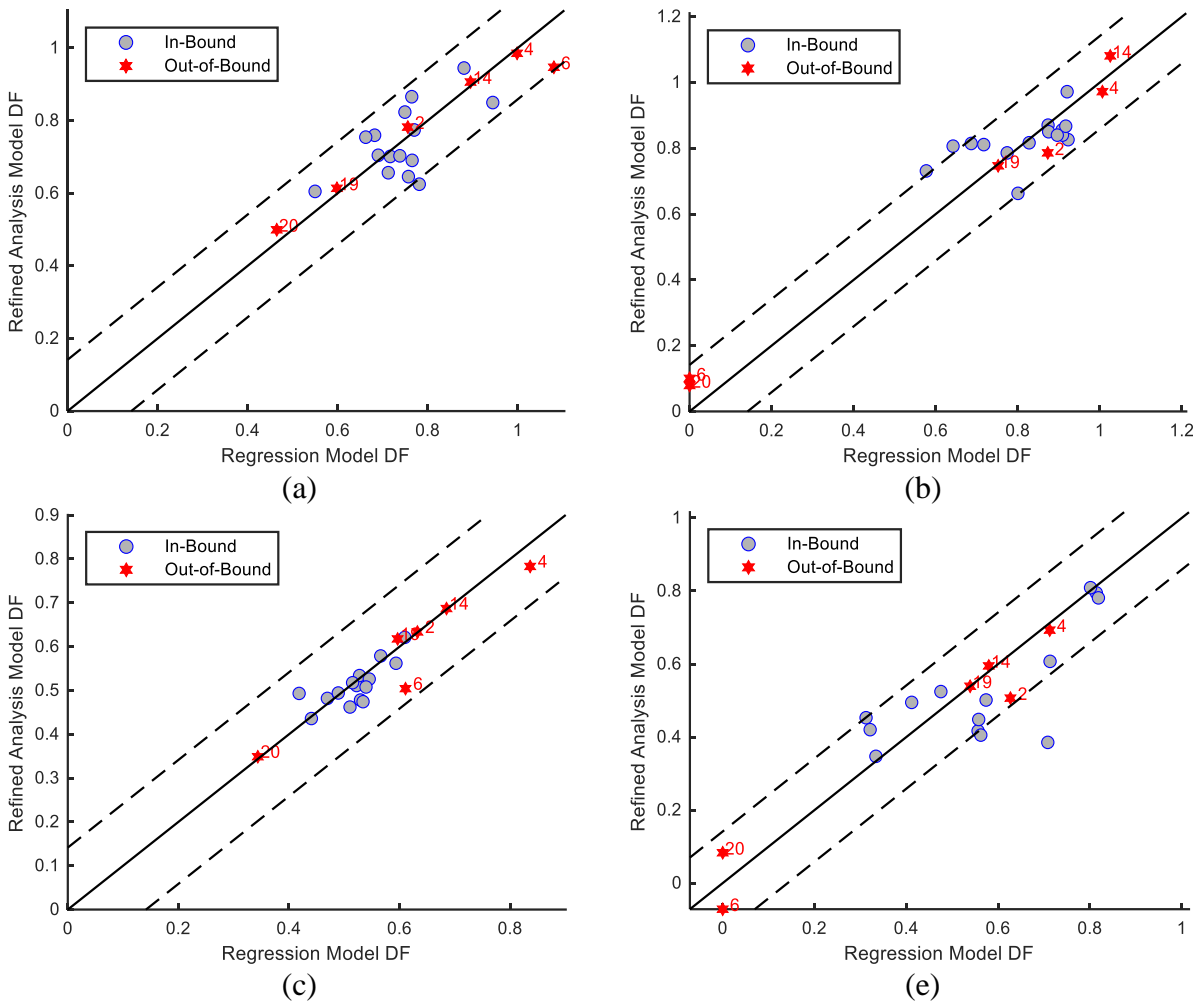**Figure 6-13.** Comparison between shear DFs from refined analysis and regression model for: interior girders (a) one lane and (b) two lanes loaded cases, and exterior girder (c) one lane and (d) two lanes loaded cases.

6.6.2   Effects of Geometrical Parameters

In this section, the effects of bridge geometrical characteristics on the obtained results is evaluated. To this end, the distribution factors computed using the develop regression models were compared with those computed using the AASHTO LRFD equations and the percent change in the DF (Δ*DFs*) was calculated using Equation (5-2). The look up tables were created to illustrate the variation of Δ*DFs* within the parameter boundaries. The obtained results are presented in Table 6-5 and Table 6-6 for moment effects and Table 6-7 and Table 6-8 for shear effects. These tables illustrate the impacts across the parameter space for distribution factor. The discussion focuses on distribution factor change with reductions in distribution factor.

The primary parameters associated with the change in distribution for interior moment are number of girders, girder depth, girder spacing, and skew. Table 6-5 shows that the change in distribution factor for interior moment can be reduced as the number of girders increases. Additionally, bridges with large skew angles will experience a greater change in distribution factor across all parameters. The greatest reduction, however, is associated with bridges with a shallow girder depth. As girder depth increases, the potential of a reduction in the distribution factor decreases. Increased girder depth, on the other hand, can result in an increase in distribution factors, particularly for bridges with a small number of girders. The girder spacing has very little effect on the change in distribution factors for bridges with skew.

Table 6-5 Percent Change in Distribution Factors for Interior Moment for Steel Girder Bridges

$d =$	25				30				35				40				45			
$N_b =$	4	5	6	7	4	5	6	7	4	5	6	7	4	5	6	7	4	5	6	7
θ=0 S=6	-1	-5	-9	-13	1	-3	-8	-12	4	-2	-7	-12	6	0	-6	-12	9	2	-5	-12
S=7	-2	-4	-7	-10	0	-3	-7	-11	2	-3	-7	-11	3	-2	-7	-12	5	-1	-7	-13
S=8	-2	-3	-5	-7	-1	-4	-6	-9	-1	-4	-7	-11	0	-4	-8	-13	1	-4	-9	-14
S=9	-2	-2	-3	-4	-2	-4	-5	-7	-3	-5	-7	-10	-3	-6	-9	-13	-4	-8	-12	-16
θ=15 S=6	-6	-13	-20	-26	0	-8	-15	-22	6	-2	-10	-19	13	3	-6	-15	19	9	-1	-11
S=7	-6	-11	-17	-22	0	-7	-13	-19	5	-2	-9	-17	10	2	-6	-14	16	7	-2	-11
S=8	-5	-9	-14	-18	0	-6	-11	-17	4	-2	-8	-15	8	1	-6	-13	13	5	-3	-11
S=9	-4	-7	-11	-14	0	-5	-9	-14	3	-2	-8	-13	6	0	-6	-12	9	3	-4	-11
θ=30 S=6	-11	-21	-30	-40	-1	-12	-22	-32	9	-2	-14	-25	19	7	-5	-17	29	16	3	-10
S=7	-10	-18	-26	-35	0	-10	-19	-28	9	-2	-12	-22	18	7	-4	-15	27	15	3	-9
S=8	-8	-15	-23	-30	0	-8	-16	-24	8	-1	-10	-19	17	7	-3	-13	25	14	3	-8
S=9	-6	-12	-19	-25	1	-6	-13	-21	8	0	-8	-16	15	6	-3	-11	22	13	3	-7
θ=45 S=6	-16	-29	-41	-54	-3	-16	-29	-42	11	-3	-17	-31	25	10	-5	-20	39	23	7	-8
S=7	-14	-25	-36	-48	-1	-13	-25	-37	12	-1	-14	-27	25	11	-3	-17	38	23	8	-6
S=8	-11	-21	-31	-42	1	-10	-21	-32	13	1	-11	-23	25	12	-1	-14	37	23	9	-4
S=9	-8	-17	-26	-36	3	-7	-17	-28	14	3	-8	-19	25	13	1	-11	35	23	10	-3

θ = skew in the bridge, in degrees; S = girder spacing, in feet; d = girder depth, in inches; N_b = number of girders

The primary parameters associated with the change in distribution factor for exterior moment are number of girder depth, span length, skew angle, and slab thickness. Table 6-6 shows that change in distribution factors for exterior moment tend to decrease less as the slab thickness increases. A decrease in distribution factor is observed as span length increases, with a larger increase observed for larger girder depths. As the skew angle increases, the potential of reducing distribution factors decreases which leads to the opportunity to increase RF above 1.0.

Table 6-6 Percent Change in Distribution Factors for Exterior Moment for Steel Girder Bridges

	$d =$	25			30			35			40			45		
	$t_s =$	7	8	9	7	8	9	7	8	9	7	8	9	7	8	9
$\theta=0$	L=45	-29	-16	-3	-37	-24	-10	-44	-31	-18	-52	-39	-26	-59	-46	-33
	L=55	-24	-11	3	-31	-18	-5	-39	-26	-13	-47	-33	-20	-54	-41	-27
	L=65	-18	-5	8	-26	-13	0	-34	-20	-7	-41	-28	-15	-48	-35	-22
	L=75	-13	0	13	-21	-7	6	-28	-15	-2	-36	-23	-9	-43	-30	-17
	L=85	-8	6	19	-15	-2	11	-23	-10	4	-31	-17	-4	-38	-24	-11
$\theta=15$	L=45	-26	-13	1	-34	-20	-7	-41	-28	-15	-49	-36	-22	-56	-43	-29
	L=55	-21	-7	6	-28	-15	-2	-36	-23	-9	-43	-30	-17	-51	-37	-24
	L=65	-15	-2	11	-23	-10	4	-30	-17	-4	-38	-25	-12	-45	-32	-19
	L=75	-10	3	17	-17	-4	9	-25	-12	1	-33	-19	-6	-40	-27	-13
	L=85	-4	9	22	-12	1	14	-20	-6	7	-27	-14	-1	-34	-21	-8
$\theta=30$	L=45	-23	-9	4	-30	-17	-4	-38	-25	-11	-46	-32	-19	-53	-39	-26
	L=55	-17	-4	9	-25	-12	2	-33	-19	-6	-40	-27	-14	-47	-34	-21
	L=65	-12	1	15	-20	-6	7	-27	-14	-1	-35	-22	-8	-42	-29	-15
	L=75	-7	7	20	-14	-1	12	-22	-9	5	-29	-16	-3	-37	-23	-10
	L=85	-1	12	25	-9	4	18	-16	-3	10	-24	-11	2	-31	-18	-5
$\theta=45$	L=45	-19	-6	7	-27	-14	-1	-35	-21	-8	-42	-29	-16	-49	-36	-23
	L=55	-14	-1	12	-22	-8	5	-29	-16	-3	-37	-24	-10	-44	-31	-18
	L=65	-9	5	18	-16	-3	10	-24	-11	3	-32	-18	-5	-39	-25	-12
	L=75	-3	10	23	-11	2	16	-19	-5	8	-26	-13	0	-33	-20	-7
	L=85	2	15	29	-6	8	21	-13	0	13	-21	-8	6	-28	-15	-1

θ = skew in the bridge, in degrees; L = span length, in feet; d = beam depth, in inches; t_s = slab thickness, in inches

The primary parameters associated with the change in distribution factor for interior shear are number of girder depth, overhang length, skew angle, and number of beams. Table 6-7 shows that bridges with characteristics that are within the defined bounds have higher distribution factors. Bridges with high skew angles and girder depths less than 30 inches may have distribution factors reduced. The magnitude of this reduction increases as the number of girders increases. Increases in girder depth almost always result in an increase in distribution factor.

Table 6-7 Percent Change in Distribution Factors for Interior Shear for Steel Girder Bridges

	$N_b =$	4			5			6			7			8		
	$Ov =$	0.4	0.8	0.12	0.4	0.8	0.12	0.4	0.8	0.12	0.4	0.8	0.12	0.4	0.8	0.12
	$d=25$	-6	10	25	1	14	27	7	18	28	14	22	30	20	26	31
	$d=30$	-1	12	26	4	15	26	10	18	27	15	21	27	20	24	28
$\theta=0$	$d=35$	3	15	27	8	17	26	12	19	25	16	20	25	21	22	24
	$d=40$	8	17	27	11	18	25	14	19	24	18	20	22	21	21	20
	$d=45$	12	20	28	14	20	25	17	19	22	19	19	20	21	19	17
	$d=25$	-8	4	17	-5	5	15	-3	5	12	0	5	10	3	5	8
	$d=30$	1	12	22	3	11	19	5	10	16	6	10	13	8	9	10
$\theta=15$	$d=35$	11	19	28	12	18	24	12	16	20	13	14	15	14	12	11
	$d=40$	20	27	34	20	24	28	20	21	23	19	19	18	19	16	13
	$d=45$	30	35	39	28	31	33	27	27	27	26	23	20	24	19	14
	$d=25$	-11	-1	8	-12	-5	2	-13	-8	-3	-14	-11	-9	-14	-15	-15
	$d=30$	4	11	19	2	7	12	0	3	5	-2	-2	-2	-4	-6	-9
$\theta=30$	$d=35$	18	24	30	15	19	22	12	13	14	9	8	6	6	2	-2
	$d=40$	33	37	40	29	30	31	25	24	23	21	17	14	17	11	5
	$d=45$	48	49	51	43	42	41	37	34	31	32	27	21	27	19	11
	$d=25$	-13	-7	0	-18	-14	-10	-23	-21	-19	-27	-28	-29	-32	-35	-38
	$d=30$	6	11	16	1	3	5	-5	-5	-6	-11	-13	-16	-16	-21	-27
$\theta=45$	$d=35$	26	29	31	19	20	20	13	10	8	6	1	-3	-1	-8	-15
	$d=40$	46	46	47	38	36	35	30	26	22	23	16	9	15	6	-3
	$d=45$	65	64	63	57	53	49	48	42	36	39	31	22	30	19	8

θ = skew in the bridge, in degrees; d = beam depth, in inches; N_b = number of girders; Ov = overhang, in feet

The primary parameters associated with the change in distribution factor for exterior shear are moment of inertia, slab thickness, span length, and girder spacing. Table 6-8 shows that distribution factors tend to have a smaller reduction potential as the slab thickness increases. The greatest reductions in distribution factors occur for bridges with a slab thickness of 7 inches and a high girder moment of inertia. The distribution factors for bridges with a slab thickness greater than 7 inches increase as the span length and girder spacing decrease.

Table 6-8 Percent Change in Distribution Factors for Exterior Shear for Steel Girder Bridges

	$t_s =$	7			8			9		
	$S =$	6	7	8	6	7	8	6	7	8
	L=45	-33	-24	-15	18	1	-16	70	26	-18
	L=55	-19	-12	-6	33	13	-6	85	39	-7
I=4500	L=65	-5	-1	3	48	26	3	101	52	4
	L=75	9	11	12	63	38	13	117	66	14
	L=85	24	22	21	78	51	23	133	79	25
	L=45	-46	-35	-25	9	-6	-22	65	23	-19
	L=55	-32	-24	-16	24	6	-12	80	36	-9
I=5500	L=65	-18	-12	-7	39	18	-2	96	49	2
	L=75	-4	-1	2	54	31	7	112	62	13
	L=85	10	11	11	69	43	17	128	76	23
	L=45	-59	-47	-35	0	-14	-28	60	19	-21
	L=55	-45	-35	-26	15	-1	-18	75	33	-10
I=6500	L=65	-31	-24	-17	30	11	-8	91	46	0
	L=75	-17	-12	-8	45	23	2	107	59	11
	L=85	-3	-1	1	60	36	11	123	72	22
	L=45	-72	-58	-45	-9	-21	-34	55	16	-23
	L=55	-58	-47	-36	6	-9	-24	71	29	-12
I=7500	L=65	-44	-35	-27	21	4	-14	86	42	-1
	L=75	-30	-24	-18	36	16	-4	102	56	9
	L=85	-16	-12	-9	51	28	6	118	69	20
	L=45	-85	-70	-54	-18	-29	-40	50	13	-25
	L=55	-71	-58	-46	-3	-16	-30	66	26	-14
I=8500	L=65	-57	-47	-37	12	-4	-20	81	39	-3
	L=75	-43	-35	-28	27	9	-10	97	52	7
	L=85	-29	-24	-19	42	21	0	113	66	18

I = girder moment of inertia, in inches[4]; L = span length, in feet; t_s = slab thickness, in inches; S = girder spacing, in feet

6.7   Summary

In this study, the live load distribution factors for 21 in-service steel girder bridges were computed using refined method of analysis. The study considered the specialized hauling vehicles and emergency vehicles as the vehicle loadings in the refined analysis. The effects of the vehicle loading and its transverse location on the computation of DFs were investigated. The DFs computed through the refined analysis and AASHTO LRFD equation were compared. In addition, regression models were created to estimate the DFs should a refined analysis based on bridge geometry be conducted. The following are the conclusions drawn from the study's findings:

- The moment and shear DFs for interior girders are governed by the design truck or tandem loading. SU and EV trucks, on the other hand, provide a higher DF for exterior girders, especially in one lane loaded case for moment and shear, and two-lane loaded scenarios for shear.

- Since the SU and EV trucks govern the computation of DFs for exterior girders, and the DFs calculated for interior girders using the SU and the EV trucks in refined analysis are very similar to those computed using the design truck and tandem, either the SU or EV trucks, instead of design truck or tandem, can be considered in refined analyses of steel girder bridges to obtain both moment and shear DFs.

- The DFs for interior girders are not affected by the transverse positioning of vehicle in the refined analysis. The largest DFs for exterior girders mostly occur for a side positioning of a truck.

- The moment and shear DFs of most steel girder bridges attain a lower value when they are computed through refined method of analysis compared to the code given equations, except for the interior shear DFs. In comparison to the AASHTO LRFD-based equations, the refined analysis may result in lower moment or shear DFs for exterior girder, indicating a high potential to improve rating factor of such members through refined analysis.

- Using refined analysis, the developed regression models can predict the DFs given certain bridge geometrical characteristics. That prediction has a coefficient of determination of at least 0.70 and can be used as an initial screening tool to obtain an idea about how the DF will change if a refined analysis is employed.

7. EVALUATION OF EFFECTIVE WIDTHS FOR CONCRETE SLAB BRIDGES

7.1 Introduction

In this section, load distribution behavior of 25 in-service reinforced concrete slab bridges was explored using refined method of analysis. The bridges were modeled using 2D plate analysis method and analyzed under either single lane loading or multi-lane loading cases. The load distribution behavior and effective width of each bridge were evaluated and compared with the effective width computed using the AASHTO LRFD equations. The percent changes in effective width of these bridges derived from the refined analyses provided the basis to evaluate the geometric parameters driving the structural response and to develop linear regression models based on these parameters.

7.2 Bridge Selection

Reinforced concrete slab bridges, representing 27% of the total number bridges in the state of Virginia, constituted the main focus of this study. The statistical distributions of concrete slab bridges within the inventory of Virginia DOT (VDOT) inventory based on the span length, deck width and skew angle are shown in Figure 7-1. A total of 25 in-service concrete slab bridges whose characteristics are also shown in Figure 7-1 were selected for this study. In the bridge selection process, the overall inventory characteristics were considered, and the bridges located on interstate and primary routes were given a priority because they are subjected to high traffic volumes. In addition, the bridges with a rating factor between 0.7 and 1.0 were chosen to explore the potential of increasing the rating factor for susceptible bridges through the computation of a refined distribution factor. Table 7-1 provides the geometrical properties of the selected bridges.

(a)

(b)

(c)
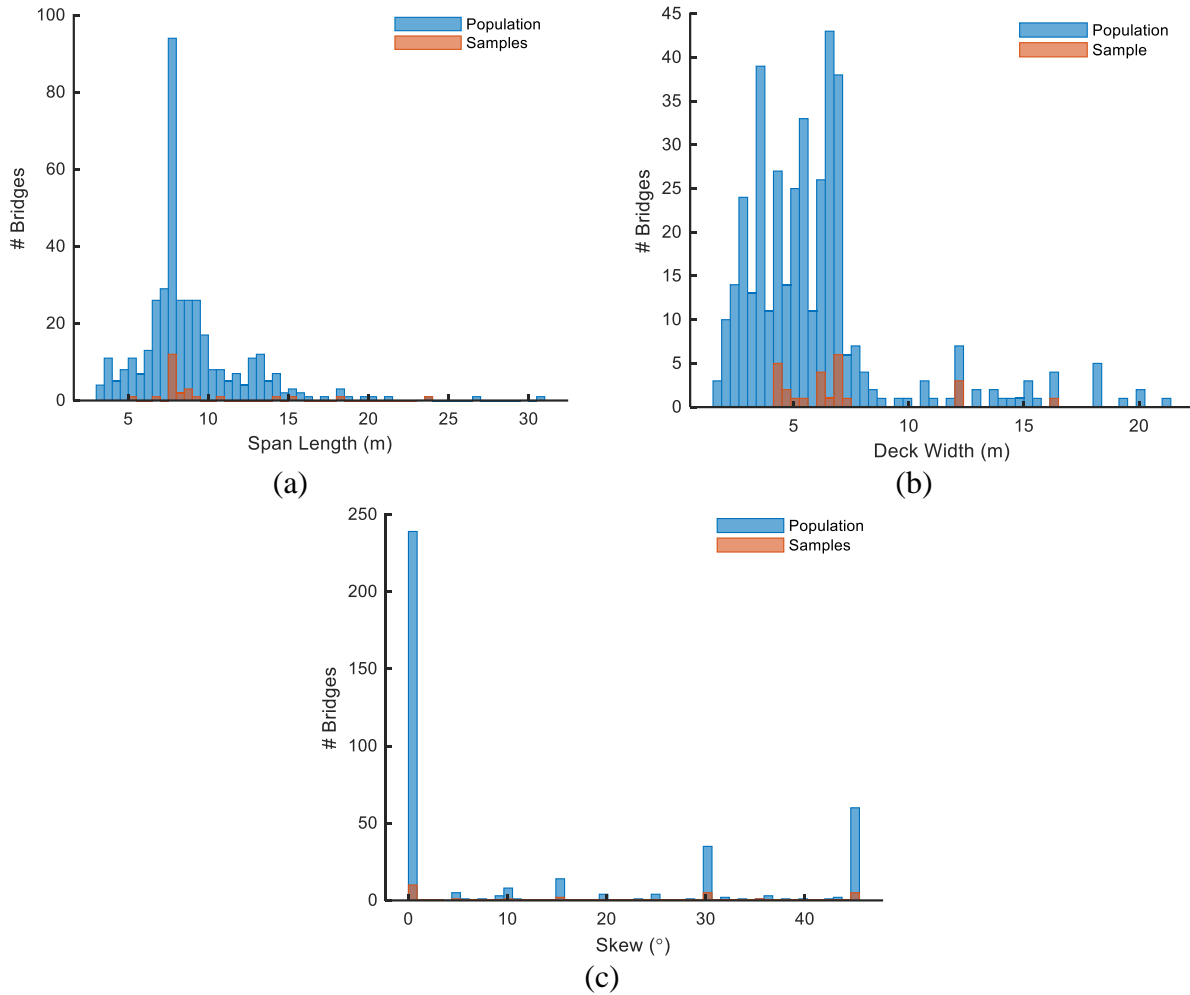
Figure 7-1: Reinforced concrete slab bridges population in terms of: (a) span length, (b) deck width, and (c) skew

Table 7-1. Selected reinforced concrete slab bridges for this study

No	Route	Span Length (m)	Parapet Width (m)	Overall Section Depth (cm)	Skew Angle (degrees)	Deck Width (m)	Lanes
1	Secondary	5.50	0.38	44.45	0	7.77	2
2	Primary	6.10	0.38	48.26	0	7.77	2
3	Primary	6.86	0.23	50.80	0	18.10	2
4	Secondary	12.19	0.28	43.18	0	9.09	2
5	Secondary	12.19	0.25	50.80	0	8.80	2
6	Primary	6.71	0.30	46.99	10	10.97	2
7	Secondary	4.60	0.30	38.10	5	7.90	2
8	Secondary	4.30	0.30	35.56	15	7.90	2
9	Secondary	16.46	0.30	50.80	15	8.53	2
10	Primary	4.60	0.51	35.56	30	15.20	2
11	Primary	6.10	0.38	48.26	30	23.50	4
12	Secondary	12.19	0.25	50.80	30	8.20	2
13	Secondary	5.20	0.32	44.45	35	6.70	2
14	Primary	7.00	0.43	45.72	45	14.30	4
15	Primary	6.10	0.51	38.10	45	8.53	2
16	Primary	4.30	0.43	35.56	45	7.90	2
17	Primary	7.01	0.37	55.88	0	7.76	2
18	Primary	7.00	0.38	55.88	0	7.77	2
19	Primary	7.00	0.23	49.53	0	7.77	2
20	Primary	4.30	0.46	53.34	0	7.92	2
21	Primary	4.30	0.43	53.34	0	7.77	2
22	Primary	6.10	0.30	52.07	30	7.62	2
23	Primary	7.30	0.19	40.64	30	8.00	2
24	Primary	4.27	0.46	46.99	45	7.62	2
25	Primary	7.01	0.23	44.45	45	5.33	1

7.3   Refined Analysis: Model Development and Computation of Distribution Factors

7.3.1   Development of Finite Element Models

The first step of the refined analysis involved creating a two-dimensional finite element model, which was then used to compute the portion of the slab effective width in resisting the applied load. With the slab bridge not containing and supporting beam elements, the model geometry was much simpler to develop and include plate elements to represent the section. The concrete slab was modeled using plate elements with four nodes. The mesh size in each bridge model was set to be equal to the half of the slab thickness or less. Pin-roller supports were set as boundary conditions for the developed models.

The live load application approaches used in the slab-on-girder bridges were also used in refined analysis of slab bridges. Models developed were subjected to live loads representing the AASHTO vehicles of interest to this study (SU4-7, design tandem, design truck (HS-20), etc.). For the analyses, only static loadings were considered as these are the primary drivers in the load sharing behavior of a bridge. For each vehicle represented in the analysis, wheel loads were

modeled as concentrated loads and applied to the corresponding nodal coordinate on the model. The loadings were positioned longitudinally on the bridge using an influence line approach to generate the maximum longitudinal response, but the transverse position(s) of the load was determined through an iterative solution systematically moving the loading transversely across the bridge. To simplify live load application to the deck model, the size of the elements was selected to eliminate the partial loading of some finite elements, i.e. the tire contact area preferably matches the area of one or a group of elements.

7.3.2   Extraction of Effective Width

The stress result obtained from the refined analysis models were used to create a plot of the longitudinal stress versus transverse location, from which the effective slab width was determined. These plots were created both single truck and two trucks placed side-by-side located at different transverse locations. The absolute maximum stress due to the maximum load effects (bending moments) at any given time was used as the reference for determining the critical effective width. The stress values at this instant for each mid transverse point were then organized into a distribution plot. A typical strain distribution plot is shown in Figure 7-2.

An idealized stress (or strain) distribution would have a relatively constant peak value (maximum stress) between the truck wheels and would decrease to zero further away from the wheels as shown in Figure 7-2. This non-uniform stress is a result of shear-lag and the concept of effective width was developed to simplify the evaluation of slabs that exhibit shear lag. The effective width section has a constant strain or stress across its width. The widely accepted definition of the effective width is "the width that would have a uniform strain equal to the maximum strain but creates the same total effect as that caused by the actual strain distribution" (Chiewanichakorn et al., 2004). Figure 7-3 conceptually illustrates how the transformed areas are determined for a wheel pair by maintaining a constant peak and determining the width to produce the same area under the curve (A2 and A3).
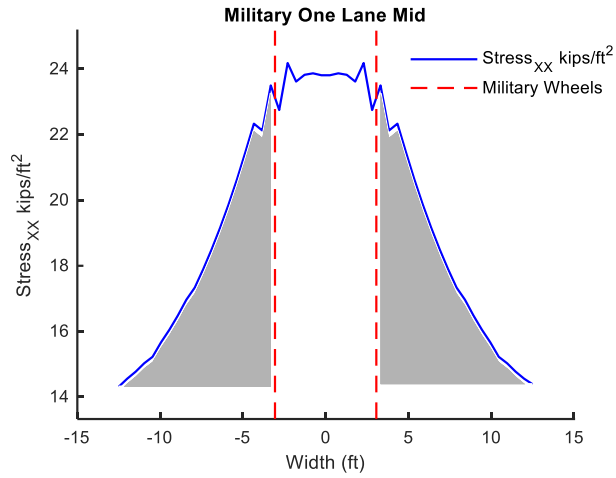
Figure 7-2. Typical Transverse Strain Distribution Plot
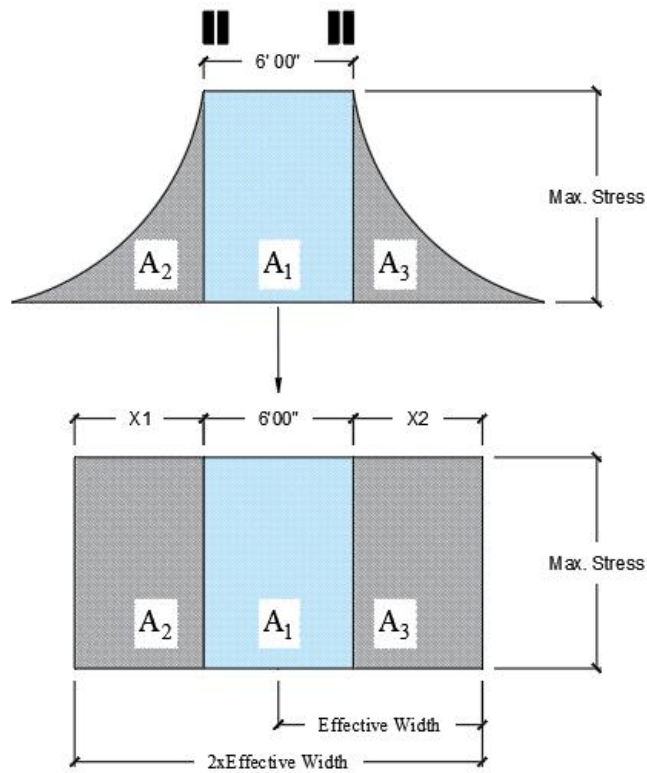
Figure 7-3. Idealized Strain Distribution and Effective Width Representation

7.3.3 *Process Automation*

Initially, the bridge geometry including section properties were specified in LARSA 4D. A mesh was generated based on the dimensions of the bridge as well as taking into consideration the computational time and the application of load. To apply the truck loads and minimize the preparation of the tedious FE data required, a MATLAB (Mathworks 2016) script was developed. A database with the axle loads of the common trucks was identified and generated in MATLAB. The MATLAB script had two main tasks: (1) read and identify the nodes associated with the truck loading for each truck and (2) write a modified LARSA 4D file with the applied loads for each case/scenario. Finally, the analysis was carried on the modified LARSA 4D file, and the results were extracted for each case. A flowchart of the procedure for determining the effective width is shown in Figure 7-4, respectively. The AASHTO trucks considered in the analyses were the HL93-Design Tandem, the HL-93/HS20-44 Design Truck, HL-93 Design Tandem and the SU Legal Truck. It was required that a number of load cases be tested in the transverse position to determine the maximum effect generated at a specific location using the trucks in the database. Therefore, for each truck, three transverse positions were considered: (1) one or two trucks placed at 2 ft from the curb of the parapets; (2) one or two trucks placed at the quarter length of the clear road width and (3) one or two trucks are placed in the mid-transverse position of the bridge. Therefore, a total of 36 load cases were considered for each bridge.
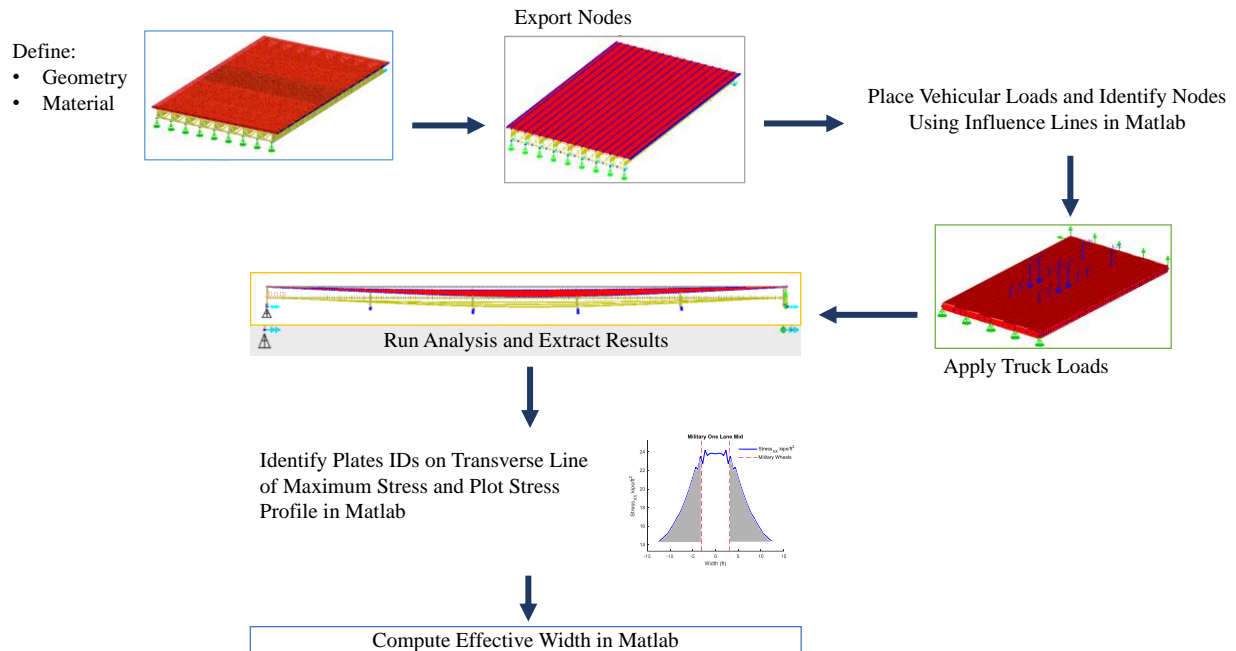
Figure 7-4. Flowchart of the Procedure Used for the Determination of Effective Width

7.3.4   Computation of Effective Width Using AASHTO LRFD and AASHTO Standards

The equation for effective width of a slab, per AASHTO LRFD, is:

For Single Lane loaded:

$$E=10.0+5.0\sqrt{L_1 W_1} \qquad (7\text{-}1)$$

For Multilane Loaded:

$$E=84.0+1.44\sqrt{L_1 W_1} \leq \frac{12.0W}{N_L} \qquad (7\text{-}2)$$

where E= Equivalent width (in.)

L_1 = Modified Span Length taken equal to the lesser of the actual span or 60 ft.

W_1 = Modified edge-to-edge width of bridge taken to be equal to the lesser of the actual width or 60.0 for multilane or 30 for single lane loading

W = Physical edge-to-edge width of bridge (ft.)

N_L = Number of design lanes

7.3.5   Computation of Effective Width through Refined Analysis

For all analyses, comparisons of performances are described relative to the design reference of the AASHTO LRFD Bridge Design Specifications. More specifically, the effective width defined in AASHTO LRFD specification served as the reference for slab bridges. The effective width for slab bridges were computed from the refined analyses and then they were compared with those computed by the AASHTO LRFD equations. Based on the results of the analysis for each bridge within the evaluation population, the cumulative worst case (i.e. smallest effective width) were compared with the AASHTO LRFD design reference as a percent change (Equation (5-2)), with a +% change indicating more of the section being effective in resisting the loading and thus an improvement in the load rating relative to the AASHTO LRFD design basis.

$$\Delta EW\ (\%) = \frac{EW_{model} - EW_{AASHTO}}{EW_{AASHTO}} \cdot 100 \tag{7-3}$$

where EW_{model} and EW_{AASHTO} represent the effective width (EW) computed using refined analysis and AASHTO LRFD Specifications, respectively; and ΔEW are the percent change in the EW when a refined analysis is conducted to compute them rather than AASHTO LRFD equations. Note that a positive change in effective width indicates an improvement in the rating factor for slab bridges. The results of changes in effective width are presented for single and multi-lane loading cases separately for slab bridges analyzed through refined analysis methods. However, the results from the worst loading case, i.e., the smallest effective width computed for single and multi-lane loading cases, were considered in the development of prediction models.

7.4   Comparison with AASHTO LRFD Distribution Factors

For the 25 reinforced concrete slab bridges the relative performance of the refined methods of analyses are presented in Table 7-2. When the measured effective widths are compared to the widths given by the AASHTO LRFD equation, it is clear that the AASHTO formula is generally conservative. The measured effective width for single truck passes was up to 81% greater than the LRFD code result. The measured effective width for side-by-side truck passes was up to 38% greater than the LRFD code result.

Table 7-2 List of the selected slab bridges

Percent Change (%) based on AASHTO LRFD			
No	One Lane EW	Two Lanes EW	Min EW
1	81	6	6
2	44	5	5
3	26	-6	-6
4	-14	-10	-14
5	4	3	3
6	61	22	22
7	68	13	13
8	80	11	11
9	2	-8	-8
10	57	17	17
11	71	38	38
12	4	1	1
13	24	0	24
14	37	24	24
15	32	12	12
16	9	2	2
17	56	5	5
18	25	3	3
19	25	3	3
20	67	5	5
21	66	9	9
22	24	7	7
23	23	2	2
24	14	6	6
25	34	0	34

Figure 7-5 shows the relative performance of the refined methods of analysis for the 25 reinforced concrete slab bridges. Presented in Figure 7-5 is a summary of the percent increase/decrease of the AASHTO LRFD effective width. It is noticed while considering the worst-case scenario (minimum effective width between one and two lanes) that the majority of the of the bridges have their effective width greater than the AASHTO LRFD effective width. The average measured effective width is even greater than the code values. When measured effective widths are compared to AASHTO LRFD equation widths, it is clear that the AASHTO formula is generally conservative.
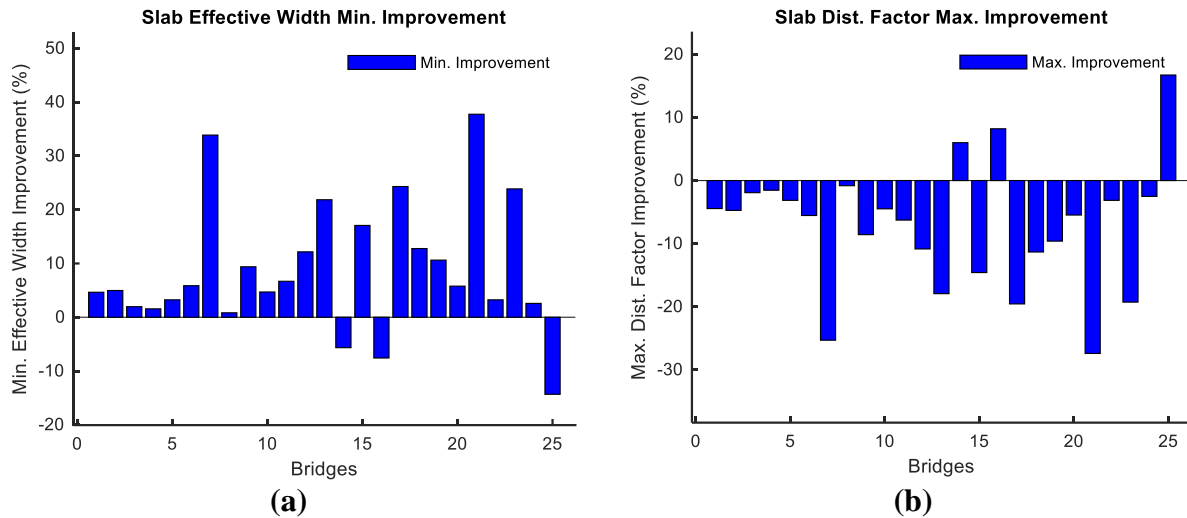
Figure 7-5 Selected Slab Bridges – Effective Width vs. AASHTO LRFD with Corresponding Impact on Load Rating Factor

7.5 Prediction Equations for Effective Width

While the limited number of concrete slab bridges were selected for the evaluation, these bridges were representative of the geometric characteristics of the overall inventory and regression models can be developed to predict the effective widths of concrete slab bridges that were not analyzed in this study. Here, the developed models utilized a best subset regression approach, which is a method that regresses multiple variables while simultaneously eliminating those that are not relevant. Best subset regression is also known as "all possible regressions" and "all possible models". This regression approach tested all possible combinations of the independent variables that were specified. After fitting all of the models using R (R Core Team, 2013), a commercial statistical analysis software package, the best models were selected using the R-squared as the statistical criteria (Hawkins and Galpin, 1986). The outcome was a presentation of the best-fit models with increasing number of independent variables up to the full model size that considers all the variables. In this study, to improve the accuracy of the prediction models, the regression equations were established considering the interaction among the selected parameters. While multi-parameter regression has the capability to extract models that best fit the dataset, the models developed in this study were limited to four parameters and their associated interactions. The choice of having four parameters in the regression models was a practical decision informed by the goal of developing look up tables that could be easily referenced. The use of more than four parameters resulted in improved predictions, but as the expense of requiring complex

visualizations. In addition, eighty percent of the observations were used as a training set, while the remaining twenty percent were used to test the models.

The regression model developed for the slab bridge effective width is shown in Equation *(7-4)*. This four-parameter model has an R^2 value of 0.905 (90.5%). The primary parameters associated with this are span length, bridge width, skew angle, and parapet width. The corresponding look-up table is presented in Table 7-3.

$$\Delta E_w = -289.4 + 23.09L + 10.07W + 57.88P_w + 10.73\theta \qquad (7\text{-}4)$$

Table 7-3 shows that bridges with smaller widths, as the span length increases, so does the effective width. When the bridge width gets larger, the effective width decreases as the span increases. The effective width of a bridge with a small width increases as the skew angle increases. However, as the width increases, the effective width decreases with increasing skew angle, with the exception of bridges with span lengths greater than 25 ft, where effective width increases with increasing skew angle. The effective width will increase as the bridge parapet width increases.

Table 7-3. Percent Change in Effective Width for Slab Bridges

	$P_w =$	1			1.12			1.25		
	$W =$	25	30	35	25	30	35	25	30	35
$L=15$	$\theta=0$	4	26	49	3	30	57	3	34	65
	$\theta=15$	8	16	24	7	18	28	6	20	34
	$\theta=30$	13	6	-1	11	6	0	9	6	2
	$\theta=45$	18	-4	-26	15	-6	-28	12	-8	-29
$L=20$	$\theta=0$	5	19	34	3	23	43	1	27	53
	$\theta=15$	8	13	18	6	16	26	5	19	34
	$\theta=30$	11	7	3	10	9	8	9	12	14
	$\theta=45$	14	1	-13	14	2	-9	13	4	-5
$L=25$	$\theta=0$	6	12	19	2	16	29	-1	20	41
	$\theta=15$	7	10	13	6	14	23	4	19	34
	$\theta=30$	9	8	7	9	12	16	9	18	26
	$\theta=45$	10	5	0	12	11	9	14	17	19
$L=30$	$\theta=0$	7	5	4	2	9	16	-4	13	29
	$\theta=15$	7	7	7	5	12	20	2	18	34
	$\theta=30$	7	9	10	8	16	24	9	23	38
	$\theta=45$	7	10	14	10	19	28	15	29	43

L: span length, in feet; *W*: slab width, in feet; P_w: parapet width, in feet; θ: skew in the bridge, in degrees

The predictions models developed were validated through a comparison of the effective width results derived from the direct refined analyses. The change in the effective width obtained from either refined analysis (x-axis) or regression model (y-axis) are shown in Figure 7-6 for each slab bridge. The solid line in the plots indicate no difference between these two parameters. The dashed lines in the plots represent the limits of 10% error between the regression model and the refined analysis model. Note that in the Table 7-3, the regression model estimates for the percent change

in the effective width are provided for the bridges with span lengths of 25 ft, 30 ft, and 35 ft. In the results presented in Figure 7-6, there were a number of bridges with a span length above 40 ft or below 15 ft, i.e., outside the model boundaries. Nevertheless, the regression models were able to make very close predictions for both bridges within and outside of the model boundaries. In particular, the mean deviation between the regression model estimate and refined analysis results for the change in the effective width is 2%.
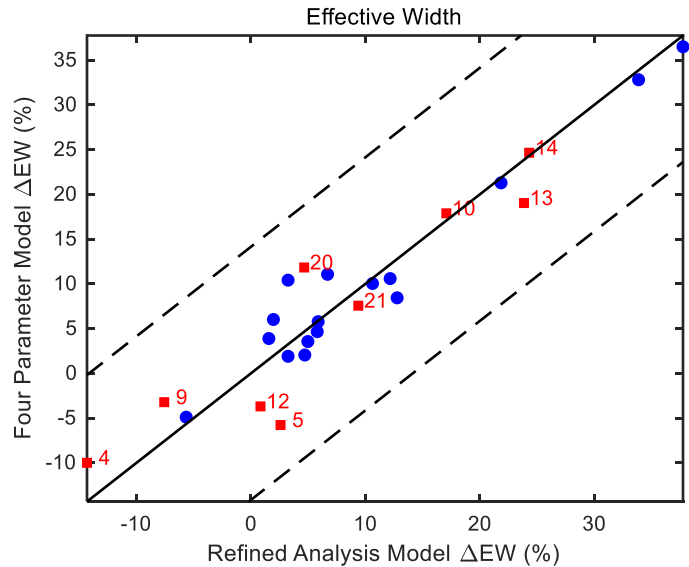
Figure 7-6. Percent Change in Effective Width for Reinforce Concrete Slab Bridges - Refined Analysis versus Regression Model. Blue markers represent bridges within the parameter ranges of regression model, while red markers represent bridges outside the parameter range of model together with corresponding bridge no.

7.6   Summary

In this chapter, a detailed numerical investigation on the effective width and load distribution factor of concrete slab bridges under various truck loads was carried out. An extensive study of simply supported concrete slab bridges was used to determine the effect of various key bridge parameters on the effective width. Based on the models results, linear regression models for the effective width of concrete slab bridges were developed based on the geometric parameters. The following conclusions can be drawn from the obtained results:

- Refined analysis tends to result in a higher effective slab width when compared to the AASHTO LRFD approach.

- Single lane loading conditions will likely have a greater increase compared to multi-lane loaded cases.

- Bridges with small span lengths mostly had a higher increase in effective width.

- The proposed expressions to predict the effective width primarily depend on bridge skewness, span length, parapet width and slab width of the bridges.

- The regression models successfully predict the effective width of concrete slab bridges within and outside of the model boundaries.

8. SUMMARY, CONCLUSIONS AND RECOMENDATIONS

8.1 Summary

State departments of transportation (DOTs) must rate the bridges in their inventory using special hauling vehicles (SHVs) and emergency vehicles (EVs) in accordance with recent amendments to federal regulations (FHWA 2013). SHVs are single-unit vehicles with several closely spaced axles, often four to seven. EVs are made to be used in emergency situations, including fires or other dangerous situations. Compared to standard vehicles used in load rating, SHVs and EVs are characterized with larger gross weights and higher axle weights. It is recognized that certain bridge types and spans may experience larger load effects (bending moment and shear) from SHVs and EVs than from previous vehicles which produce lower ratings (Sivakumar 2007). Since some bridges may need posting when rated with these specialist vehicles, this presents a challenge for state DOTs.

Bridge owners need to periodically evaluate the live load carrying capacity of their bridges. According to the most recent evaluation methodologies (AASHTO 2015), a bridge's operating load capacity is determined in terms of equivalent tonnage based on a specific vehicle configuration that may cross the bridge and rating factors (RFs). Since dead loads typically are not exposed to large alterations, rating factor is mainly dependent on live load effects and nominal capacity due to existing condition. As a result, increased live load demands, such as those imposed by SHVs and EVs, can have a negative impact on the rating.

The live load distribution factor (DF) has a direct and significant influence on the bridge rating factor. In particular, a lower DF leads to a higher the rating factor. The analytical formulas in the AASHTO LRFD Specification for computing the live load DFs were produced in NCHRP 12-26 project (NCHRP 2007), where extensive finite element (FE) analyses were conducted on single span bridges. The results were then used to formulate a set of equations that can predict the DFs using a few geometric characteristics of bridges. However, these AASHTO LRFD were obtained based on a set of assumptions such as equal girder spacing. The distribution behavior was assumed to be governed by the HS-20 design vehicle. Furthermore, the impacts of other essential elements in load distribution, such as cross-frames (Alawi et al. 2022, Khaloo and Mirzabozorg 2003, Mertz 2001, Benitez et al. 2022, Barr et al. 2001, Allawi et al. 2019, Stallings et al. 1996, McConnell 2020, Gull and Azizinamini 2014), diaphragms and barriers (Roddenberry et al. 2011, Eamon and

Nowak 2002, Bakht and Jaeger 1992), and deck cracking (Chung and Sotelino 2006, Sotelino aet al. 2004) were not considered in the construction of these expressions.

Refined analysis commonly refers a more elaborate modeling and structural analysis in bridge design and evaluation (Adams et al. 2019, Adams et al. 2019). It usually involves the development and analysis of a FE model with adequate complexity to better reveal the state of stress in a bridge structure. If implemented properly for bridge load rating, it can avoid unnecessary postings and rehabilitations. Therefore, refined analysis can be used to evaluate a more accurate rating factor for bridges susceptible to the SHV and EV loadings.

This dissertation explores the evaluation of live load distribution factors for girder bridges and live load resisting effective bridge widths for slab bridges through refined analysis. Considering the population of bridges affected by the SHV ratings and route importance, three bridge classes (simple span steel girder bridges, reinforce concrete T-beam bridges, and concrete slab bridges) were selected for the refined analysis as described in Section 3. Girder bridges were modeled using the plate with an eccentric beam analysis approach, while plate elements were used to model slab bridges within the LARSA 4D software package. The selected modeling approaches were validated through the simulation of the bridge structures with available field-testing results from the literature as presented in Section 4. A total of 71 in-service bridges belonging to the three selected bridge classes were then modeled and analyzed to compute the load distribution factors for girder bridges or effective widths for slab bridges, and the results were compared with those obtained from the code-specified equations. Using the data obtained from these numerical simulations, a series of multi-parameter linear regression models were developed to predict the percent change in distribution factor and effective width, respectively for girder and slab bridges with different geometrical characteristics.

Specifically, Section 5 explores the use of refined analysis methods to potentially increase load ratings of concrete T-beam bridges by obtaining a decrease in live load distribution factors. The studied T-beam bridges are vulnerable to posting under consideration of the new federal regulations and when using conventional, simplified equations for load distribution factors. Finite element models for a total of 25 in-service bridges were developed and analyzed under different vehicle loadings including special hauling vehicles (SHVs). The effect of transverse positioning of the vehicle load on the computation of the distribution factors was also considered. The moment

and shear effects in each girder were extracted and the distribution factors for the interior and exterior girders of the selected bridges were computed. These distribution factors were compared to those obtained from the AASHTO code-specified equations. The results were used to develop regression models to predict the percent change in distribution factors if a refined analysis is implemented. Furthermore, a support vector machine (SVM) was used to identify the governing truck type based on geometrical properties of bridges.

In Section 6, refined analysis method was used to compute live load distribution factors of steel girder bridges considering the impacts of SHVs and EVs on the load distribution behavior. To determine the load distribution factors for interior and exterior girders under different lane loading conditions, finite element models of twenty-one steel girder bridges from the state of Virginia were developed and then analyzed. The effects of vehicle type and transverse position on the results of the refined analysis were evaluated. The results were comparatively evaluated with those obtained using AASHTO LRFD equations. The distribution factor of steel girder bridges with various geometrical parameters were predicted using a series of linear regression models that were built using the data from the numerical simulations.

Section 7 explores the effective width calculations for concrete slab bridges considering the effects of different vehicles on the load distribution behavior. Finite element models of 25 reinforced slab bridges in Virginia were developed and then analyzed to determine the effective width for interior and exterior girders under different lane loading conditions. The results were compared to those obtained using the AASHTO LRFD equations. A series of linear regression models built using data from the numerical simulations were used to predict the change in effective width of the bridges with various geometrical parameters.

8.2 Conclusions

The major finding of this dissertation can be summarized as follows:

- The bridges in the VDOT inventory that are susceptible to load posting due to SHVs and EVs primarily consist of steel girder-concrete deck, reinforced concrete T-beam, and slab bridges.

- The plate with eccentric beam analysis (for girder bridges) and plate analysis (for slab bridges) are effective refined analysis methods in representing the load distribution behavior when modeling with LARSA 4D. For the eccentric beam analysis, LARSA 4D allows generating

models automatically with little effort by using built-in templates that can also be modified using spreadsheets. While the basic grid analysis approach can work for both of these types of structures, using this method in LARSA 4D requires additional effort in placing grid lines and calculating some sectional properties.

- The moment distribution factors obtained from the refined analysis will likely result in improved rating factors compared to those using distribution factors computed through the AASHTO LRFD approach, as is the case for the shear distribution factors for exterior girders.

- However, the shear distribution factors for interior girders will likely be greater. Consequently, the rating factors for those bridges controlled by the shear capacity of interior beams will likely be lower.

- For the slab bridges, refined analysis tends to result in a higher effective slab width when compared to the AASHTO LRFD approach. Single lane loading conditions will likely have a greater increase compared to multi-lane loaded cases.

- The proposed equations for predicting load distribution provide a quick and easy way to evaluate the load distribution factors.

- When bridges are vulnerable to posting from both newly introduced specialized vehicles and previously existing load rating classifications, the developed models can be used to identify bridges whose rating factor can be improved through refined analysis.

As discussed above, for each selected bridge class, a series of multi-parameter linear regression models were developed to predict the percent change in distribution factor for slab-on-girder bridges and percent change in effective width for slab bridges using four variables that described the geometrical characteristics of the bridges. Using these regression equations, the following observations can be made on the effects of bridge geometric characteristics on the load distribution behavior:

For reinforced concrete T-beam bridges:

- For interior moment effects, as the number of girders increased, the reduction of distribution factor could be larger. For bridges with a small number of girders, the distribution factor mostly increased. An increase in girder spacing lead to a higher reduction in the distribution factor. Bridges with a shorter span length and a higher number of girders had the highest potential of experiencing a reduction in the distribution factor.

- For exterior moment effects, as the slab thickness increased, the distribution factors tended to have a smaller reduction. For bridges with a slab thickness of 7 or 8 inches, as the number of girders increased, the potential reduction in distribution factor decreased. On the other hand, for bridges with a slab thickness of 9 inches, an increase in the number of girders mostly resulted in a higher possibility of reduction in distribution factors.

- For interior shear effects, increasing numbers of girders mostly leads to an increase in distribution factor. Bridges with a high skew angle (30 or 45 degrees) and high girder spacing may have a reduction in the distribution factor. The magnitude of this reduction increases with a decrease in span length.

- For exterior shear effects, as the skew angle increases the reduction in distribution factor tend to decrease. As the moment of inertia increases, the distribution factors tend to have a lower reduction potential except for bridges with a skew angle of 0 and slab thickness of 7 inches.

For steel girder bridges:

- For interior moment effects, as the number of girders increased, the greater the possibility of reducing the distribution factor. As the girder depth increased, there was a lower potential of a reduction in the distribution factor. For the bridges with a high girder depth and small number of girders, even a small increase in the distribution factors can be observed. Girder spacing had minimal effect on the change in distribution factors.

- For exterior moment effects, as the slab thickness decreased; the distribution factors tended to be larger relative to the AASHTO-calculated factors. An increase in span length resulted in a decrease in potential reduction in distribution factor. As the skew angle increased, the potential of reduction in distribution factors somewhat decreased.

- For interior shear effects, the distribution factors mostly increased for bridges with characteristics that are within the bounds considered in this study. In other words, the rating factor for bridges could be expected to decrease when using refined analysis methods and the rating is controlled by shear capacity of interior beams.

- For exterior shear effects, as the slab thickness increased, the distribution factors tended to have a lower possibilty of a reduction. For bridges with slab thickness of 7 inches, the largest reductions in distribution factors occurred for bridges with short span lengths and high girder moments of inertia.

For concrete slab bridges:

- Effective width mostly increased for bridges with characteristics that were within the defined bounds. Bridges with small span lengths mostly had a higher potential of an increase in effective width. An increase in bridge width mostly lead to an increase in effective width. Bridges with larger parapet widths had a higher potential of an increase in effective width.

8.3   Recommendations for Future Work

This study has proposed several regression equations to obtain distribution factor for girder bridges and effective width for slab bridges. Field testing of a select number of bridges can be conducted to evaluate accuracy of these equations as compared to AASHTO LRFD equations.

One of the limitations of this investigation is that the number of bridges selected for each category were limited (ranged from 21 to 25). Thus, the regression equations derived based on the selected bridges cannot represent bridges with all geometric characteristics. Here, the goal was to choose the bridges so that the variance in the developed formula was as small as possible.

Other constraints include the selection of bridges tested for validation. The bridges we chose for strain gage testing and evaluation were carefully chosen. However, more bridges could have been chosen to perform field testing to increase the veracity of our models.

According to the findings of this investigation, finite-element analysis could be used to compute a more accurate distribution factor and effective width of the rating process for girder and slab bridges, respectively. Further research can be planned to integrate the refined analysis methods into a comprehensive and reliability-based procedure for rating girders and concrete slab bridges.

The equivalent width based on measured strains from the finite element models and linear material properties may not be realistic for slab bridges with significant cracks, and these bridges should be analyzed with nonlinearity in the material properties in mind.

For transverse positioning of trucks, more transverse locations can be considered in the analysis to make sure the load effects are maximized not only at the exterior position when the

trucks are placed at what is defined as the exterior position (0.6m away from the curb) and at different point for the interior location instead at the quarter or mid position.

This study only looked at cases involving simply supported interior girders with multiple-lane loading. Similar research can be conducted on other bridge types, including continuous girder bridges, to inform about the load distribution behavior of these bridges for load rating.

Other bridge types, such timber deck girder bridges, can also benefit from similar studies to learn more about how loads are distributed on these types of bridges and how much weight they can support.

APPENDICES

Regression Equations for Evaluation of Distribution Factors for Concrete T-Beam Bridges:

Moment – Interior Girders – One-lane:

$$\Delta DF_{M\text{-}int\text{-}1L} = -3879 + 257.28L + 217.16t_s + 62.28d + 754O_v - 14.45L \cdot t_s - 4.27L \cdot d$$
$$-32.90L \cdot O_v - 3.61t_s \cdot d - 47.34t_s \cdot O_v + 1.11d \cdot O_v + 0.25L \cdot t_s \cdot d + 2.24L \cdot t_s \cdot O_v \qquad (1)$$
$$-0.3192L \cdot d \cdot O_v + 0.19t_s \cdot d \cdot O_v$$

Moment – Interior Girders – Two-lanes:

$$\Delta DF_{M\text{-}int\text{-}2L} = -3704 + 188L + 222.48t_s + 64.27d + 828O_v - 12.18L \cdot t_s - 3.65L \cdot d$$
$$+134.54L \cdot O_v - 3.91t_s \cdot d - 75.06t_s \cdot O_v + 20.72d \cdot O_v + 0.23L \cdot t_s \cdot d - 3.83L \cdot t_s \cdot O_v \quad (2)$$
$$-0.96L \cdot d \cdot O_v + 1.62t_s \cdot d \cdot O_v$$

Moment – Exterior Girders – One-lane:

$$\Delta DF_{M\text{-}ext\text{-}1L} = 4244 - 1116.2L - 1094S + 19.74d + 38.31O_v + 427.78L \cdot S$$
$$+9.34L \cdot d + 980.15L \cdot O_v - 21.64S \cdot d - 1083.3S \cdot O_v - 134.32d \cdot O_v \qquad (3)$$
$$-3.06L \cdot S \cdot d - 343.20L \cdot S \cdot O_v - 3.05L \cdot d \cdot O_v + 75.35S \cdot d \cdot O_v$$

Moment – Exterior Girders – Two-lanes:

$$\Delta DF_{M\text{-}ext\text{-}2L} = 154.8 - 5.67L - 3.40d + 19.21\theta - 23.23O_v + 0.15L \cdot d - 2.75L \cdot \theta$$
$$-2.9L \cdot O_v - 0.15d \cdot \theta + 0.1d \cdot O_v - 3.07\theta \cdot O_v + 0.03L \cdot d \cdot \theta \qquad (4)$$
$$+0.07L \cdot d \cdot O_v + 1.35L \cdot \theta \cdot O_v - 0.2d \cdot \theta \cdot O_v$$

Shear – Interior Girders – One-lane:

$$\Delta DF_{S\text{-}int\text{-}1L} = -579.08 - 139.26L + 37.74t_s + 193.52N_b + 1347.5O_v + 7.50L \cdot t_s + 26.18L \cdot N_b$$
$$+77.08L \cdot O_v - 11.76t_s \cdot N_b - 94t_s \cdot O_v - 414.34N_b \cdot O_v - 1.47L \cdot t_s \cdot N_b \qquad (5)$$
$$-2.73L \cdot t_s \cdot O_v - 5.16L \cdot N_b \cdot O_v + 27.61t_s \cdot N_b \cdot O_v$$

Shear – Interior Girders – Two-lanes:

$$\Delta DF_{S\text{-}int\text{-}2L} = 120 - 2.87L - 104.86S - 22.67\theta - 68.72N_b + 4.21L \cdot S$$
$$+0.57L \cdot \theta + 4.06L \cdot N_b + 7.43S \cdot \theta + 45.99S \cdot N_b + 4.97\theta \cdot N_b \qquad (6)$$
$$+0.01L \cdot S \cdot \theta - 2.73L \cdot S \cdot N_b - 0.12L \cdot \theta \cdot N_b - 1.70S \cdot \theta \cdot N_b$$

Shear – Exterior Girders – One-lane:

$$\Delta DF_{S\text{-}ext\text{-}1L} = 1482 - 167.37L - 776S - 10.94d - 239.41O_v + 80.78L \cdot S + 1.75L \cdot d$$
$$+119.39L \cdot O_v + 6.75S \cdot d + 168.76S \cdot O_v - 21.26d \cdot O_v - 0.88L \cdot S \cdot d \qquad (7)$$
$$-55.97L \cdot S \cdot O_v + 0.09L \cdot d \cdot O_v + 8.52S \cdot d \cdot O_v$$

Shear – Exterior Girders – Two-lanes:

$$\Delta DF_{S\text{-}ext\text{-}2L} = -127.5 + 66.88S + 97.97 \times 10^{-4}I - 63.55\theta + 3.09N_b - 5.38 \times 10^{-5}S \cdot I + \qquad (8)$$

$$26.35S \cdot \theta - 4.68S \cdot N_b + 3.50 \times 10^{-5} I \cdot \theta + 2.65 \times 10^{-5} I \cdot N_b + 12.50\theta \cdot N_b$$
$$-1.46 \times 10^{-5} S \cdot I \cdot \theta - 0.87 \times 10^{-5} S \cdot I \cdot N_b - 5.26S \cdot \theta \cdot N_b$$

Regression Equations for Evaluation of Load Distribution Factors for Steel Girder Bridges

<u>Full Regression Equations for Moment DFs:</u>

- Interior Girders – One-lane:

$$DF_{M\text{-}int\text{-}1L} = 0.364 - 0.005L + 0.115S - 0.001\theta - 0.025N_b \tag{1}$$

- Interior Girders – Two-lanes:

$$DF_{M\text{-}int\text{-}2L} = -0.508 - 0.061L + 0.584S + 0.019\theta + 5.911O_v + 0.213L \cdot S + 0.001 \times 10^{-2} L \cdot \theta$$
$$-0.006L \cdot O_v - 0.009S \cdot \theta - 2.452 \cdot O_v - 0.005\theta \cdot O_v \tag{2}$$

- Exterior Girders – One-lane:

$$DF_{M\text{-}ext\text{-}1L} = 0.843 + 0.271S - 0.055t_s - 0.005\theta - 0.057N_b + 0.38 \times 10^{-2} L \cdot t_s$$
$$-0.002S \cdot \theta - 0.034S \cdot N_b + 0.5 \times 10^{-3} t_s \cdot \theta + 0.55 \times 10^{-2} t_s \cdot N_b$$
$$+0.270 \times 10^{-3} \theta \cdot N_b \tag{3}$$

- Exterior Girders – Two-lanes:

$$DF_{M\text{-}ext\text{-}2L} = -0.313 - 0.060L + 0.479S + 0.025\theta + 3.710Ov + 0.021L \cdot S + 0.08 \times 10^{-3} L \cdot \theta$$
$$+0.017L \cdot O_v - 0.105S \cdot \theta - 1.84S \cdot O_v - 0.87 \times 10^{-3} \theta \cdot O_v \tag{4}$$

<u>Full Regression Equations for Shear DFs:</u>

- Interior Girders – One-lane:

$$DF_{S\text{-}int\text{-}1L} = 3.25 + 6.769 \times 10^{-3} L - 1.51S - 0.078t_s - 0.054N_b - 0.045L \cdot S + 0.005L \cdot t_s$$
$$+0.7 \times 10^{-3} L \cdot N_b + 0.059S \cdot t_s + 0.268S \cdot N_b - 0.031t_s \cdot N_b \tag{5}$$

- Interior Girders – Two-lanes:

$$DF_{S\text{-}int\text{-}2L} = -3.80 - 0.162L + 1.624S + 0.063d + 0.418N_b + 0.135L \cdot S$$
$$-0.08 \times 10^{-3} L \cdot d + 0.79 \times 10^{-2} L \cdot N_b - 0.016S \cdot d - 0.147S \cdot N_b - 0.003d \cdot N_b \tag{6}$$

- Exterior Girders – One-lane:

$$DF_{S\text{-}ext\text{-}1L} = 0.03 + 0.19S + 1.672 \times 10^{-3}d - 0.001\theta - 0.224O_v \qquad (7)$$

- Exterior Girders – Two-lanes:

$$
\begin{aligned}
DF_{S\text{-}ext\text{-}2L} = &-3.854 - 0.290L + 0.238t_s + 0.121d - 0.250N_b + 0.013L \cdot t_s - \\
&0.470 \times 10^{-4}L \cdot d - 0.35 \times 10^{-2}L \cdot N_b \qquad (8)\\
&-0.569 \times 10^{-2}t_s \cdot d + 0.307 \times 10^{-2}t_s \cdot N_b + 0.198 \times 10^{-2}d \cdot N_b
\end{aligned}
$$

Regression Equation for Evaluation of Effective Width for Concrete Slab Bridges:

$$
\begin{aligned}
\Delta E_w = &-289.4 + 23.09L + 10.07W + 57.88P_w + 10.73\theta - 8.102 \times 10^{-1}L \cdot W - 14.94L \cdot P_w \\
&- 52.89L \times 10^{-2}L \cdot \theta - 78.40 \times 10^{-2}W \cdot P_w - 30.06 \times 10^{-2}W \cdot \theta + 41.26 \times 10^{-2}P_w \cdot \theta \\
&+ 49.21 \times 10^{-2}L \cdot W \cdot P_w + 14.71 \times 10^{-3}L \cdot W \cdot \theta + 13.97 \times 10^{-2}L \cdot P_w \cdot \theta \\
&- 11.93 \times 10^{-2}W \cdot P_w \cdot \theta
\end{aligned}
$$

REFERENCES

AASHTO (2002). Standard Specifications for Highway Bridges, 17th Ed., American Association of State Highway and Transportation Officials (AASHTO), Washington, D.C.

AASHTO (2012). LRFD Bridge Design Specifications, 5th Ed., American Association of State Highway and Transportation Officials (AASHTO), Washington, D.C.

AASHTO. (2010). AASHTO LRFD bridge design specifications, 5th Ed., Washington, DC.

Adams, A., Galindez, N., Hopper, T., Murphy, T., Ritchie, P., Storlie, V. and Weisman, J., 2019. *Manual for Refined Analysis in Bridge Design and Evaluation* (No. FHWA-HIF-18-046). United States. Federal Highway Administration. Office of Infrastructure.

Allawi, A.A., Said, A.I., Al-Sherrawi, M.H., Albayati, A., Al Gharawi, M. and El-Zohairy, A., 2022. Evaluation of Live Load Distribution Factors of a Highway Bridge. In *Geotechnical Engineering and Sustainable Construction* (pp. 531-543). Springer, Singapore.

Allawi, Abbas, Mohannad Al-Sherrawi, Mohanned Al Gharawi, and Ayman El-Zohairy. "A case study to evaluate live load distributions for pre-stressed RC bridge." In Challenges in Mechanics of Time-Dependent Materials, Volume 2, pp. 73-85. Springer, Cham, 2019.

Amer, A., Arockiasamy, M. and Shahawy, M. (1999). Load distribution of existing solid slab bridges based on field tests. Journal of Bridge Engineering, 4(3), pp.189-193.

American Association of State and Highway Transportation Officials (AASHTO) (2015). "Manual for Bridge Evaluation. 2nd Ed. with 2016 Interim Revisions." American Association of State Highway and Transportation Officials, Washington, DC.

American Association of State and Highway Transportation Officials (AASHTO) (2019). Manual for Bridge Evaluation. 3rd Ed. with 2019 Interim Revisions. American Association of State Highway and Transportation Officials, Washington, DC.

American Association of State Highway and Transportation Officials (AASHTO) (2017). AASHTO LRFD Bridge Design Specifications. 8th Ed. American Association of State Highway and Transportation Officials, Washington, DC.

Angulo, C., X. Parra, and A. Catala. 2003. K-SVCR. A support vector machine for multi-class classification. *Neurocomputing*, 55(1-2), pp.57-77.

Bae, H. U., & Oliva, M. G. (2012). Moment and shear load distribution factors for multigirder bridges subjected to overloads. Journal of Bridge Engineering, 17(3), 519-527.

Bagheri, Abdollah, Mohamad Alipour, Osman E. Ozbulut, and Devin K. Harris. "A nondestructive method for load rating of bridges without structural properties and plans." Engineering Structures 171 (2018): 545-556.

Bakht, B., & Jaeger, L. G. (1992). Ultimate load test of slab-on-girder bridge. Journal of Structural Engineering, 118(6), 1608-1624.

Barker, M.G. (2001). Quantifying field-test behavior for rating steel girder bridges. Journal of Bridge Engineering, 6(4), pp.254-261

Barr, P. J., M. O. Eberhard, and J. F. Stanton. 2001. "Live-load distribution factors in prestressed concrete girder bridges." *Journal of Bridge Engineering*, 6(5), pp.298-306.

Barr, P. J., N. Yanadori, M. W. Halling, and K. C. Womack. 2007. "Live-load analysis of a curved I-girder bridge." *Journal of Bridge Engineering*, 12(4), pp.477-484.

Benítez, José Miguel Parra, José M. Benjumea, and Vladimir Guilherme Haach. "Theoretical and computational simulation of the effect of the number of intermediate diaphragms on the live load distribution factors and structural response of a precast girder bridge." Latin American Journal of Solids and Structures 19 (2022).

Cai, C. S. 2005. "Discussion on AASHTO LRFD load distribution factors for slab-on-girder bridges." *Practice periodical on structural design and construction*, 10(3), pp.171-176.

Catbas, F.N., Gokce, H.B. and Gul, M. (2012). Practical approach for estimating distribution factor for load rating: Demonstration on reinforced concrete T-beam bridges. Journal of Bridge Engineering, 17(4), pp.652-661.

Chiewanichakorn, M., Aref, A.J., Chen, S.S. and Ahn, I.S. (2004). Effective flange width definition for steel–concrete composite bridge girder. Journal of Structural Engineering, 130(12), pp.2016-2031.

Chung, W., J. Liu, and E. D. Sotelino. 2006. "Influence of secondary elements and deck cracking on the lateral load distribution of steel girder bridges." *Journal of Bridge Engineering*, 11(2), pp.178-187.

Conner, S., and X. S. Huo. 2006. "Influence of parapets and aspect ratio on live-load distribution." *Journal of Bridge Engineering*, 11(2), pp.188-196.

Davids, W.G., Poulin, T.J. and Goslin, K. (2013). Finite-element analysis and load rating of flat slab concrete bridges. Journal of Bridge Engineering, 18(10), pp.946-956.

DePolo, D. S., and D. G. Linzell. 2008. "Evaluation of live-load lateral flange bending distribution for a horizontally curved I-girder bridge." *Journal of Bridge Engineering*, 13(5), pp.501-510.

Dicleli, M., S. Erhan. 2009. "Live load distribution formulas for single-span prestressed concrete integral abutment bridge girders." *Journal of Bridge Engineering*, 14(6), pp.472-486.

Dymond, Benjamin Z., Catherine EW French, and Carol K. Shield. "Investigation of shear distribution factors in prestressed concrete girder bridges." (2016).

Dymond, Benjamin Z., Catherine EW French, and Carol K. Shield. "Torsional effects on load tests to quantify shear distribution in prestressed concrete girder bridges." Special Publication 323 (2018): 10-1.

Dymond, B.Z., French, C.E. and Shield, C.K. (2019). Recommendations for More Accurate Shear Rating of Prestressed Concrete Girder Bridges. Journal of Bridge Engineering, 24(12), p.04019117.

Eamon, C. D., & Nowak, A. S. (2002). Effects of edge-stiffening elements and diaphragms on bridge resistance and load distribution. Journal of Bridge Engineering, 7(5), 258-266.

Ebeido, T., and J. B. Kennedy. 1996. "Girder moments in continuous skew composite bridges." *Journal of Bridge Engineering*, 1(1), pp.37-45.

Eom, J. and Nowak, A.S. (2001). Live load distribution for steel girder bridges. Journal of Bridge Engineering, 6(6), pp.489-497.

Eom, J., and A. S. Nowak. 2001. "Live load distribution for steel girder bridges." *Journal of Bridge Engineering*, 6(6), pp.489-497.

Fanous, F., J. May, and T. Wipf. 2011. "Development of live-load distribution factors for glued-laminated timber girder bridges." *Journal of Bridge Engineering*, 16(2), pp.179-187.

Federal Highway Administration (FHWA) (2013). Action: Load Rating of Specialized Hauling Vehicles. Federal Highway Administration, McLean, VA.

Federal Highway Administration (FHWA) (2016). Fixing America's surface transportation act or 'FAST Act'. Federal Highway Administration, McLean, VA.

FHWA, Action: Load Rating of Specialized Hauling Vehicles. 2013, Federal Highway Administration: McLean, VA.

Gheitasi, A. and D.K. a (2015). "Implications of Overload Distribution Behavior on Load Rating Practices in Steel Stringer Bridges." Transportation Research Record: Journal of the Transportation Research Board, 2522, pp 47–56.

Gull, J.H. and Azizinamini, A., 2014. Steel plate girder diaphragm and cross bracing loads (No. BDK80-977-20). Florida. Dept. of Transportation.

Harris, D. K. 2010. "Assessment of flexural lateral load distribution methodologies for stringer bridges." *Engineering Structures*, 32(11), pp.3443-3451.

Harris, D. K., O. E. Ozbulut, A. Bagheri, M. S. Dizaji, A. K. Ndong, and M. Alipour. 2020. "Load Rating Strategies for Bridges with Limited or Missing As-Built Information (No. FHWA/VTRC 20-R27)." Virginia Transportation Research Council (VTRC).

Harris, D.K., Ozbulut, O., Bagheri, A., Dizaji, M.S., Ndong, A.K. and Alipour, M. (2020). Load Rating Strategies for Bridges With Limited or Missing As-Built Information (No. FHWA/VTRC 20-R27). University of Virginia.

Hawkins, D.M. and Galpin, J.S. (1986). Selecting a Subset of Regression Variables so as to Maximize the Prediction Accuracy at a Point. Journal of Applied Statistics, 13, pp.187199.

Hayworth, Rebecca, X. Sharon Huo, and Lei Zheng. "Effects of State Legal Loads on Bridge Rating Results Using the LRFR Procedure." Journal of Bridge Engineering 13, no. 6 (2008): 565-572.

Herzberg, P. A. "The Parameters of Cross-Validation (Psychometric Monograph No. 16). Richmond, VA: Psychometric Society." (1969).

Huang, D. 2004. "Field test and rating of Arlington curved-steel box-girder bridge: Jacksonville, Florida." *Transportation Research Record*, 1892(1), pp.178-186.

Huang, D. 2008. "Full-scale test and analysis of a curved steel-box girder bridge." *Journal of Bridge Engineering*, 13(5), pp.492-500.

Islam, S. (2018). Load Rating Study of Effects of Special Hauling Vehicle Loads on Ohio Bridges (Doctoral dissertation, University of Toledo).

Jáuregui, D.V., Licon-Lozano, A. and Kulkarni, K., 2007. Improved load rating of reinforced concrete slab bridges (No. NM05STR-02). New Mexico. Dept. of Transportation. Research Bureau.

Kennedy, J. B., and N. F. Grace. 1983. "Load distribution in continuous composite bridges." *Canadian Journal of Civil Engineering*, 10(3), pp.384-395.

Khaloo, A.R. and Mirzabozorg, H., 2003. Load distribution factors in simply supported skew bridges. *Journal of Bridge Engineering*, *8*(4), pp.241-244.

Kim, S. and Nowak, A.S. (1997). Load distribution and impact factors for I-girder bridges. Journal of Bridge Engineering, 2(3), pp.97-104.

LARSA 4D 7.01.69 [Computer software]. Melville, NY, LARSA

LARSA, Inc. LARSA, Melville, NY.

Lawson, W. D., H. Seo, J. G. Surles, and S. M. Morse. 2018. "Impact of Specialized Hauling Vehicles on Load Rating Older, Bridge-Class, Reinforced Concrete Box Culverts." *Transportation Research Record*, 2672(41), pp.87-100.

Mabsout, M., Tarhini, K., Jabakhanji, R. and Awwad, E. (2004). Wheel load distribution in simply supported concrete slab bridges. Journal of Bridge Engineering, 9(2), pp.147-155.

Mathworks, Inc. MATLAB, Natick, MA.

MATLAB (2016a). "The MathWorks, Natick, 2016.

McConnell, J., Radovic, M. and Keller, P., 2020. Holistic finite element analysis to evaluate influence of cross-frames in skewed steel I-girder bridges. Engineering Structures, 213, p.110556.

Mensah, Salahudin A., and Stephan A. Durham. "Live load distribution factors in two-girder bridge systems using precast trapezoidal U-girders." Journal of Bridge Engineering 19, no. 2 (2014): 281-288.

Mertz, D.R., 2015. Steel bridge design handbook: Load rating of steel bridges (No. FHWA-HIF-16-002-Vol. 18). United States. Federal Highway Administration. Office of Bridges and Structures.

Morcous, G., Hanna, K. and Tadros, M.K., 2010. Load rating of complex bridges (No. SPR-1 (10) P329). Nebraska Transportation Center.

NCHRP Project 12-63 (Report 575, 2007)

Mott, R. and Diaz, M.A., 2010. Distribution factors for short-haul vehicular loads on prestressed concrete open box beam (U-Beam) bridges. Practice Periodical on Structural Design and Construction, 15(2), pp.101-108.

Nouri, G. and Ahmadi, Z. (2012). Influence of skew angle on continuous composite girder bridge. Journal of Bridge Engineering, 17(4), pp.617-623.

Nowak, A.S. and Eom, J. (2001). Verification of Girder Distribution Factors and Dynamic Load Factors by Field Testing. Current and future trends in bridge design, construction and maintenance 2: Safety, economy, sustainability and aesthetics (pp. 414-423). Thomas Telford Publishing.

Nowak, A.S., J. Eom, A. Sanli, and R. Till. 1999. "Verification of girder-distribution factors for short-span steel girder bridges by field testing." *Transportation Research Record*, 1688(1), pp.62-67.

Puckett, J. A., S. X. Huo, M. Jablin, and D. R. Mertz. 2011. "Framework for simplified live load distribution-factor computations." *Journal of Bridge Engineering*, 16(6), pp.777-791.

R Core Team (2013). R: A language and environment for statistical computing. R Foundation for Statistical Computing, Vienna, Austria

Roddenberry, M. R., Chipperfield, J., and Tawfiq, K. S. (2011). "Effect of secondary elements on load distribution in prestressed bridge girders." Proc., 2011 Structures Congress, ASCE, Reston, VA, 215–226.

Sivakumar, B. (2007). "NCHRP 12-63: Legal truck loads and AASHTO legal loads for posting." *Report 575*, National Cooperative Highway Research Board, Washington, D.C.

Snyder, R. and Beisswenger, J. (2017). Implementation of a Refined Shear Rating Methodology for Prestressed Concrete Girder Bridges (No. MN/RC 2017-48). Minnesota. Dept. of Transportation. Research Services & Library.

Sotelino, E.D., Liu, J., Chung, W. and Phuvoravan, K., 2004. Simplified load distribution factor for use in LRFD design.

Stallings, J.M., Cousins, T.E. and Stafford, T.E., 1996. Effects of removing diaphragms from steel girder bridge. Transportation Research Record, 1541(1), pp.183-188.

Stawska, Sylwia, Andrzej S. Nowak, Jacek Chmielewski, and Anjan Ramesh Babu. "Bridge rating for vehicles with grandfather provisions." Journal of Bridge Engineering 26, no. 9 (2021): 04021066.

Team, R. C. 2013. "R: A language and environment for statistical computing."

Virginia Department of Transportation (VDOT) (2019). State of the Structures and Bridges Report. Virginia Department of Transportation, Richmond, VA.

Wang, N., Ellingwood, B. R., & Zureick, A. H. (2011b). Bridge rating using system reliability assessment. II: Improvements to bridge rating practices. Journal of Bridge Engineering, 16(6), 863-871.

Wang, N., O'Malley, C., Ellingwood, B. R., & Zureick, A. H. (2011a). Bridge rating using system reliability assessment. I: Assessment and verification by load testing. Journal of Bridge Engineering, 16(6), 854-862.

Yan, W., Hunt, L., Sheng, Q., & Szlavnies, Z. (2000). R: Development Core Team (2005): R: a language and environment interaction for statistical computing. R Foundation for Statistical Computing, Vienna, Austria, www. R-project. org.

Yoo, C. H., K. Kim, K. C. Lee, and J. Kang. 2013. "Bending strength of a horizontally curved composite I-girder bridge." *Journal of Bridge Engineering*, 18(5), pp.388-399.

Yost, J.R., J. L. Schulz, and B. C. Commander. 2005. "Using NDT data for finite element model calibration and load rating of bridges." *In Structures Congress 2005: Metropolis and Beyond* (pp. 1-9).

Yousif, Zaher, and Riyadh Hindi. "AASHTO-LRFD live load distribution for beam-and-slab bridges: Limitations and applicability." Journal of Bridge Engineering 12, no. 6 (2007): 765-773.

Zokaie, T. 2000. "AASHTO-LRFD live load distribution specifications." Journal of bridge Engineering, 5(2), pp.131-138.

Zokaie, T., Imbsen, R. A., and Osterkamp, T. A. (1991). Distribution of Wheel Loads on Highway Bridges, National Cooperative Highway Research Program (NCHRP 12-26). Transportation Research Board, Washington, USA.

Zokaie, T., R. A. Imbsen, and T. A. Osterkamp. 1991. "Distribution of wheel loads on highway bridges." Transportation Research Record, 1290, pp.119-126.